DISCOVERY AND CHARACTERIZATION OF REGULATORY MECHANISMS AFFECTING THE HETEROMERIC ACETYL-COENZYME A CARBOXYLASE IN ARABIDOPSIS

A Dissertation

presented to

the Faculty of the Graduate School

at the University of Missouri-Columbia

In Partial Fulfillment

of the Requirements for the Degree

Doctor of Philosophy

---

by

MATTHEW JACOB SALIE

Dr. Jay J. Thelen, Dissertation Supervisor

MAY 2016

The undersigned, appointed by the dean of the Graduate School, have examined the Dissertation entitled

DISCOVERY AND CHARACTERIZATION OF REGULATORY MECHANISMS AFFECTING THE HETEROMERIC ACETYL-COENZYME A CARBOXYLASE IN ARABIDOPSIS

Presented by

MATTHEW JACOB SALIE

A candidate for the degree of

Doctor of Philosophy

And hereby certify that, in their opinion, it is worthy of acceptance

---

Jay J. Thelen

Jan A. Miernyk

Melissa G. Mitchum

Abraham J.K. Koo

David W. Emerich

ACKNOWLEDGEMENTS

Many people have helped me accomplish this work. First and foremost, I would like to thank my parents for raising me with strong morals and work ethic that allowed me to endure the many failed experiments and exciting discoveries that come with graduate research. I would like to thank Jay Thelen for putting the time and investment into my training that has prepared me for the next step in my career, and my committee for the advice and encouraging conversations during my publication struggles. I thank Severin Stevenson and Kirby Swatek for the time and expertise they gave to me when I began in the lab. Their effort saved me months of time and I am very grateful. I thank my previous mentors who encouraged me to enter into a career in science and gave me invaluable experience in a lab: Larry Louters and Scott Tamminga. I especially want to thank my lab mate and trusted friend, Rashaun Wilson. She has helped me more than I can possibly thank her for over the years as we have celebrated the highs and carried each other through the lows. I wish her all the best as we go our separate ways. And finally, I want to thank my beautiful fiancé, Li Zhe. Thank you for all of your support and love. I love you, and I can't wait to spend our lives together.

TABLE OF CONTENTS

LIST OF TABLES

LIST OF FIGURES

ABSTRACT

Fatty acid biosynthesis (FAS) is an essential metabolic pathway used by all organisms to generate fatty acids. A staple component of this pathway is the enzyme acetyl-CoA carboxylase (ACCase), which catalyzes the committed step by converting acetyl-CoA to malonyl-CoA. The heteromeric form of this enzyme requires four different subunits for activity: biotin carboxylase, biotin carboxyl carrier protein (BCCP), and α- and β-carboxyltransferase (CT). Heteromeric ACCase is present in prokaryotes and the plastids of most plants, and has been a focus of biotechnology research due to its prominent role in FAS. Many different regulatory mechanisms have been identified in both plants and *E. coli*. However, it is still unknown how most of these regulatory mechanisms are mediated. For example, ACCase is known to be feedback inhibited by 18:1-acyl carrier protein in plants, yet it is unknown how this inhibition is exerted on the enzyme. Therefore it was posited that other unknown factors, such as proteins or post-translational modifications, might play a role in ACCase regulation.

To identify suspected regulatory factors associated with ACCase, we performed *in vivo* co-immunoprecipitation (co-IP) using subunit-specific antibodies to isolate the ACCase complex from *Arabidopsis thaliana* leaves. Quantitative mass spectrometry of these co-IPs revealed all four known subunits to ACCase and two unknown proteins annotated as 'biotin/lipoyl attachment domain containing' (BADC) proteins. The BADC proteins are a family of three proteins in *A. thaliana* and resemble the BCCP subunit to ACCase, but lack the conserved biotinylation motif. All three BADC proteins interacted with the two *A. thaliana* BCCP isoforms and the biotin carboxylase subunit of ACCase based on yeast two-hybrid and heterologous co-expression analyses. None of the

BADC proteins were biotinylated *in planta* or when expressed in *Escherichia coli*, unlike BCCP controls. Gene orthologs to BADC were found only in plant and green algae species that contain a heteromeric ACCase suggesting BADC genes co-evolved with this form of ACCase. Expression of BADC proteins in a temperature-sensitive *E. coli* BCCP mutant in minimal media strongly inhibited cell growth through interaction with the homologous, bacterial ACCase. Also, addition of recombinant BADC protein to *in vitro* ACCase activity assays significantly reduced enzyme activity. Finally, partial silencing of one of the BADC genes in *A. thaliana* seed led to a slight, yet significant, increase in seed oil content. We conclude the BADC proteins are ancient BCCPs that acquired a new function through mutation of the biotinylation motif. We propose a poisoned complex model whereby BADCs function as negative regulators of ACCase by competing with BCCP for access to the holo-ACCase complex.

In addition, a study was performed to identify the role of phosphorylation of the α-CT subunit. Multiple studies had identified two phosphorylation sites on the C-terminal domain of α-CT in *A. thaliana*. This C-terminal domain is not found in all plant species and has an unknown function. To determine the potential regulatory effect of phosphorylation on this domain, phosphomimic and phospho-deficient α-CT mutants were made and expressed in wild type *A. thaliana*. Multiple independent transgenic lines containing at least two-fold α-CT protein compared to empty vector controls were screened for seed oil content. The resulting data showed no clear phenotype that could be attributed to expression of the mutants. This result could be explained by a number of factors such as the presence of endogenous α-CT, the complexity of the seed oil phenotype, or a large margin of technical error in some lines. However, *in vitro* ACCase

activity assays showed that a transgenic line overexpressing native α-CT contained increased specific activity of the enzyme compared to controls. Furthermore, analysis of transgenic lines expressing phosphomimic or phospho-deficient α-CT mutants also showed increased ACCase specific activity which was indistinguishable from the native α-CT overexpression line, regardless of the mutation. Therefore it appears that increased α-CT expression can increase ACCase activity by allowing for the formation of more active complexes. This observation suggests that α-CT is the limiting subunit of the ACCase complex in the stroma.

CHAPTER I: REVIEW

REGULATION AND STRUCTURAL CHARACTERISTICS OF HETEROMERIC ACETYL-COA CARBOXYLASE

The following chapter is adapted from the publication in press in
Biochimica et Biophysica Acta – Molecular and Cell Biology of Lipids

Title: Regulation and structure of the heteromeric acetyl-CoA carboxylase

Authors: Matthew J. Salie and Jay J. Thelen

Abstract:

The enzyme acetyl-CoA carboxylase (ACCase) catalyzes the committed step of the *de novo* fatty acid biosynthesis (FAS) pathway by converting acetyl-CoA to malonyl-CoA. Two forms of ACCase exist in nature, a homomeric and heteromic form. The heteromeric form of this enzyme requires four different subunits for activity: biotin carboxylase; biotin carboxyl carrier protein; and α- and β-carboxyltransferase. Heteromeric ACCases (htACCase) can be found in prokaryotes and the plastids of most plants. The plant htACCase is regulated by diverse mechanisms reflected by the biochemical and genetic complexity of this multienzyme complex and the plastid stroma where it resides. In this review we summarize the regulation of the plant htACCase and also describe the structural characteristics of this complex from both prokaryotes and plants.

1.0 Introduction

1.1 Role of acetyl-CoA carboxylase in de novo fatty acid synthesis

Acetyl-CoA carboxylase (EC 6.4.1.2; ACCase) catalyzes the committed step of *de novo* fatty acid synthesis (FAS) in all organisms. The enzyme uses bicarbonate, ATP, acetyl-CoA, and biotin cofactor to produce malonyl-CoA, the building block of fatty acid synthesis (Figure 1) (1,2). In nature there are two functional forms of this enzyme, each contain the four different components required for activity: biotin carboxylase (BC; EC 6.3.4.14); biotin carboxyl carrier protein (BCCP); and α- and β-carboxyltransferase (CT). One form is heteromeric, for which all four enzymatic components are expressed as individual subunits that associate to form a multienzyme complex (3). The heteromeric form of ACCase (htACCase) is found in prokaryotes and the plastids of algae, bryophytes, pteridophytes, gymnosperms, non-graminaceous monocots, and dicots (3-5). A few archaea have been identified to contain a hybrid CT gene that encodes the α and β subunits in tandem, however, these enzymes carboxylate both acetyl-CoA and propionyl-CoA (6-8). The other form is described as homomeric, whereby all four enzymatic components are concatenated into a single polypeptide. The homomeric ACCase (hmACCase) is the predominant form for *de novo* fatty acid synthesis in the cytosol of animals and fungi, and the plastids of graminaceous monocots. In addition, the cytosol of all plants contains a hmACCase isoform that provides malonyl-CoA for fatty acid elongation as well as polyketide biosynthesis, malonylation reactions, and other specialized metabolic processes (9). A hmACCase has also been discovered in the plastid of dicot species (10), but its metabolic role is

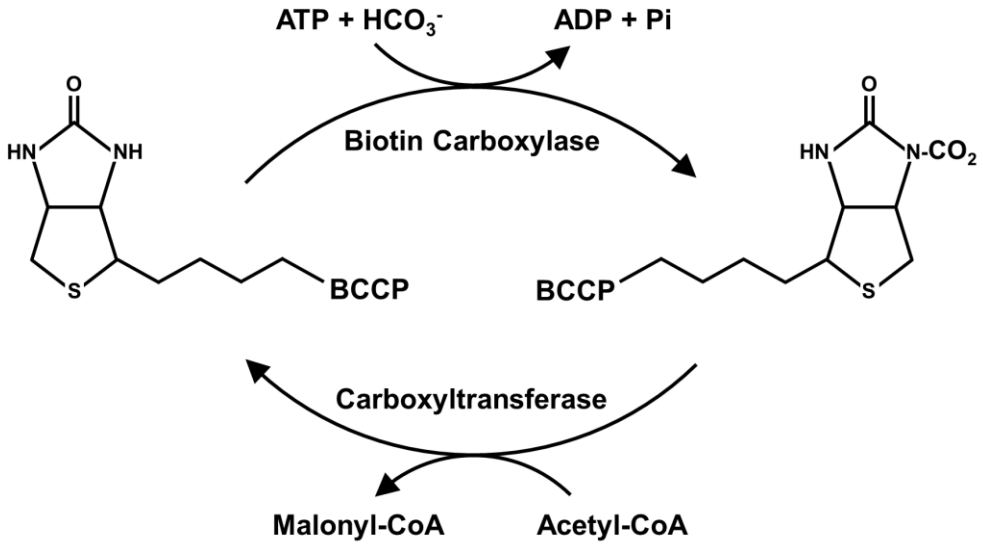

Figure 1. Reaction mechanism of ACCase. Adapted from (11). The ATP-dependent carboxylation of the biotinyl moiety with the biotin carboxyl carrier protein (BCCP) is catalyzed by biotin carboxylase (BC). The activated carboxyl group is then transferred to acetyl-coenzyme A by carboxyltransferase (CT) to produce malonyl-coenzyme A. Active site coupling between the BC and CT half reactions is facilitated by the flexible biotinyl-lysine arm within the holo-BCCP.

presently unclear.

Due to its complexity and key role in *de novo* FAS, the htACCase is the most extensively studied form of ACCase in plants. There is evidence that increasing htACCase activity leads to increased carbon flux into *de novo* FAS in both microbes (12) and plants (13). Therefore understanding the regulatory factors that affect htACCase activity will be important in developing successful biotechnology strategies involving lipid metabolism. This review will consequently focus on the recent discoveries related to the regulation and structure of htACCase in both plants and prokaryotes. For a more historical perspective on hmACCase or an in-depth discussion of fatty acid synthesis in plants we recommend the following reviews (14-16).

1.2 The half-reactions of htACCase occur on separate subcomplexes

The htACCase catalyzes two distinct half-reactions and is made up of two separable "subcomplexes", BC-BCCP and α-CT-β-CT (11,17,18). These two components catalyze the enzymatic half-reactions noted in Figure 1. The biotin-containing subunit, BCCP, links the two reactions through an active site coupling mechanism analogous to that of the lipoyl domain of the α-keto acid dehydrogenase complexes (19). The two subcomplexes readily dissociate during conventional purification techniques, but the subcomplexes themselves remain intact, suggesting that these subcomplexes are more stable compared to the whole htACCase complex (17,18). The first active site is on the BC subunit, where ATP is bound and hydrolyzed to catalyze the carboxylation of biotin cofactor covalently bound to a conserved Lys within the BCCP. The carboxylated, biotinyl-Lys arm is then transferred to the active site on the CT subcomplex. This active

site is produced by the assembly of both the α- and β-CT subunits, and binds acetyl-CoA as the terminal carboxy acceptor (20).

1.3 htACCase gene localization

The genes encoding the catalytic subunits for htACCase were first discovered in *E. coli* (2,21-23) and subsequently plants (24-27). In the reference dicot plant Arabidopsis (*Arabidopsis thaliana*), each catalytic subunit is encoded by a single gene except for BCCP, which is encoded by two genes (25,28,29). Each of these genes is encoded within the nuclear genome except for *accD* (encoding the β-CT subunit), which resides in the plastid genome. This is the only known FAS-related gene that is encoded in the plastid genome (30). Presumably, each of the genes for the ACCase subunits initially resided in the plastid genome after the original endosymbiotic event in algae and have undergone sequential transfer to the nuclear genome (5). It is unclear why the *accD* gene was retained in the plastid. In *E. coli*, the CT subunits have been suggested to regulate their own gene expression by binding the mRNAs that encode the subunits (31). Perhaps retaining the *accD* gene in the plastid allows the plant to partially maintain this form of transcriptional regulation. However, this function must not be essential, as evidence of stochastic *accD* gene transfer to the nucleus has been observed for some land plant species (32-38).

2.0 Genetic regulation

2.1 htACCase gene expression in plants

The genes for htACCase subunits are expressed in all plant tissues, though at different levels. Steady-state transcript levels are most abundant in developing seed,

during which transcript levels of htACCase, as well as many other FAS enzymes, follow a bell-shaped curve that crests between 8 and 11 days after flowering (DAF) (39). This precedes the maximal accumulation of seed oil, which occurs between 9 and 13 DAF (39).

One of the contributors to the increase in FAS gene expression during seed filling is the transcription factor WRINKLED1 (WRI1). The *wri1* mutant was first isolated in Arabidopsis by Focks and Benning, and was later shown to encode an APETALA2/ ethylene-responsive element-binding protein (40,41). Further study showed that WRI1 is responsible for increasing the expression of at least 18 genes involved in FAS (39,40). Of these, only the BCCP2 subunit gene of htACCase is significantly induced (39,42). Gene expression is directly affected by binding of WRI1 to an 'AW box' in the promoter region of the BCCP2 gene (42,43). Interestingly, the promoter region of the BC and α-CT genes also contain this AW box and can be bound by WRI1 (42). However, BC and α-CT expression is unchanged in *wri1* mutant and WRI1 overexpression lines, suggesting that other cis-elements might be involved in expression of these genes (42). It should also be noted that WRI1 can affect htACCase activity by regulating the expression of genes required for biotin synthesis (44).

2.2 Genetic attempts to modulate htACCase gene expression

As the committed step of *de novo* FAS, ACCase is considered the gatekeeper for carbon flow into this pathway. Thus increasing ACCase levels, and ultimately activity, may enhance flux through this pathway. For example, overexpression of all four htACCase subunits in *E. coli* resulted in an approximate 100-fold and six-fold increase in malonyl-CoA production and FAS rate, respectively (12). This result confirms that

increased htACCase activity does increase carbon flux through FAS in a model bacterium. The situation in plants, however, is still unclear.

Attempts to increase fatty acid synthesis by modifying htACCase gene expression have had mixed results. Overexpression of the BC subunit had no significant effect on *de novo* FAS and did not result in a concomitant increase in BCCP protein levels, providing the first clue that up-regulation of any one catalytic subunit does not result in a compensatory increase in other catalytic subunits (45). In contrast, overexpression of β-CT in tobacco led to increased expression of the other catalytic subunits to the htACCase. However, this did not significantly enhance seed oil content, suggesting that post-transcriptional regulation might be another important layer governing overall htACCase activity (46). It is worth noting the β-CT overexpression lines did produce approximately double the amount of seeds per plant.

Both seed-specific overexpression and constitutive reduction of the BCCP2 subunit in Arabidopsis unexpectedly produced similar results. Down-regulation of BCCP2 by antisense silencing led to an average 9% reduction in total seed oil content (47). In addition, overexpression of the BCCP2 subunit led to a reduction in seed oil content (23%) associated with incomplete biotinylation of overexpressed BCCP2. Over half of the BCCP2 protein present in developing siliques was in the non-biotinylated, apo form, resulting in a 65 percent reduction in htACCase activity. Quantitative immunoblot analysis of the BCCP2 overexpression lines showed that expression of the other catalytic subunits to htACCase did not significantly change in abundance, while the biotin synthesis pathway was up-regulated at both the transcript and protein levels (48). Additionally, an uncharacterized protein annotated a “biotin attachment domain-

containing" protein was upregulated at both the transcript and protein levels. This uncharacterized protein is discussed further in section 3.4 on regulatory proteins for htACCase. These observations illustrate the importance of the biotin synthetic pathway in htACCase function and the necessity for a fully biotinylated BCCP for proper htACCase function. In addition, this study confirmed results from Shintani et al., 1997 that upregulation of a single nuclear-encoded ACCase subunit does not produce a compensatory increase in any of the other subunits to the complex.

Analysis of BCCP1 and BCCP2 T-DNA lines in Arabidopsis determined the functional redundancy of the two isoforms to be unidirectional (49). Lack of BCCP2 expression results in no obvious phenotype, while marginal reduction of BCCP1 expression results in a number of defects including reduced growth and increased seed abortion (49). Furthermore, complete loss of BCCP1 expression appears to be lethal. The lack of functional redundancy can be explained in part by the seed-specific nature of BCCP2 expression. Additionally, BCCP1 appears to comprise a majority of the total BCCP pool in developing siliques with an estimated BCCP1:BCCP2 ratio of 5:1 (49).

2.3 RNA editing of accD (β-CT)

RNA editing of plastid-localized *accD* gene encoding the β-CT subunit has been shown to be important for CT activity. The conversion of a specific base, C794 (for the Arabidopsis gene), to U converts the original Ser codon to Leu. Recombinant β-CT translated from unedited mRNA causes loss of CT activity *in vitro* (50). The presence of a Leu codon at this position in *E. coli* and some plants suggests that this amino acid plays a critical role in structure or function (51). Multiple RNA editing proteins have been

observed to edit β-CT in Arabidopsis (51-54), further highlighting the role this modification has for proper CT activity.

3.0 Biochemical regulation

Many different forms of biochemical regulation have been discovered for htACCase in plants, reflecting its critical role as the committed step in the *de novo* FAS pathway.

3.1 Light activation (or dark de-activation)

In leaves, *de novo* FAS is strictly dependent on light (55,56). Likewise, the activity of htACCase in leaves increases about three-fold within minutes of plastid illumination (55). Many changes occur in the plastid upon light adaptation, including an increase in pH from 7.1 to 8, increased thioredoxin activity, as well as increased concentrations of ATP, NADPH, and magnesium chloride (57). Of these changes, two separate studies observed that thioredoxin activity (58) and pH change (59) had the most significant effect on htACCase activity. Though it should be noted that ATP is a substrate for ACCase, and reductant (both NADH and NADPH) is required for each two carbon extension during FAS. The availability of each of these metabolites increases during photosynthesis. However, these regulatory mechanisms only apply to plastids in the leaves. Plastids in other tissues, such as roots are not photosynthetic, and therefore likely control d*e novo* FAS rates and htACCase activity through different regulatory mechanisms.

3.2 Feedback inhibition by acyl-acyl carrier protein

The final product of *de novo* FAS, acyl-acyl carrier protein (ACP), has been observed to have an effect on htACCase activity in *E. coli* (60,61) and *Brassica napus* (62). In *B. napus*, inhibition was most strongly exerted by the final product of plastidial *de novo* FAS, 18:1-ACP. In contrast, inhibition in *E. coli* was exerted by acyl-ACPs of various chain lengths from short (C6) to long (C20) (61). Acyl-ACP acts as a mixed inhibitor of htACCase under varying acetyl-CoA concentrations in *E. coli* (61). This finding suggests that feedback inhibition is at least partially exerted through competitive interaction with the acetyl-CoA binding site on CT. In addition, acyl-ACP likely binds to an allosteric site on htACCase, but a specific interaction with a subunit of the complex has not yet been identified.

3.3 Redox regulation

As mentioned previously, thioredoxin has been shown to increase htACCase activity *in vitro* (58). When htACCase was partially purified from pea chloroplast lysates, enzyme activity increased up to seven-fold in the presence of the reducing agents DTT or thioredoxin f (AT3G02730) (58). In a different study, when crude chloroplast lysates from spinach were assayed, pH was observed to have a greater effect on htACCase activity than reductant (59). This was resolved by further analysis of htACCase activity in spinach chloroplast lysates, whereby DTT was shown to double enzymatic activity when htACCase activity was initially low. It was later shown that redox regulation of ACCase resides with the CT half reaction through a regulatory disulfide bond , specifically Cys-267 and Cys-442 of the *Pisum sativum* α-CT and β-CT, respectively (63). This CT disulfide bond was observed *in vivo* and was more prevalent in dark versus light conditions, suggesting CT reduction enhances htACCase activity.

3.4 Regulatory proteins

Recently, two proteins have been shown to directly interact with the BCCP subunit. The first interaction has been observed in both plants and *E. coli* and involves the PII (AT4G01900) (64) and orthologous GlnB (65) proteins, respectively. PII is a small, homotrimeric protein involved in the regulation of nitrogen metabolism by acting as a 2-oxoglutarate sensor (66). Further analysis of this interaction determined that PII has a negative effect on htACCase activity, dependent on ATP; ATP is not consumed but must bind to the homotrimer to be active. Activated PII binds to the biotin moiety of BCCP, reducing the V_{max} of htACCase by up to 50 percent, based upon *in vitro* activity assays (67). This reversible interaction is relieved by 2-oxoglutarate binding as well as uridylylation of the PII monomers (67). In plants, PII inhibition was also relieved by oxaloacetate and pyruvate (64). This last finding is important for regulation of htACCase in the plastid, whereby high pyruvate concentrations would lead to increased acetyl-CoA substrate for the enzyme through the action of the plastid pyruvate dehydrogenase complex (pPDC). Therefore PII appears to integrate both nitrogen and carbon metabolism by sensing both 2-oxoglutarate and pyruvate, respectively, as well as energy status (ATP/ADP ratio).

The second interaction involves a family of proteins annotated as “biotin attachment domain-containing” and are thus abbreviated as BADC. We recently observed these proteins to co-immunoprecipitate with htACCase from Arabidopsis crude chloroplast extracts (Chapter II). Through subsequent yeast two-hybrid analysis and co-purification in *E. coli*, a direct interaction between BADC and the BCCP subunit of htACCase was observed (Chapter II). The BADC proteins were previously observed to

localize to the plastid and co-elute with htACCase by size-exclusion chromatography, among a collection of other proteins (68). The BADC proteins are a family of three in Arabidopsis that share 25 to 30 percent amino acid sequence identity with the BCCP isoforms. Despite the similarity to BCCP proteins, BADCs lack the canonical biotinylation motif (AMKL) and were not observed to be biotinylated *in vivo* (Chapter II). BADC genes are present only in green algae and land plant species that contain htACCase, suggesting that BADC function is linked to htACCase. Although prokaryotes do not contain BADC genes, expression of Arabidopsis BADC protein in *E. coli* was shown to significantly reduce htACCase activity (Chapter II). The mechanism of BADC inhibition of htACCase activity is still unknown.

3.5 Membrane association and non-catalytic domains of plant CT subunits

Multiple studies have observed an association of the htACCase with the plastid inner envelope membrane (24,27,69,70). Further biochemical analysis demonstrated this envelope membrane association to be specific to the CT subunits (69). Although no specific protein-protein interaction or acyl modifications have been identified, the CT subunits interact through a non-ionic mechanism as salt washing was unable to abrogate this association (69). In Arabidopsis, both α- and β-CT proteins contain large, non-catalytic domains which are not found in prokaryotic orthologs and have no known function. For α-CT, this approximately 300 amino acid non-catalytic domain is located at the C-terminus and is predicted to contain coiled-coil structure. For β-CT, the domain is at the N-terminus and is approximately 200 amino acids in length. Removal of these domains does not affect CT activity *in vitro* (63). Thus these domains may serve a

regulatory function, and could be involved in the interaction with the plastid envelope membrane.

3.6 Post-translational modifications

Other than the disulfide bridge for CT and biotinylation of BCCP, only two other types of post-translational modifications (PTMs) have been observed on any of the subunits to a plant htACCase. Ser phosphorylation was observed for the pea β-CT subunit (71), although the specific site was not determined. It was noted that β-CT phosphorylation was more prevalent under illuminated conditions. Dephosphorylation of pea chloroplast extracts also caused reduced CT activity, suggesting that phosphorylation has a positive effect on htACCase. Additionally, phosphorylation was observed on three 2D gel spots corresponding to α-CT in Arabidopsis (72); and three separate phosphoproteomic studies identified phosphorylation on sites Ser741 and Ser744 of the Arabidopsis α-CT (73-75). These phosphorylation sites are contained in the non-catalytic C-terminal domain of α-CT. The role of these phosphorylation events is unknown. One possibility could be that phosphorylation in the coiled-coil domain of α-CT may affect protein-protein interactions.

Glutathionylation of htACCase has also been observed on the BCCP subunit for *C. reinhardtii* (76) and the BC subunit in Arabidopsis (77). No functional role has been discovered for this PTM. However, it is thought that one of the prominent roles of glutathione is to protect proteins from irreversible oxidation under stress conditions (78). Due to the potential for buildup of reactive oxygen species in the plastid, this PTM might increase the longevity of the htACCase.

4.0 Structural insights from *E. coli* htACCase

4.1 Crystal structures of the BC-BCCP and CT subcomplexes

At present, our structural understanding of the htACCase is based entirely on the *E. coli* model. The crystal structure of the BC-BCCP subcomplex indicated it is a heterooctomer comprised of two BC dimers and four BCCP monomers, producing a 1:1 stoichiometry and four potential active sites (79). In contrast, proteomics (80,81), *in vivo* labeling (82), and ribosome profiling studies (83) have observed a BC-BCCP ratio of 1:2, respectively. The conflicting crystal structure could be due to the use of artificial translation initiation sites that allowed for abnormal subunit expression and complex formation. In both cases, four biotinyl sites are present in the BC-BCCP subcomplex (Figure 2).

The CT subcomplex from *E. coli* was determined to be a $\alpha_2\beta_2$ heterotetramer (20). Each pair of CT subunits shares a single active site, where α-CT binds carboxybiotin and β-CT binds acetyl-CoA. The β-CT subunit in prokaryotes and plants contains a Zn binding motif that is an atypical Cys4 'zinc ribbon' and functions as a DNA-binding domain (20,84). Thus CT has three binding ligands: DNA, acetyl-CoA, and carboxybiotin. Ligand binding is competitive, whereby DNA binding prevents acetyl-CoA and carboxybiotin binding, and vice versa (84). This Zn binding motif has also been observed to act as an active-site 'lid' in tRNA synthetases (85-87). The Zn motif in β-CT is near the active site and, when removed, abolishes CT activity (63), suggesting it also plays a role in CT catalysis.

4.2 BCCP dimerization

Dimerization of the BCCP subunit has been shown in *E. coli* and was discovered through the unexpected finding of apo-BCCP rescuing a temperature-sensitive (Ts) BCCP mutant. In this study, the L8 strain of *E. coli* contained a temperature-sensitive (Ts) mutation in *accB,* creating a BCCP protein that is unstable at 37 °C. As a result, these cells lacked ACCase activity and showed no growth in minimal media (88). Unexpectedly, expression of an apo-BCCP mutant protein whereby the biotinyl Lys was replaced with a Cys or Arg, complemented the Ts BCCP due to partial restoration of ACCase activity. This was attributed to a stabilization effect on Ts BCCP and suggested that BCCP actually functions as a dimer. This finding may be critical in the understanding of htACCase regulation. With the discovery of BADC proteins that interact with BCCPs, it is likely that these proteins can form heterodimers with a regulatory function. In even the simplest context for Arabidopsis, many possible heterodimers could form between the three BADC isoforms and the two BCCP isoforms present in that species; and the combinatorial possibilities are much higher in polyploid crops. Incorporation of these heterodimers could lead to many variations in htACCase activity allowing for fine-tuned control of the enzyme and FAS pathway.

4.3 Thumb domain of BCCP

The BCCP subunit also contains a 'thumb' domain that is essential for BCCP function (88). This domain spans ten residues (T90-E100, *E. coli* numbering) and is only conserved in biotin-dependent carboxylases that catalyze malonyl-CoA synthesis. Site-directed mutations to the thumb domain severely reduced htACCase activity, suggesting that it acts as a lid for the BC active site during biotin carboxylation and is an important

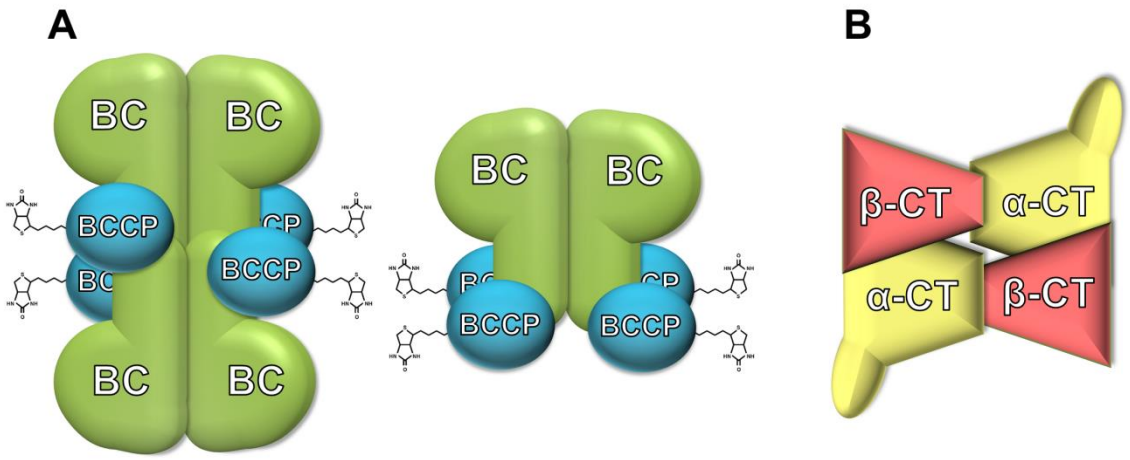

Figure 2. **Subcomplexes of htACCase.** The structure of whole htACCase in plants is still unclear, but is known to consist of two separate subcomplexes. **A** The bacterial literature provides evidence of a BC-BCCP subcomplex consisting of a 1:1 ratio (left) or a 1:2 ratio (right) (79-83). In both cases, the subcomplex contains four biotin cofactors available for carboxylation. **B** The CT half reaction is a heterotetramer containing two α- and β-CT subunits (20).

structural component of BCCP function. The BADCs, which share 25 to 30 percent identity with BCCP, have a modified thumb domain that is three residues longer and contains six more basic residues than BCCP. This difference might play a role in BADC function.

4.4 The in vivo htACCase complex is larger than its calculated size

Multiple studies have observed that native htACCase can form large complexes *in vivo* (Table 1). The *E. coli* BC-BCCP subcomplex was observed to be approximately 640 kDa by size exclusion chromatography (SEC) (79). Pea htACCase was observed to be 650-700 kDa in size by gel filtration (24). In soybean, BC-BCCP and CT subcomplexes were observed to be approximately 800 and 600 kDa, respectively, even under high salt (0.5M KCl) concentrations (17). Finally, the Arabidopsis htACCase subunits were identified in the 1-2 MDa range by SEC (68). Variations in the technique used could explain the differences observed, but in all cases the observed size of the plant htACCase and its subcomplexes were larger than expected based upon structural predictions from bacterial models. Assuming the BC-BCCP subcomplex has a 1:2 ratio and the CT subcomplex is a heterotetramer, the approximate size for the Arabidopsis BC-BCCP and CT subcomplexes should be 190 kDa and 270 kDa, respectively. Therefore, htACCase may form larger oligomers, interact with another large complex, or contain additional factors. Perhaps higher order structure of plant htACCase occurs through the plant-specific coiled-coil domains of α-CT. Additionally, other proteins may be involved in these large complex formations. The previously identified interactors with htACCase, PII and BADC, are small proteins and by themselves could not account for

Subunit	Gene name		Apparent protein mass (kDa)*	
	E. coli	*A. thaliana*	*E. coli*	*A. thaliana*
Catalytic subunits				
BC	*accC*	*CAC2*	50[3]	51[69]
BCCP1	*accB*	*CAC1A*	23[22]	38[69]
BCCP2	-	*CAC1B*	-	25[89]
α-CT	*accA*	*CAC3*	35[23]	97[69]
B-CT	*accD*	*accD*	32[23]	86[69]
Regulatory subunits				
PII	*GlnB*	*GLB1*	17[67]	18[127]
BADC1	-	*BLP3*	-	30
BADC2	-	*BLP1*	-	29
BADC3	-	*BLP2*	-	27

Complex	Observed mass (kDa)†	
	E. coli	Plant
BC-BCCP	640[83]	800[16]
CT	130[20]	600[16]
htACCase		>1,000[68]

Table 1. **Observed mass of the htACCase complex and individual subunits.** The accepted gene names and apparent protein mass for each catalytic and regulatory subunit of htACCase are shown. The observed mass for the htACCase complex as well as its constituent subcomplexes are also noted. References are denoted in superscript. *Apparent mass observed by SDS-PAGE. †Observed mass by size-exclusion chromatography.

the large complexes observed. It is possible that other large multienzyme complexes, such as the pPDC or fatty acid synthase, interact with htACCase and contribute to the MDa complex. Indeed, the E2 subunit of pPDC was observed to co-elute with htACCase by SEC (68).

5.0 Concluding remarks

It is clear based on the research summarized here that the htACCase is an important multienzyme complex with diverse regulatory properties (Figure 3). The discovery of new, interacting proteins with regulatory implications is particularly intriguing and suggests there is much more to understand about this key step in *de novo* FAS. We highlight some of the major unanswered questions here.

First, many details of the htACCase complex assembly remain unknown. Although progress has been made in understanding bacterial subunit stoichiometry, the nature of the plant complex is still unclear. Additionally, in organisms that contain multiple copies of each gene, like soybean, do the different copies play distinct roles? This appears to be true for the two BCCP isoforms which show different expression patterns (39,89). The formation of complexes containing BCCP1 or BCCP2 might behave very differently, as reported for *in vitro* activity assays (89), but this has yet to be determined *in vivo*.

Second, the mediation of feedback inhibition on htACCase is still unknown. A direct interaction between acyl-ACP and htACCase has yet to be identified. It is possible that the interaction has remained hidden due to the small size of the ACP, making it difficult to observe with typical tryptic digestion-based proteomic procedures. At present, there

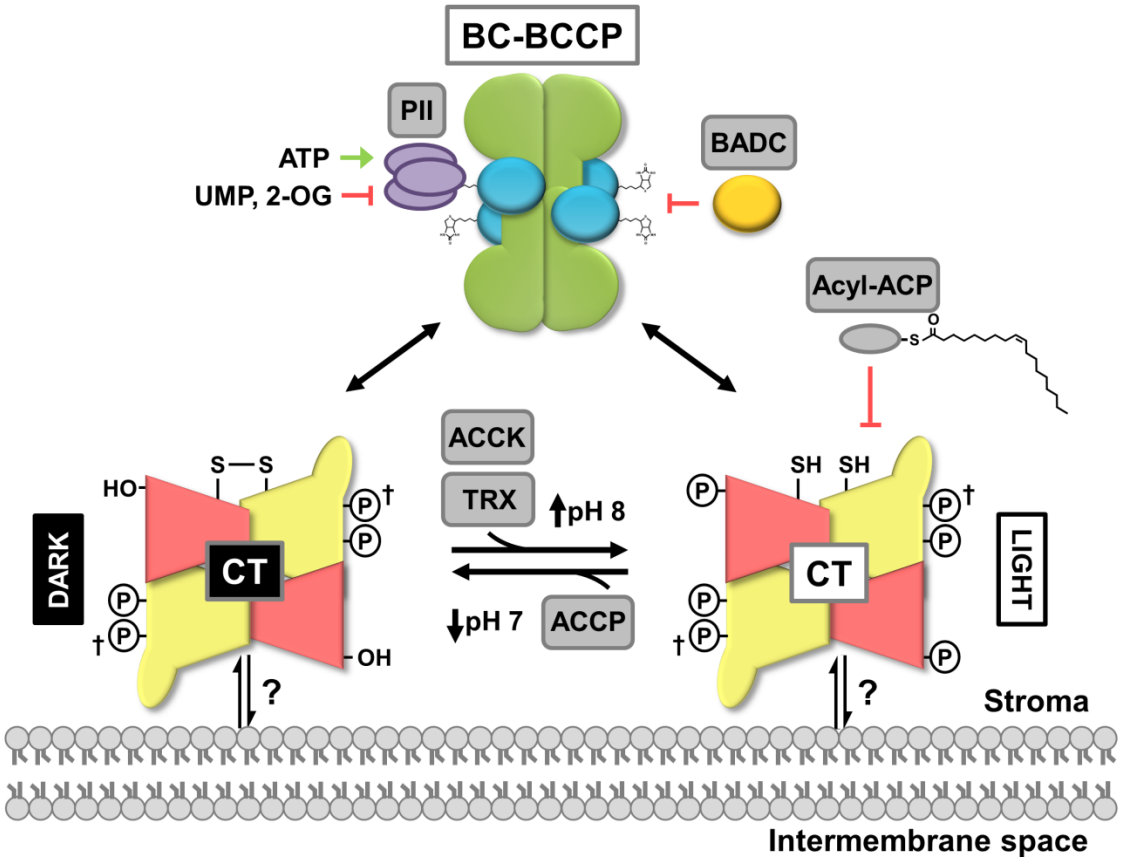

Figure 3. Regulatory factors affecting heteromeric ACCase in plants. Diagram shows the known factors that affect htACCase activity. Effector proteins are labelled in grey. The BC-BCCP subcomplex (top) can be inhibited by PII and BADC proteins. For this diagram, the BC:BCCP ratio was assumed to be 1:1. The two CT subcomplexes depict the known changes due to light exposure. In the dark (bottom left), a disulfide bond links the α (yellow) and β (salmon) subunits and the β subunit is not phosphorylated. In the light (bottom right), the disulfide bond is reduced by TRX and the β subunit is phosphorylated, resulting in a more active complex. Acyl-ACP exerts feedback inhibition on the CT subcomplex. Unknown factors are denoted by: ?, CT associates with the inner envelope through an unknown non-ionic interaction; †, light-dependency of α-CT phosphorylation is unknown. Abbreviations: BC, biotin carboxylase; BCCP, biotin carboxyl carrier protein; BADC, biotin/lipoyl attachment domain containing protein; ACP, acyl carrier protein; 2-OG, 2-oxoglutarate; ACCK, kinase of htACCase; TRX, thioredoxin; ACCP, phosphatase of htACCase; CT, carboxyltransferase.

is still the possibility that other factors could be required to mediate feedback inhibition. This information will be valuable to implement biotechnological strategies aimed at preventing feedback inhibition of htACCase.

Third, the membrane association of the CT subunits has yet to be fully understood. Although multiple groups have observed the interaction with the plastid envelope (24,27,69,70), there is no evidence for a direct protein-protein interaction with a membrane protein. The CT subunits have also not been identified to contain any acyl modifications that would allow for incorporation into the membrane. Due to the implication of other FAS enzymes that associate with the inner envelope (90-92), membrane association may allow for metabolon formation and substrate channeling to occur. Indeed, the stromal concentrations of acetyl-CoA and other FAS intermediates in the plastid were calculated to be insufficient to account for the observed FAS rates, suggesting that substrate channeling likely occurs *in vivo* (93). Metabolon formation might also account for the over 1 MDa observed size of htACCase *in vivo*. Further research is required to address this topic.

CHAPTER II

DISCOVERY AND CHARACTERIZATION OF NOVEL REGULATORS TO THE HETEROMERIC ACETYL-COA CARBOXYLASE: THE ‘BIOTIN/LIPOYL ATTACHMENT DOMAIN CONTAINING’ PROTEIN FAMILY

The following chapter is adapted from a publication to submitted to
The Plant Cell

Title: The BADC proteins – negative regulators of heteromeric acetyl-CoA carboxylase from autotrophs

Authors: Matthew J. Salie, Ning Zhang, Veronika Lancikova, Dong Xu, Jay J. Thelen

Author contributions: MJS designed and performed the experiments, and wrote the manuscript. NZ and DX performed the evolutionary analysis. VL performed the qPCR and RT-PCR analysis. JJT conceived the idea for the project, and wrote the manuscript with MJS.

ABSTRACT

Acetyl-CoA carboxylase (ACCase) catalyzes the committed step of *de novo* fatty acid synthesis and regulates flux through this central metabolic pathway. In prokaryotes, green algae, and most plants, this enzyme is a heteromeric complex requiring four different subunits for activity. The plant complex is recalcitrant to conventional purification schemes and hence the structure and composition of the full assembly is unknown. *In vivo* co-immunoprecipitation using subunit-specific antibodies identified a novel family of proteins in *Arabidopsis thaliana* annotated as 'biotin/lipoyl attachment domain containing' (BADC) proteins. Results from yeast two-hybrid and co-expression in *Escherichia coli* confirmed that all three BADC proteins interact with the two biotin carboxyl carrier protein (BCCP) isoforms of Arabidopsis ACCase. These proteins resemble BCCP (25-30% sequence identity) but are not biotinylated due to a mutated biotinylation motif. We demonstrate that BADC proteins significantly inhibit ACCase activity in both *E. coli* and *A. thaliana.* We conclude the BADC proteins are negative regulators of ACCase, and propose a functional model.

INTRODUCTION

Plant oils are an important renewable source of hydrocarbons for food, energy, and industrial feedstocks(94,95). Acyl chains stored as triacylglycerol are produced by the *de novo* fatty acid synthesis (FAS) pathway. The committed step of *de novo* FAS is catalyzed by the heteromeric acetyl-coenzyme A carboxylase (htACCase) which carboxylates acetyl-CoA to form malonyl-CoA in a two-step reaction requiring ATP, bicarbonate, and biotin cofactor. In prokaryotes, and in plastids of dicots and non-

graminaceous monocots, htACCase is a complex requiring four distinct subunits: biotin carboxylase (BC), biotin carboxyl carrier protein (BCCP), and α- and β-carboxyltransferase (CT) (3,96). Graminaceous monocots possess a homomeric form of plastid ACCase wherein the catalytic components are fused in tandem as a single polypeptide. A homomeric form of ACCase has also been identified in the plastid of dicot species (10), but its metabolic role is still unclear. Structural models for the plant htACCase are based on the *Escherichia coli* homolog. The *E. coli* htACCase is composed of two enzymatic subcomplexes: an α/β-CT heterotetramer and a BC/BCCP heterooctamer (11,16,69,97). The components of each subcomplex form stable associations while the two subcomplexes themselves show a relatively weak interaction with one another. This property has contributed to the difficulties in biochemical and structural characterization of htACCase from plants.

As expected for the first irreversible step in a pathway, regulation of the plant htACCase is sophisticated. First, htACCase is activated by light, during which activity increases several fold in the plastid. This activation occurs within minutes and is reportedly due to the increase in stromal pH from 7.0 to 8.0 (59) and thioredoxin-dependent reduction of a disulfide bond in CT (58,63). Second, htACCase activity is suppressed by feedback inhibition through increased levels of acyl-acyl carrier protein (61,62). Third, an interaction between htACCase and a 2-oxoglutarate-binding protein PII reduces htACCase activity (64). Recombinant PII protein was shown to pulldown BCCP from chloroplast lysates in the absence of 2-oxoglutarate, likely through a direct interaction with the biotin cofactor. Addition of 2-oxoglutarate abrogated the interaction.

Lastly, two types of BCCPs were identified in plants and have been shown to be under different transcriptional control (89). The BCCP1 isoform is constitutively expressed in all organs and tissues analyzed, while BCCP2 is predominantly expressed in the seed under the control of the WRINKLED1 transcription factor (28,39). Of these two isoforms, BCCP2 was shown to be more active *in vitro* (89).

Additional properties of the plant htACCase suggest additional, non-catalytic components may be involved in function or regulation. For example, the observed size of the plant htACCase complex is larger than the calculated mass of the known subunits (17,68). Additionally, the α- and β-CT subunits contain large domains of 200 to 300 residues which are not required for catalytic activity, are not present in prokaryotic orthologs, and have no known function (11,63). In α-CT, this domain contains three strongly predicted coiled-coil regions which are often involved in protein-protein interactions (98). Previous observations showed a strong, non-ionic association between the CT subcomplex and the plastid inner envelope, though the mechanism and potential mediating factor has yet to be determined (69). The a-CT subunit is phosphorylated on multiple sites (Ser^{741}, Ser^{744}, Ser^{755}, Ser^{756}, Ser^{758}) and may be associated with light activation (59). Finally, with some exceptions (32-34,36-38) the genes encoding the subunits to the plant htACCase reside in both the nuclear and plastid genomes (16). Collectively, these regulatory, structural, and genomic observations suggest that this enzyme may possess additional, non-catalytic factors to facilitate the various forms of regulation. To discover novel interactors with htACCase, we employed co-immunoprecipitation coupled with liquid chromatography-tandem mass

spectrometry (LC-MS/MS). The results we present here show a family of uncharacterized genes, annotated to encode “biotin attachment domain-containing (BADC)” proteins interact with and inhibit htACCase activity in both *E. coli* and *A. thaliana*.

RESULTS

Two novel proteins, BADC1 and BADC2, co-immunoprecipitate with htACCase - To discover unknown protein interactors with the htACCase, quantitative co-IP analyses were performed. Clarified chloroplast lysates from 14-d-old *A. thaliana* seedlings were incubated with Protein A-Sepharose beads coated with polyclonal antibodies against either BCCP2 or α-CT. Control precipitations were performed using uncoated beads. Precipitated proteins were identified by LC-MS/MS analysis of trypsin-digested peptides. A protein was considered a putative interactor if it was identified in control samples less than half of the number of times it was identified in trial precipitations (eg 2 control identifications and 5 trial identifications). In this way, naturally abundant proteins that would be present in the control but might also interact with htACCase were not excluded. Comprehensive lists of putative interacting proteins are shown in Table 2 and Table 3. From thirteen biological replicates of the α-CT co-IPs, all four catalytic subunits to the htACCase complex were identified. Likewise, all catalytic subunits, except β-CT, were identified from co-IPs with antibodies against BCCP2 (Fig. 4A and 4B). As expected, the BC/BCCP and α/β-CT subcomplexes were more abundant in the BCCP2 and α-CT co-IPs, respectively. Additionally, two proteins of unknown function containing a

presumptive “biotin attachment domain-containing” region, hereafter termed BADC1 (AT3G56130) and BADC2 (AT1G52670), were identified from both sets of co-IPs. The BADC1 protein was present in seven and one replicate of the BCCP2 and α-CT co-IPs, respectively, while BADC2 was present in six and two replicates of the BCCP2 and α-CT co-IPs, respectively. The BCCP1 protein was present in seven and seven replicates of the BCCP2 and α-CT co-IPs, respectively, while BC was present in seven and nine replicates of the BCCP2 and α-CT co-IPs, respectively. The normalized, relative abundance of BADC proteins was more commensurate with BC and BCCP abundance than α and β-CT from both co-IP analyses. Reciprocal co-IPs using antibodies specific to BADC1 and BADC2 precipitated both BCCP isoforms (Fig. 4C and 4D). Thus, BADC1 and BADC2 appear to preferentially interact with the BC/BCCP component of htACCase.

Yeast two-hybrid and heterologous co-expression confirm direct interactions between BADC and BCCP isoforms from A. thaliana - To confirm the co-IP results and directly determine which htACCase subunit interacts with BADC1 and BADC2, targeted yeast two-hybrid analysis was employed. In addition to the two experimentally-identified BADCs we also tested a third, putative BADC isoform, termed BADC3 (AT3G15690) identified by BLAST interrogation of the *A. thaliana* genome. This protein shares 61% amino acid sequence identity with BADC2, suggesting similar function. Yeast two-hybrid analyses showed each of the three BADC proteins interacted with each BCCP isoform (Fig. 5A). Additionally, the BADC isoforms are capable of interacting with each other.

To further verify the interaction between BADC and BCCP, *A. thaliana* BCCP1 was co-expressed with each of the three *A. thaliana* BADC proteins in *E. coli*. In these experiments, either the BADC or BCCP1 protein was expressed with a His_6-tag, while the other contained no affinity tag. When the His_6-tagged protein was purified by Ni^{2+}-NTA affinity chromatography, the respective "untagged" protein was present in the same elution fractions (Fig 5B). As a control, it was verified that untagged proteins were unable to bind to the affinity column. This approach confirmed the interaction between BADC and BCCP isoforms.

Biotin is not required for BADC-BCCP interaction – To determine if the BCCP-BADC interaction involves the biotin cofactor, as previously reported for PII interaction with htACCase (67), the biotinyl Lys245 residue on BCCP1 was mutated to Arg by site-directed mutagenesis. This mutation prevents biotinylation of BCCP1 (Fig. 11A). Using this 'apo-BCCP1', we repeated yeast two-hybrid and co-expression analysis with BADCs. All BADC isoforms were shown to interact with apo-BCCP1 (Fig. 11B, 11C).

Recombinant AtBADC1 and AtBADC3 form homodimers through a disulfide bond – Previous analysis of *E. coli* BCCP suggested that this subunit forms functional homodimers *in vivo* (88). Through intact mass analysis of purified recombinant BCCP2, we observed that plant BCCP can also form homodimers (Fig. 12A). In addition, analysis of recombinant BADCs showed that BADC1 and BADC3, but not BADC2, can form homodimers (Fig. 12A). The observed monomer size for each BADC was in agreement with the predicted mass, suggesting these proteins are unmodified. In the absence of DTT, purified recombinant BCCP2, BADC1, and BADC3 show a monomer

and dimer band when denatured and resolved by SDS-PAGE (Fig. 12B). Recombinant BADC2 shows only a monomer band. Increasing DTT concentration led to the disappearance of the dimer band, suggesting a disulfide bond is involved in dimer formation of BADCs and plant BCCPs.

The mature primary sequence of the BADC proteins from *A. thaliana* contains only two or three Cys residues. Of these, only one Cys residue is conserved in BADC1 and BADC3, but not BADC2 (Fig 12C). This Cys residue is likely involved in disulfide bond formation. Similarly, the BCCP subunits contain a conserved Cys residue fifteen residues downstream that is also likely involved in disulfide bond formation (Fig. 12C).

BADCs resemble BCCPs but are not biotinylated – The ability to form homodimers is a shared characteristic between BADCs and BCCPs. Interestingly, the three BADC isoforms share many other characteristics with the two BCCP isoforms from *A. thaliana.* Firstly, these proteins contain a canonical plastid target peptide and are plastid localized based upon proteomic analysis of purified chloroplasts (68). Secondly, the BADC isoforms share 24 to 29% amino acid sequence identity with the BCCP isoforms (Fig. 14). Lastly, structural predictions of the BADC and BCCP proteins show similar β-sheet secondary structure with a characteristic 'thumb motif' as previously observed for the *E. coli* BCCP (88)(Fig. 13). Despite these similarities, the BADC proteins lack the canonical biotinylation motif (Fig. 6A). The tetrapeptide (Ala/Val)-Met-Lys-(Met/Leu) is the known biotinylation motif and is usually located 34 or 35 residues from the C-terminus (99,100). The BADC proteins do, however, possess a conserved Lys residue in a similar (Val/Ile)-(Leu/Val)-Lys-(Leu/Ile) motif located near the C-terminus

suggesting the possibility of a non-canonical biotinylation motif. To test this possibility, we purified recombinant BADC proteins expressed in *E. coli* and the native BADC1 protein from *A. thaliana* seedlings, and probed for biotinylation using a biotin-specific antibody (Fig. 6B and 6C). Results of these experiments confirmed that the BADC proteins are not biotinylated *in vivo*, unlike BCCP controls.

Identification of BADC orthologs and co-occurrence analysis suggests BADCs first appeared in red algae – The evidence of a direct BADC-BCCP interaction suggests that BADC function is linked to htACCase. If true, orthologs to *A. thaliana* BADCs (AtBADC) would be found only in organisms that contain the heteromeric form of ACCase, not the homomeric form that predominates in eukaryotes. To search for the presence of AtBADC orthologous proteins, the primary sequence of each AtBADC was used to search against the KEGG Sequence Similarity database (101). Putative orthologs were confirmed by reciprocal BLAST searches against the *A. thaliana* proteome. All AtBADC orthologs lacked the conserved biotinyl Lys found in BCCPs. In total, 30, 7, and 31 orthologous proteins were identified for AtBADC1, AtBADC2, and AtBADC3, respectively, across 36 different species of dicots, non-graminaceous monocots, and algae (Fig. 15). The full-length protein sequences of identified AtBADC orthologs were used to generate a maximum-likelihood phylogenetic tree (Fig. 15). Green algae contained orthologs to BADC3 alone. All of the species that harbor a putative BADC ortholog also contain the heteromeric form of ACCase. No BADC orthologs were detected in organisms that contain only the homomeric ACCase. Additionally, no BADC orthologs were detected in prokaryotes (both bacteria and

archaea), which also contain a heteromeric ACCase. The presence of orthologs in algae but not prokaryotes suggests that BADCs first appeared in algae.

To determine if BADCs arose from a previously functional BCCP in algae, co-occurrence analysis was performed. Figure 16 shows the species containing AtBCCP and/or AtBADC orthologs that were used in this analysis. With the exception of two red algae and *Cyanophora paradoxa* all species contained AtBCCP and AtBADC orthologs. In red algae, only one putative AtBADC1 ortholog (GenBank ID: XP_005708748.1) was identified in the species *Galdieria sulphuraria*. This protein shares the same number of identical (31) and conserved (46) amino acid residues with both AtBADC1 and AtBADC2, as well as 30 identical and 44 conserved amino acid residues with AtBADC3. However, the BLAST search attributed the highest score to AtBADC1, suggesting that this protein is an AtBADC1 ortholog. In addition, two putative BCCP proteins were identified in the red algae species *Chondrus crispus* and *Cyanidioschyzon merolae* to lack the biotin motif residue but shared higher sequence similarity to AtBCCP2 than AtBADCs (GenBank ID XP_005715802.1 and XP_005535248.1, respectively), which suggests that BADCs might have originated from BCCP gene duplication and loss-of-function mutation in red algae. From this observation we can infer not only that BADCs and BCCPs are related, but that the branch point between these proteins occurred in red algae. In particular, one of the few characterized red algae species contains BADC proteins, while glaucophytes, which are more ancient than red algae, do not have BADC.

BADC expression reduces htACCase activity in a temperature-sensitive E. coli mutant- Due to their similarity with BCCPs but lack of a conserved biotinylation motif it

was hypothesized that BADCs are negative regulators of htACCase activity. As *E. coli* contain htACCase but lack BADC orthologs, this was an appropriate system to test this theory *in vivo*. Growth assays in *E. coli accb* strain L8 were performed to evaluate the potential effect of the BADC proteins on htACCase activity. This strain has been studied in detail (22,88,102) and it is known that cell growth at 37°C is directly proportional to htACCase activity when lacking an exogenous source of fatty acids. This phenotype is due to temperature-sensitive (Ts) mutations in the BCCP gene (*accB*) that prevents *de novo* FAS. Experiments were performed in a minimal medium containing only glucose and glycerol as carbon sources. To complement the Ts phenotype, the native *E. coli* BCCP (EcBCCP) gene was cloned into L8 cells in a T7 polymerase expression system. Although this strain does not contain a T7 polymerase for optimal expression, a basal level of expression was observed by western blotting (data not shown). Expression of EcBCCP rescued cell growth at 37 °C in media lacking fatty acids while empty vector controls showed minimal growth (Fig. 7A). In the same way, the *A. thaliana* BADC3 gene was cloned into L8 cells and was unable to complement the Ts phenotype. BADC3 was chosen since it appears to be the founding member of the protein family based on phylogenetic analysis. However, co-expression of BADC3 with EcBCCP reduced the complementing effect of EcBCCP expression by approximately 72% after 23 h growth. Affinity pull down assays with tagged BADC3 confirmed the inhibition was mediated by interaction with EcBCCP (data not shown). This result demonstrated that the BADC proteins affect the ability of EcBCCP to form holo-ACCase complexes.

Recombinant BADC inhibits plant htACCase activity - To test if the BADCs can also inhibit plant htACCase, enzyme activity assays were performed on ten day-old *A. thaliana* silique extracts. The activity of htACCase was monitored *in vitro* by measuring the incorporation of $H^{14}CO_3$ into acid-stable products. Assays were performed in the presence of 10 μM recombinant BADC1, BADC2, BADC3, BCCP2, or apo-BCCP1 and compared to buffer control (WT). The average of four biological replicates showed that all three BADCs inhibited htACCase activity by 25 to 37%, while BCCP2, apo-BCCP1, and BSA showed no effect (Fig. 7B). These results, in addition to the *E. coli* expression results (Fig. 7A), confirm the BADCs can negatively affect htACCase activity.

Expression profiles of BADC and htACCase subunits respond differently to light – As mentioned previously, activity of htACCase is dependent on light. Absolute transcript levels of the BADCs and nuclear-encoded htACCase subunits were monitored in ten d old *A. thaliana* siliques to determine the effect of light on gene expression. Siliques were harvested after dark-adaption or exposure to various lengths of light. Quantitative PCR analysis of RNA extracts from these samples showed that htACCase subunit expression increases significantly in response to light. After six hours, expression of BCCP1, BCCP2, and α-CT increased approximately 15-fold, while BC expression increased 35-fold (Fig. 8A). Expression of the β-CT gene was not monitored due to its plastid localization. In contrast, BADC1 and BADC2 expression was reduced approximately ten-fold, while BADC3 expression increased eight-fold. Despite the conflicting changes in BADC isoforms, total BADC transcript level was reduced by half after six hours light exposure (Fig. 8B). The total BADC:BCCP transcript ratio is approximately 9:1 prior to

light exposure, and then shifts to almost 1:4 after six hours light exposure (Fig. 8B), suggesting that BADC protein levels are relatively greater than BCCP protein levels in the dark, and vice versa in the light.

Seed specific RNAi-silencing of BADC1 increases seed oil content in A. thaliana – Biochemical analysis showed that BADCs can function as negative regulators of htACCase. Therefore molecular genetic reduction of BADC expression *in planta* might increase htACCase activity. Since ACCase activity has previously been shown to correlate with seed oil content in transgenic lines altered in ACCase function (13,47), RNAi-silencing of BADC1 in *A. thaliana* using a seed-specific promoter was performed. Seed oil content analysis showed a significant increase in oil in three of six independent T_2 lines (Fig. 9A). Additionally, RT-PCR analysis of whole silique tissue showed a significant reduction in BADC1 transcript level of approximately 22% on average in the three lines containing significantly higher seed oil (Fig. 9B). The fractional silencing is partly due to the use of whole silique tissue instead of isolated seed for RT-PCR analysis. These results agree with those shown in Fig. 7, demonstrating that BADC proteins are negative regulators of htACCase.

DISCUSSION

The BADC proteins described here are annotated as proteins with unknown function. When mentioned in previous reports, these proteins were labeled as BCCP-'like' due to their sequence similarity with BCCP. The BADCs were observed to co-elute with *A. thaliana* htACCase during size-exclusion chromatography (68). These proteins were

also detected in pull-down experiments with 2-oxoglutarate-binding protein PII along with both BCCP isoforms in *A. thaliana* (64). In both cases, a direct interaction involving the BADCs was never established and a functional role was neither determined nor proposed. Here we present conclusive evidence that the BADCs not only directly interact with htACCase, but also function as negative regulators of this multienzyme complex. Thus we have termed them BADCs to avoid confusion with BCCPs. Three lines of evidence demonstrate these proteins are not functional BCCPs: 1) the BADCs are not biotinylated (Fig. 6); 2) BADC protein expression cannot complement the Ts BCCP in L8 *E. coli* (Fig. 7A); 3) addition of recombinant BADCs to *A. thaliana* silique extracts inhibits htACCase activity while biotinylated BCCP2 has no effect (Fig. 7B). Furthermore, seed specific silencing of BADC gene expression resulted in increased seed oil content (Fig. 9A). Therefore we conclude that the BADC proteins function as negative regulators of htACCase activity.

Current evidence suggests the BADCs function as competitive inhibitors of htACCase. Given the similarity of BADC and BCCP primary amino acid sequence (Fig. 14), predicted structure (Fig. 13), and dimerization capability (Fig. 12), a prevailing theory is the BADC proteins inhibit htACCase activity by competing with BCCP for binding to other ACCase subunits. The crystal structure of the *E. coli* BC/BCCP subcomplex consists of two dimers of BC held together by four BCCPs, thus having a BCCP:BC ratio of 1:1 (97). In contrast, proteomics (80,81), *in vivo* labeling (82), and ribosome profiling studies (83) have observed a BCCP:BC ratio of 2:1. Our co-IP experiments do not clearly distinguish between these possibilities in plants. In either

case, the subcomplex theoretically allows for the incorporation of up to four BADC proteins, and enables BADC proteins to exert concentration-dependent inhibition on htACCase. Assuming a BCCP:BC ratio of 1:1, we propose a model where multiple BC/BCCP/BADC subcomplexes can be formed (Fig. 10). Coupled with the observation that BADC proteins can interact with one another (Fig. 5A) it appears that minimally five different BC/BCCP/BADC subcomplexes are possible. With two BCCP and three BADC isoforms in *A. thaliana* the combinatorial possibilities increase exponentially. Such a mechanism would enable fine control of htACCase function through variable BCCP and BADC expression.

Since the BADCs resemble BCCP but are not biotinylated, a BC/BCCP/BADC subcomplex could be considered pseudo-poisoned. Natural examples of pseudo-poison complex regulation are rare; though at least one bioengineered example has been reported. Overexpressing BCCP2 in *A. thaliana* seed markedly reduced both htACCase activity and seed oil content due to increased levels of apo-BCCP (47,48). Pseudo-poisoned htACCase complexes were formed, reducing carbon flux through *de novo* FAS. This mechanism appears to be similar for BADC proteins, whereby they act as natural, apo-BCCP mimics and thus htACCase agonists. We can conceive of at least one advantage this novel form of metabolic regulation provides for *de novo* FAS. This proposed regulatory model would simplify the genetic control necessary for htACCase activity, as the cell would require strict control over only the BADC or BCCP genes rather than the entire complement of plastid and nuclear htACCase genes. Subtle expression

variations in either BADC or BCCP, both of which reside in the nuclear genome, could determine htACCase complex activity, like a molecular rheostat.

Such a model implies that BCCP and BADC proteins are under differential regulation and are potentially inducible. We show evidence of differential gene regulation in *A. thaliana* siliques (Fig. 8). After exposing dark-adapted siliques to six hours light, total BADC transcript levels decreased approximately two-fold, while total BCCP transcript levels increased approximately 15-fold (Fig. 8A). Therefore, during dark adaption the total BADC transcript level is approximately nine-fold higher than total BCCP transcript level (Fig. 8B). After six hours light exposure, the total BCCP transcript level becomes three-fold higher than the total BADC transcript level. If the BADC and BCCP protein levels change in accordance with transcript levels even to a small degree, our competitive model suggests that htACCase activity will be higher in light conditions and lower in dark conditions. As mentioned previously, htACCase activity is known to increase in response to light. Therefore the competitive model of BADC regulation is consistent with previous reports on the light activation of htACCase.

The literature also gives evidence of the inducible nature of BADC and BCCP gene expression. First, transcriptomic analysis of the *A. thaliana WRI1* mutant, a transcription factor which regulates approximately 18 enzymes from central metabolism, showed differential expression for only the BCCP2, BADC2 and BADC3 subunits to htACCase (39). Second, overexpression of WRI1 significantly increased expression of only the BCCP2 subunit to htACCase (42,44). Third, global transcriptome and proteomic analysis of BCCP2 overexpression lines in *A. thaliana* showed that targeted

upregulation of BCCP2 produced a concomitant increase in BADC2 transcript and protein; quantitative immunoblotting showed no changes to the other htACCase subunits (48). Thus, it appears that expression of BADC and BCCP subunits are under different transcriptional control than other htACCase subunits.

Regulation of htACCase by BADCs must now be considered among the other regulatory mechanisms for this multienzyme complex. As mentioned previously, these mechanisms include feedback inhibition, PII-mediated inhibition, light, and redox chemistry. However, regulation of htACCase by the BADC family of proteins distinguishes itself from each of the aforementioned regulatory properties by the potential for near complete control of the multi-enzyme complex solely at the transcription level. Purified, recombinant BADC, lacking any post-translational modifications, by itself was sufficient to inhibit htACCase *in vivo* (Fig. 7A). By extension, targeted down-regulation of one BADC gene was also sufficient to enhance ACCase function and accumulation of triacylglyerol in the seed (Fig. 9A). From these observations it is tempting to speculate what effect reduction of all three BADC genes might have on seed oil content or plant function in general. Given their efficacy it is likely to produce unintended, deleterious effects particularly if silencing is not targeted to cell types capable of storing excess fatty acids originating from the plastid, i.e. developing embryonic cells. This is presently being explored by systematic tandem RNAi and the collection of T-DNA knockout lines available for Arabidopsis.

In conclusion, our results implicate the BADC proteins as negative regulators of htACCase in diverse autotrophs. Due to the essential role of htACCase in *de novo* FAS

and the identification of BADC orthologs in almost every major oil crop and green algae species currently in use to produce biofuels (Fig. 15), further study could provide new mechanisms for engineering increased oil content in these species.

EXPERIMENTAL PROCEDURES

Nomenclature- For the purposes of this manuscript, we refer to the accessions AT3G56130, AT1G52670, and AT3G15690 as BADC1, BADC2, and BADC3, respectively.

Accessions- α-CT, AT2G38040; β-CT, ATCG00500; BC, AT5G35360; BCCP1, AT5G16390; BCCP2, AT5G15530; BADC1, AT3G56130; BADC2, AT1G52670; BADC3, AT3G15690

Plant materials and growth conditions- Wild type *A. thaliana* (ecotype-Columbia-0) were grown in a growth chamber with 12 h day (23 °C, 50% humidity, 50 μmol m^{-2} s^{-1}) and 12 h night (20 °C, 50% humidity) conditions. For co-immunoprecipitation experiments, 8.5 cm x 8.5 cm pots were filled with moist soil (Sunshine Mix #6, Sun Gro Horticulture), covered with screen (1 mm^2 pore size), and coated with seeds. For htACCase activity experiments, two plants were grown in opposite corners of 8.5 x 8.5 cm pots.

Co-immunoprecipitation of htACCase from A. thaliana seedlings. Crude chloroplasts were isolated from approximately 10 g 14-d-old *A. thaliana* seedlings after 1 h light exposure. Fresh leaves were homogenized in ice-cold grinding buffer (50 mM HEPES-KOH pH 8.0, 330 mM sorbitol, 1.5 mM $MnCl_2$, 2 mM $MgCl_2$, 2 mM EDTA, 0.1%

(w/v) BSA) using a Waring blender. Homogenate was filtered through two layers of Miracloth and centrifuged at 2,600 *g* at 4° C for 20 min. Chloroplasts were lysed for 30 min in ice-cold lysis buffer (50mM HEPES-KOH pH 8.0, 10% (v/v) glycerol, 0.5% (v/v) Triton X-100). Lysates were homogenized ten times in a Dounce homogenizer on ice and then centrifuged at 30 k *g* for 20 min at 4° C. Then 1 mL of the 30 k *g* supernatant was added to 25 µL Protein A Sepharose beads (Sigma Aldrich) either uncoated (control) or coated with antibody specific for α-CT, BCCP, BADC1, or BADC2. Co-immunoprecipations (co-IP) were carried out at 4° C for 3 h with gentle mixing. The beads were washed twice with 1 mL ice-cold lysis buffer and precipitated protein was eluted by adding 30 µL 6x SDS sample buffer (350 mM Tris-HCl, pH 6.8, 350 mM SDS, 30% (v/v) glycerol, 100 mM dithiothreitol, 2.5 mM bromophenol blue) and heating at 65 °C for 10 min. Eluted proteins were resolved on 10% SDS-PAGE gels for western and mass spectrometry analysis.

Mass spectrometry sample preparation and analysis- Precipitated proteins from co-IPs were resolved by 10% SDS-PAGE and stained with colloidal Coomassie Brilliant Blue (CBB) G-250. Each lane was separated into 0.5 cm segments and subsequently diced into approximately 1 mm^3 gel pieces. Gel pieces were digested with trypsin and peptides were extracted as described previously (103). Tryptic peptides were lyophilized and stored at -20 °C until analysis by liquid chromatography-tandem mass spectrometry (LC-MS/MS). Lyophilized peptides were prepared for mass spectrometry analysis as described previously (104). Samples were analyzed on a LTQ Orbitrap XL ETD (Thermo Fisher Scientific) with the same settings as in (105), except that peptides were

eluted using a 30 min acetonitrile gradient (5-43% acetonitrile), the top 8 masses from the precursor scan were selected for data-dependent acquisition, and precursor ions were fragmented using CID (collision-induced dissociation). Dynamic exclusion was enabled with the following settings: repeat count, 3; repeat duration, 30 s; exclusion list, 50; and exclusion list duration, 30 s.

Database searching- Acquired spectra were searched against the TAIR10 protein database (70,773 entries, downloaded on 06/11/2012), concatenated to a randomized TAIR10 database as a decoy. Search parameter settings of SEQUEST were static modification of cysteine-carboxyamidomethylation and variable modification of methionine-oxidation. Other search parameter settings of SEQUEST included two missed tryptic cleavage sites, absolute threshold: 1000, minimum ion count: 10, mass range: 650-3500, and a parent and fragment ion tolerance of 1 Da and 1000 ppm, respectively. Search result files were loaded into Proteome Discoverer 1.3 (Thermo Fisher Scientific). Identified peptides were filtered to <1% false discovery rate using the following criteria: 10 ppm peptide mass deviation, 'Xcorr versus charge state', and 2 and 1 peptide minimum for co-IPs and 2D BN-SDS PAGE, respectively. Protein grouping was also enabled. False discovery rate was calculated manually using spectral counting (106). Files generated for each biological replicate by Proteome Discoverer 1.3 were exported into Microsoft Excel for further analysis.

Filtering of co-immunoprecipitation protein identifications- Proteins identified from SEQUEST searches were compared against uncoated Sepharose bead controls that had been treated in an identical manner to the htACCase subunit co-IPs. Proteins that

were only identified in the htACCase subunit co-IPs were considered as putative interacting clients. All other proteins were disregarded. The htACCase subunits were never identified in controls.

Yeast two-hybrid construct design- The ORF of genes of interest were inserted into bait and prey vectors PGBKT7 and pGADT7. Primers were designed to exclude the N-terminal target peptide from the coding region, as predicted by TargetP (107,108). Predicted target peptide lengths were: BCCP1, 82; BCCP2, 87; BADC1, 56; BADC2, 47; BADC3, 54 amino acids. Genes were amplified from cDNA clones obtained from the Arabidopsis Biological Resource Center. Amplicons were first inserted into Zero Blunt TOPO vector (Life Technologies) and checked for errors by DNA sequencing. Error-free amplicons were then subcloned into either pGBKT7 or pGADT7 vector. Completed constructs were transformed into competent DH5α cells. Cells transformed with pGBKT7 and pGADT7 were grown on LB media agar plates containing 50 µg/mL kanamycin (Kan) and 100 µg/mL ampicillin (Amp), respectively. Plasmids were purified from 5 mL culture of positive colonies using QIAprep Spin Miniprep kit (Qiagen).

Targeted yeast two-hybrid assays- Targeted yeast two-hybrid assays were performed using an adaptation of the lithium acetate method (109). Strain AH109 yeast were transformed with 100 ng of bait and prey vector. Pelleted transformed cells were resuspended in 300 uL sterile water. Aliquots of 100 µL cell suspension were plated on synthetic dropout (SD) media lacking leucine, tryptophan, and histidine. Plates were incubated at 30° C for 4 d and then imaged. Images shown are representative of at least three replicate experiments.

Recombinant protein expression and purification- The ORFs of BCCP1, BCCP2, BADC1, BADC2, and BADC3 were amplified via PCR from cDNA clones U15855, U85042, U12534, C00214, and U15571, respectively (ABRC). The primer pairs for these amplifications were the same as those used in the yeast two-hybrid construct formation. These primers were designed to remove the transit peptide, as predicted by TargetP. The amplified ORF of all five genes were cloned into either the expression vector pET28a or pET11a producing an N-terminal His-tagged fusion protein or an untagged recombinant protein, respectively. All constructs were sequence confirmed via DNA sequencing. Constructs were then transformed into *E. coli* strain BL21 (B2685: Sigma). Recombinant protein was expressed and purified from transformed BL21 cells as described in (104). For co-expression experiments, ~200 ng of each plasmid was used to transform BL21 cells.

Immunoblotting- Proteins resolved by SDS-PAGE were transferred to PVDF membrane and stained with the appropriate primary antibody overnight at 4° C for western blot analysis. All antibodies were used at 1:5000 dilution in PBS-T (10 mM NaH_2PO_4-NaOH pH 7.2, 150 mM NaCl, 0.3% (v/v) Tween 20). Antibodies used in this study were derived from rabbits immunized with recombinant *P. sativum* α-CT (69), recombinant *A. thaliana* BCCP2 (47), recombinant *A. thaliana* BADC2 short peptide (48), or recombinant *A. thaliana* BADC1. Blots were rinsed twice in PBS-T, probed in secondary antibody for 1 h at room temperature, and developed as described previously (69). Goat anti-rabbit IgG secondary antibody conjugated to alkaline phosphatase was obtained from Sigma-Aldrich (St. Louis, MO).

Antibody production – A. thaliana BADC1 antibody was raised against recombinant BADC1 protein in rabbits (Cocalico Biologicals, Reamstown, PA). Protein was expressed in BL21 *E. coli* cells using the pET28a clone described above and purified by Ni^{2+}-NTA affinity chromatography. Antibody from the fourth bleed was used in this study.

BADC orthologs identification and maximum-likelihood tree construction - Representative splicing forms of BCCP and BADC proteins in *Arabidopsis thaliana* were used to search against KEGG SSDB (Sequence Similarity DataBase) (101) for their potential orthologous proteins, respectively. SSDB contains pre-built all-vs-all Smith-Waterman (110) alignments among all protein-coding genes in species with the whole genome information. The following criteria were applied to obtain orthologs with high confidence: 1) reciprocal best hits only; 2) Smith-Waterman alignment score greater than 300; 3) fragment sequences (less than 100 amino acid residues) were removed. All predicted ortholog relationships were further confirmed by independent reciprocal BLAST searches. For BCCP orthologs, search was limited to Eukaryotes belonging to the KEGG ORTHOLOGY group K02160. Full-length protein sequences of orthologs were retrieved from the KEGG or NCBI database. Biotin/lipoyl attachment domains were extracted using HMMER (3.0) (111) and Pfam (112) annotations (PF00364). Multiple sequence alignments were performed using MUSCLE (3.8.31) (113) for both full-length and domain sequences. Maximum likelihood phylogenetic tree of BADC full-length sequences was constructed with 1000 rapid bootstrapping iterations implemented in RAxML (8.2.4) (114) and CIPRES Science Gateway. We applied CAT for

evolutionary rate heterogeneity approximation and general time reversible (GTR) amino acid substitution model (using the “RAxML -m PROTCATGTR” option).

Co-occurrence analysis - The primary sequences of confirmed BCCP and BADC orthologs from all species present in the maximum-likelihood tree were used for co-occurrence analysis. In addition, BCCP and BADC orthologs from *Cyanophora paradoxa* and three red algae species with whole genome sequences were included to trace the origin of BADC proteins. The ortholog assignment was confirmed by reciprocal BLAST searches. We generated the species tree using phyloT (http://phylot.biobyte.de) based on NCBI Taxonomy and the Tree of Life project (http://tolweb.org/tree/). The protein co-occurrence pattern was drawn using ggtree (http://bioconducter.org/packages/release/bioc/html/ggtree.html).

Growth assays in L8 strain E. coli cells- The temperature-sensitive (Ts) L8 strain *E. coli* was obtained from the Coli Genetic Stock Center (Yale, New Haven, CT). The accb (BCCP) gene was sequenced and found to contain point mutations that changed Ile83 to Val and Gly133 to Ser. Chemically competent L8 cells were transformed with the vectors in the text using the heat shock method. Cells were then plated on Kan, Amp, or Kan+Amp plates to select for transformants containing pET28a, pET11a or both, respectively. Plates were incubated at 30°C for two days. PCR positive colonies were added to 2 mL LB media (1% tryptone (w/v), 0.5% NaCl (w/v), 0.5% yeast extract (w/v)) culture and grown overnight at 30°C, 250 rpm. Glycerol stocks were made from these cultures and stored at -80°C. To prevent loss of the Ts phenotype, all experiments were performed using the original glycerol stock for each transformant. Experiments

were begun by inoculating 5 mL LB media with a stab of glycerol stock and incubating at 30°C overnight, 250 rpm. Then overnight cultures were centrifuged at 3,000 *g* and resuspended in 5 mL sterile deionized water. Cultures were centrifuged again and resuspended in M63 minimal media to make OD_{600} = 3.75. Then a 200 µL cell suspension was added to 7 mL M63 media plus antibiotics in sterile culture tubes. Cultures contained Kan, and Amp if necessary, at 50 µg/mL each as well as 1 µM isopropyl β-D-1-thiogalactopyranoside at T=0.

RNAi silencing of BADC1 in A. thaliana- Inverted repeats targeting AtBADC1 were inserted into the pMU103 vector. The repeats coded for bases 774 to 1034 of the cDNA sequence (accession AT3G56130.1). Primers used to amplify the sequence were 5'-GTGTTAGTCACATCTCCCGCAGT-3' and 5'-GATGTTGATGTCGTGGAAAGATGGC-3'. The 5' repeat was inserted using the restriction enzymes AscI and AvrII. The 3' repeat was inserted using the restriction enzymes SacI and XmaI. Repeats were placed on either side of the Rice Waxy-A intron. Expression of the mRNA was driven by the seed-specific glycinin promoter. A sequence confirmed construct was transformed into *A. thaliana* ecotype Col-0 using the floral dip method (115). Basta herbicide screening was used to identify independent lines. For monitoring seed oil content, T_2 plants from each independent line were grown to maturity alongside wild type plants. Dry seed was harvested for analysis.

RT-PCR and qPCR analysis - RNA for RT-PCR and qPCR analysis was extracted from 10 d old siliques using the RNeasy Plant Mini Kit (Qiagen). cDNA was synthesized from 500 ng RNA of four biological replicates. Primers used in analysis

were: BADC1 sense, 5'-GCTCCTAGCCCATCTCAAGC-3'; BADC1 antisense, 5'-TCCAGATGCCTCCAAAGCAG-3'; Actin 8 sense, 5'-CCAGATCTTCATCGTCGTGGT-3'; Actin 8 antisense, 5'-ATCCAGCCTTAACCATTCCAGT-3'. qPCR assays were performed on an ABI 7500 system (Applied Biosystems). Reaction volumes were 20 µL and contained SYBR Green PCR Master Mix (Applied Biosystems). Control reactions contained no template and were performed in triplicate. Amplicon identity was confirmed through melting curve analysis. For qPCR analysis, absolute transcript quantities were calculated using a standard curve of serially diluted amplicons of known concentrations.

Fatty acid methyl ester (FAME) analysis- Seed oil was derivatized as described previously (116). Heptadecanoic acid was used as an internal standard. FAMEs were analyzed by a Hewlett Packard 6890 gas chromatograph as described previously (117). For WT and each independent line, 5 mg seed from thirteen and four plants, respectively, were analyzed. Seeds were dried over desiccant for one week prior to analysis.

ACCase activity assays- HtACCase activity was directly monitored in ten-d-old siliques through the incorporation of $^{14}CO_2$ into acid-stable products as in (47). *A. thaliana* WT Col-0 plants were grown in long day conditions (16 h light, 50% humidity, 100 µmol m^{-2} s^{-1}) and siliques were harvested after six hours of light exposure. In each trial, four biological replicates of three siliques were assayed. Siliques were pulverized in homogenization buffer (20 mM TES, pH 7.5, 10% glycerol, 5 mM EDTA, 2 mM DTT, 2 mM benzamidine, 2 mM PMSF, 1% Triton X-100), centrifuged at 10 k *g* for 15 s, and assayed within 5 minutes of harvest to minimize loss of htACCase activity. Assays were

performed in the presence of 10 uM haloxyfop to eliminate homomeric ACCase activity. Enzyme activity values for –acetyl-CoA controls were subtracted from +acetyl-CoA trials to determine the true htACCase activity levels. Purified recombinant protein was added to assay tube prior to addition of silique lysate.

Acknowledgements: We thank John Ohlrogge for the α-CT and BCCP antibody, Melissa Mitchum for the yeast strain and two-hybrid vectors, Brian Mooney and Beverly DaGue for the intact mass analysis, and Shannon King for aiding the study of BADC dimerization.

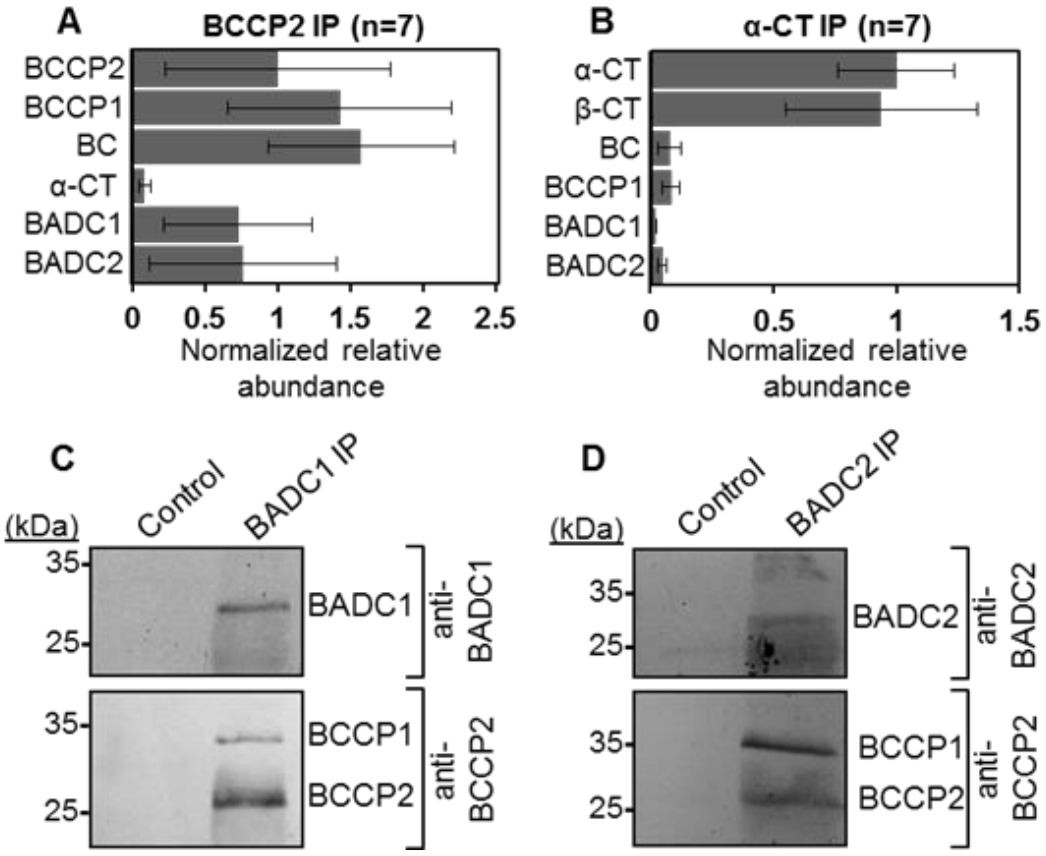

FIGURE 4. Co-immunoprecipitation of ACCase and BADC proteins from *Arabidopsis thaliana* seedlings. *A*, *B*, Proteins were precipitated from *A. thaliana* crude chloroplast lysate using antibodies specific for ACCase subunits BCCP2 (*A*) or α-CT (*B*) and identified by LC-MS/MS. Control precipitations were performed with uncoated Protein A sepharose beads. For both sets of experiments, n=7. Normalized relative abundance averages signify the average number of peptide spectral matches divided by the protein molecular weight and normalized to BCCP2 (*A*) or α-CT (*B*). Error bars represent standard deviation of normalized relative abundance among replicates in which the protein was identified. Semi-quantitative normalized relative abundance values were determined by dividing total spectral matches for each protein by protein size and normalizing to the antibody-specific protein. (*C, D*) Protein blot analysis of reciprocal co-IPs from the same *A. thaliana* lysate showed that the BCCP subunits of ACCase co-precipitated with BADC1 (*C*) and BADC2 (*D*). Blots are representative of three biological replicates.

Protein Name	Protein Accession	No. of replicates identified (n=13)	No. of control replicates identified (n=13)	Average Peptides	Average PSMs	Coiled coil potential
acetyl Co-enzyme a carboxylase carboxyltransferase alpha subunit	AT2G38040.1	13	0	47.8	231.0	y
acetyl-CoA carboxylase carboxyl transferase subunit beta	ATCG00500.1	13	0	5.0	19.6	n
acetyl Co-enzyme a carboxylase biotin carboxylase subunit	AT5G35360.1	9	0	6.1	14.3	y
calcium sensing receptor	AT5G23060.1	9	5	7.1	21.3	y
heat shock protein 60	AT3G23990.1	9	0	5.2	8.3	y
light-harvesting chlorophyll-protein complex II subunit B1	AT2G34430.1	9	4	3.8	63.8	n
NAD(P)-binding Rossmann-fold superfamily protein	AT3G18890.1	9	4	5.4	12.9	n
Ribosomal L29 family protein	AT5G65220.1	9	1	3.7	9.6	y
thylakoid rhodanese-like	AT4G01050.1	9	2	3.0	7.1	n
Translation protein SH3-like family protein	AT5G54600.1	9	2	3.8	8.4	n
chloroplast ribosomal protein S4	ATCG00380.1	8	2	4.5	15.1	n
NAD(P)-linked oxidoreductase superfamily protein	AT5G53580.1	8	1	3.3	6.6	n
ribosomal protein L12-C	AT3G27850.1	8	3	3.5	9.0	y
ribosomal protein L9	AT3G44890.1	8	3	3.6	7.9	y
chloroplastic acetylcoenzyme A carboxylase 1	AT5G16390.1	7	0	2.4	6.4	n
Clp ATPase	AT3G48870.1	7	1	3.7	6.9	y
lipoxygenase 2	AT3G45140.1	7	3	9.3	23.6	y
NAD(P)-binding Rossmann-fold superfamily protein	AT4G35250.1	7	2	3.9	7.9	n
Protein of unknown function (DUF1118)	AT5G08050.1	7	2	2.1	5.4	n
ribosomal protein S9	AT1G74970.1	7	1	3.4	9.3	n
ribosomal protein L15	AT3G25920.1	6	2	4.3	11.3	n

Table 2. Putative interacting proteins identified by α-CT co-immunoprecipitation. Table lists the proteins identified to be present in α-CT immunoprecipicates by tandem mass spectrometry. Proteins are ranked by number of times identified in trial replicates containing α-CT antibody (No. of replicates identified, n=13). Proteins were excluded if identified in control replicates greater than half the number of times identified trial replicates (eg 3 control identifications, 4 trial identifications). In order from left to right, columns list the protein annotation, protein accession number, number of trial replicates the protein was identified in (n=13), number of control replicates protein was identified in (n=13), average number of peptides identified by tandem mass spectrometry, average number of peptide spectral matches (PSMs) to the protein, and coiled coil potential of the protein. Coiled-coil potential was determined by predicting coiled-coil domains from the full protein sequence using MARCOIL (y, at least one region showed over 50% probability to contain a coiled coil; n, no region of the protein sequence showed over 50% probability of a coiled coil)

Protein Name	Protein Accession	No. of replicates identified (n=13)	No. of control replicates identified (n=13)	Average Peptides	Average PSMs	Coiled coil potential
ribosomal protein L22	ATCG00810.1	6	0	3.2	9.8	n
Ribosomal protein S13/S18 family	AT5G14320.1	6	2	4.0	9.7	y
Thioredoxin superfamily protein	AT3G26060.1	6	1	3.5	11.8	n
peroxisomal NAD-malate dehydrogenase 2	AT5G09660.2	6	3	5.6	14.1	n
chloroplast ribosomal protein S15	ATCG01120.1	5	2	4.4	11.0	y
dicarboxylate diiron protein, putative (Crd1)	AT3G56940.1	5	1	3.8	8.0	y
elongation factor Ts family protein	AT4G29060.1	5	0	4.6	5.6	y
FtsH extracellular protease family	AT5G42270.1	5	2	5.0	7.6	y
photosynthetic electron transfer C	AT4G03280.1	5	2	4.0	11.2	n
photosystem II light harvesting complex gene 2.1	AT2G05100.1	5	2	3.2	12.2	n
plastid ribosomal protein l11	AT1G32990.1	5	1	2.4	3.6	n
ribosomal protein L16	ATCG00790.1	5	2	3.2	12.0	n
Ribosomal protein L17 family protein	AT3G54210.1	5	1	3.0	7.2	n
Ribosomal protein L19 family protein	AT5G47190.1	5	0	2.6	4.8	y
ribosomal protein S2	ATCG00160.1	5	2	5.6	12.2	y
rubredoxin family protein	AT5G17170.1	5	2	3.4	8.6	n
CLPC homologue 1	AT5G50920.1	4	0	4.8	8.5	y
cyclophilin 38	AT3G01480.1	4	1	3.8	8.5	y
photosystem II family protein	AT1G03600.1	4	0	2.0	4.5	y
Plastid-lipid associated protein PAP / fibrillin family protein	AT2G35490.1	4	1	2.5	5.0	y
protochlorophyllide oxidoreductase A	AT5G54190.1	4	1	2.0	5.5	y
Ribosomal protein L13 family protein	AT1G78630.1	4	1	2.0	4.0	n
ribosomal protein S11	ATCG00750.1	4	1	3.5	20.5	n
DEAD box RNA helicase (RH3)	AT5G26742.3	4	0	5.3	12.8	y

Table 2 continued.

Protein Name	Protein Accession	No. of replicates identified (n=13)	No. of control replicates identified (n=13)	Average Peptides	Average PSMs	Coiled coil potential
FtsH extracellular protease family	AT2G30950.1	3	1	4.0	6.0	y
glutamate-1-semialdehyde 2,1-aminomutase 2	AT3G48730.1	3	0	2.7	4.7	n
heat shock protein 60-2	AT2G33210.1	3	0	3.3	4.3	y
Molecular chaperone Hsp40/DnaJ family protein	AT4G39960.1	3	0	2.7	4.7	y
NAD(P)-binding Rossmann-fold superfamily protein	AT1G24360.1	3	0	2.7	4.3	y
one-helix protein 2	AT1G34000.1	3	0	2.7	4.7	y
phosphoglycerate kinase 1	AT3G12780.1	3	1	4.3	14.0	y
photosystem I light harvesting complex gene 2	AT3G61470.1	3	1	3.0	11.7	n
photosystem I P subunit	AT2G46820.1	3	0	3.0	5.3	n
photosystem II light harvesting complex gene 2.3	AT3G27690.1	3	1	4.0	15.7	n
photosystem II reaction center PSB29 protein	AT2G20890.1	3	0	2.7	4.3	y
plastid transcriptionally active 4	AT1G65260.1	3	0	2.0	3.7	y
Ribosomal L28 family	AT2G33450.1	3	0	5.0	8.3	n
Ribosomal protein L10 family protein	AT5G13510.1	3	0	4.3	9.3	n
ribosomal protein L12-A	AT3G27830.1	3	0	3.7	8.7	y
ribosomal protein L14	ATCG00780.1	3	0	3.0	6.0	n
ribosomal protein L20	ATCG00660.1	3	1	3.0	5.3	n
ribosomal protein S1	AT5G30510.1	3	1	2.0	3.3	y
Ribosomal protein S10p/S20e family protein	AT3G13120.1	3	0	3.0	7.0	n
Ribosomal protein S21 family protein	AT3G27160.1	3	0	3.0	7.3	n
ribosomal protein S8	ATCG00770.1	3	0	2.7	5.0	n
translocon at the inner envelope membrane of chloroplasts 110	AT1G06950.1	3	1	5.7	12.3	y
unknown protein	AT2G21960.1	3	1	2.7	7.0	n
63 kDa inner membrane family protein	AT2G28800.4	2	0	2.5	5.0	y

Table 2 continued.

Protein Name	Protein Accession	No. of replicates identified (n=13)	No. of control replicates identified (n=13)	Average Peptides	Average PSMs	Coiled coil potential
ADP/ATP carrier 1	AT3G08580.1	2	0	2.0	4.5	n
Aldolase superfamily protein	AT1G69740.1	2	0	2.5	6.5	n
Aldolase-type TIM barrel family protein	AT4G18360.1	2	0	2.3	6.0	n
Aldolase-type TIM barrel family protein	AT3G14420.1	2	0	2.0	4.0	y
GTP binding Elongation factor Tu family protein	AT1G07920.1	2	0	3.5	13.5	n
hydroxypyruvate reductase	AT1G68010.1	2	0	2.0	3.0	n
Plastid-lipid associated protein PAP / fibrillin family protein	AT3G26070.1	2	0	2.5	3.0	y
Protein of unknown function (DUF1118)	AT1G74730.1	2	0	2.0	4.5	n
Ribosomal protein L21	AT1G35680.1	2	0	2.5	6.5	n
ribosomal protein large subunit 27	AT5G40950.1	2	0	2.0	8.0	n
ribosomal protein S19	ATCG00820.1	2	0	4.0	6.0	y
Single hybrid motif superfamily protein	AT1G52670.1	2	0	2.5	3.5	n
Translation initiation factor 3 protein	AT2G24060.1	2	0	2.0	2.0	y
unknown protein	AT4G01150.1	2	0	3.0	5.0	y
unknown protein	AT1G67700.1	2	0	2.0	4.5	n
biotin/lipoyl attachment domain-containing protein	AT3G56130.1	1	0	2.0	5.0	n
Chaperone protein htpG family protein	AT2G04030.1	1	0	2.0	3.0	n
chaperonin 20	AT5G20720.1	1	0	2.0	4.0	n
chloroplast RNA-binding protein 33	AT3G52380.1	1	0	2.0	5.0	y
chloroplast signal recognition particle 54 kDa subunit	AT5G03940.1	1	0	2.0	5.0	y
chorismate synthase, putative / 5-enolpyruvylshikimate-3-phosphate phospholyase, putative	AT1G48850.1	1	0	2.0	2.0	y
dicarboxylate transporter 1	AT5G12860.1	1	0	2.0	3.0	n
dihydrolipoyl dehydrogenases	AT4G16155.1	1	0	3.0	7.0	n

Table 2 continued.

Protein Name	Protein Accession	No. of replicates identified (n=13)	No. of control replicates identified (n=13)	Average Peptides	Average PSMs	Coiled coil potential
disease resistance protein (TIR-NBS-LRR class) family	AT5G46470.1	1	0	2.0	6.0	y
DNA-directed RNA polymerase family protein	ATCG00170.1	1	0	3.0	4.0	n
DNAJ heat shock family protein	AT2G22360.1	1	0	4.0	9.0	y
Enoyl-CoA hydratase/isomerase family	AT4G29010.1	1	0	2.0	2.0	n
Eukaryotic aspartyl protease family protein	AT3G54400.1	1	0	2.0	4.0	n
FKBP-like peptidyl-prolyl cis-trans isomerase family protein	AT3G10060.1	1	0	2.0	4.0	n
glucoside glucohydrolase 2	AT5G25980.2	1	0	2.0	4.0	n
glutamate synthase 2	AT2G41220.1	1	0	2.0	4.0	y
glutamate tRNA synthetase	AT5G64050.1	1	0	3.0	8.0	n
glutamate-1-semialdehyde-2,1-aminomutase	AT5G63570.1	1	0	2.0	4.0	n
haloacid dehalogenase-like hydrolase family protein	AT1G56500.1	1	0	2.0	2.0	n
high cyclic electron flow 1	AT3G54050.1	1	0	2.0	5.0	n
Leucine-rich repeat protein kinase family protein	AT3G02880.1	1	0	2.0	6.0	n
lipoamide dehydrogenase 1	AT3G16950.1	1	0	2.0	5.0	n
MAR binding filament-like protein 1	AT3G16000.1	1	0	6.0	6.0	y
NAD(P)-binding Rossmann-fold superfamily protein	AT5G18660.1	1	0	3.0	6.0	y
NAD(P)-binding Rossmann-fold superfamily protein	AT2G34460.1	1	0	2.0	3.0	n
Nucleic acid-binding proteins superfamily	AT3G23700.1	1	0	2.0	4.0	n
Nucleotidylyl transferase superfamily protein	AT2G25840.1	1	0	2.0	4.0	n
Oxidoreductase, zinc-binding dehydrogenase family protein	AT1G23740.1	1	0	2.0	3.0	n
PGR5-LIKE A	AT4G22890.4	1	0	2.0	2.0	y
photosystem II subunit P-2	AT2G30790.1	1	0	2.0	9.0	n
photosystem II subunit R	AT1G79040.1	1	0	3.0	8.0	n

Table 2 continued.

Protein Name	Protein Accession	No. of replicates identified (n=13)	No. of control replicates identified (n=13)	Average Peptides	Average PSMs	Coiled coil potential
Plastid-lipid associated protein PAP / fibrillin family protein	AT2G42130.3	1	0	2.0	4.0	n
plastid-specific 50S ribosomal protein 5	AT3G56910.1	1	0	2.0	7.0	y
P-loop containing nucleoside triphosphate hydrolases superfamily protein	AT1G80380.2	1	0	2.5	5.0	n
P-loop containing nucleoside triphosphate hydrolases superfamily protein	AT5G35970.1	1		3.0	7.0	n
pyruvate dehydrogenase E1 alpha	AT1G01090.1	1	0	2.0	4.0	y
Ribosomal L18p/L5e family protein	AT1G48350.1	1	0	3.0	6.0	n
ribosomal protein L36	ATCG00760.1	1	0	2.0	4.0	n
Ribosomal protein L7Ae/L30e/S12e/Gadd45 family protein	AT2G47610.1	1	0	2.0	2.0	y
ribosomal protein S12A	ATCG00065.1	1	0	2.0	5.0	n
serine hydroxymethyltransferase 2	AT5G26780.1	1	0	2.0	3.0	y
thiazole biosynthetic enzyme, chloroplast (ARA6) (THI1) (THI4)	AT5G54770.1	1	0	3.0	5.0	y
Thioredoxin family protein	AT5G03880.1	1	0	3.0	5.0	n
Thioredoxin superfamily protein	AT3G52960.1	1	0	2.0	3.0	n
Translation elongation factor EFG/EF2 protein	AT1G62750.1	1	0	2.0	2.0	y
Translation initiation factor 3 protein	AT4G30690.1	1	0	2.0	2.0	y
TUDOR-SN protein 1	AT5G07350.1	1	0	2.0	6.0	y
unknown protein	AT5G37360.1	1	0	3.0	7.0	n
unknown protein	AT5G58250.1	1	0	2.0	3.0	n
unknown protein	AT1G18060.1	1	0	5.0	15.0	n
uridylyltransferase-related	AT1G16880.1	1	0	2.0	3.0	n

Table 2 continued.

Protein Name	Protein Accession	No. of replicates identified (n=13)	No. of control replicates identified (n=13)	Average Peptides	Average PSMs	Coiled coil potential
Uroporphyrinogen decarboxylase	AT2G40490.1	1	0	2.0	2.0	y
vegetative storage protein 1	AT5G24780.1	1	0	2.0	6.0	n
zeaxanthin epoxidase (ZEP) (ABA1)	AT5G67030.1	1	0	3.0	5.0	n
zeta-carotene desaturase	AT3G04870.1	1	0	3.0	4.0	y

Table 2 continued.

Protein Name	Protein Accession	No. of replicates identified (n=7)	No. of control replicates identified (n=7)	Average Peptides	Average PSMs
acetyl Co-enzyme a carboxylase biotin carboxylase subunit	AT5G35360.1	7	0	14.5	67.6
biotin carboxyl carrier protein 2	AT5G15530.1	7	0	2.9	15.1
plastid transcriptionally active 4	AT1G65260.1	7	0	12.6	54.3
biotin/lipoyl attachment domain-containing protein	AT3G56130.1	7	0	3.7	13.7
Single hybrid motif superfamily protein	AT1G52670.1	6	0	2.6	14.4
alpha-amylase-like 3	AT1G69830.1	6	0	12.5	35.3
chloroplastic acetylcoenzyme A carboxylase 1	AT5G16390.2	6	0	4.5	15.5
Clp ATPase	AT3G48870.1	6	1	3.2	5.2
heat shock protein 60	AT3G23990.1	6	0	7.5	16.8
heat shock protein 60-2	AT2G33210.2	6	0	5.5	11.2
pyruvate dehydrogenase E1 alpha	AT1G01090.1	6	0	6.3	14.7
structural constituent of ribosome	ATCG00800.1	6	2	5.2	12.7
calcium sensing receptor	AT5G23060.1	5	2	6.2	16.4
DEAD box RNA helicase (RH3)	AT5G26742.1	5	1	5.0	10.4
dihydrolipoyl dehydrogenases	AT4G16155.1	5	0	5.6	20.4
Glycogen/starch synthases, ADP-glucose type	AT5G24300.1	5	0	3.8	7.6
lipoxygenase 2	AT3G45140.1	5	2	11.8	30.4
photosynthetic electron transfer B	ATCG00720.1	5	2	2.4	6.6
photosynthetic electron transfer C	AT4G03280.1	5	2	2.8	7.0
ribosomal protein L9	AT3G44890.1	5	1	2.8	6.4
TCP-1/cpn60 chaperonin family protein	AT3G13470.1	5	0	6.0	14.6
2-oxoacid dehydrogenases acyltransferase family protein	AT3G25860.1	4	0	5.0	23.8
2-oxoacid dehydrogenases acyltransferase family protein	AT1G34430.1	4		6.0	17.8
chloroplast ribosomal protein S4	ATCG00380.1	4	1	3.5	7.5
peroxisomal NAD-malate dehydrogenase 2	AT5G09660.2	4	1	5.0	15.5
Ribosomal L29 family protein	AT5G65220.1	4	1	3.0	5.3

Table 3. Putative interacting proteins identified by BCCP2 co-immunoprecipitation. Table lists the proteins identified to be present in BCCP2 immunoprecipicates by tandem mass spectrometry. Proteins are ranked by number of times identified in trial replicates containing BCCP2 antibody (No. of replicates identified, n=7). Proteins were excluded if they were identified in control replicates greater than half the number of times identified trial replicates (eg 3 control identifications, 4 trial identifications). In order from left to right, columns list the protein annotation, protein accession number, number of trial replicates the protein was identified in (n=7), number of control replicates protein was identified in (n=7), average number of peptides identified by tandem mass spectrometry, and average number of peptide spectral matches (PSMs) to the protein.

Protein Name	Protein Accession	No. of replicates identified (n=7)	No. of control replicates identified (n=7)	Average Peptides	Average PSMs
Ribosomal L5P family protein	AT4G01310.1	4	0	3.0	7.3
ribosomal protein L16	ATCG00790.1	4	1	2.5	8.3
Translation protein SH3-like family protein	AT5G54600.1	4	1	4.0	9.0
acetyl Co-enzyme a carboxylase carboxyltransferase alpha subunit	AT2G38040.1	3	0	4.0	5.7
Aldolase superfamily protein	AT1G69740.1	3	0	3.7	7.3
Aldolase superfamily protein	AT1G12230.1	3	0	2.0	4.0
chloroplast ribosomal protein S15	ATCG01120.1	3	1	3.0	8.5
Cystathionine beta-synthase (CBS) family protein	AT4G34120.1	3	0	2.0	2.7
L-Aspartase-like family protein	AT4G18440.1	3	1	2.3	4.3
lipoamide dehydrogenase 1	AT3G16950.1	3	0	4.0	13.0
NAD(P)-binding Rossmann-fold superfamily protein	AT4G35250.1	3	1	3.7	10.3
NAD(P)-binding Rossmann-fold superfamily protein	AT1G24360.1	3	0	3.3	6.3
Photosystem I, PsaA/PsaB protein	ATCG00350.1	3	1	6.0	17.0
photosystem II reaction center PSB29 protein	AT2G20890.1	3	0	3.0	7.0
pyruvate dehydrogenase E1 beta	AT1G30120.1	3	0	3.3	9.3
ribosomal protein L15	AT3G25920.1	3	0	3.3	7.0
Ribosomal protein L17 family protein	AT3G54210.1	3	1	3.7	7.3
Ribosomal protein L19 family protein	AT5G47190.1	3	0	2.0	4.0
ribosomal protein L22	ATCG00810.1	3	0	3.0	9.0
ribosomal protein large subunit 27	AT5G40950.1	3	1	2.0	7.7
ribosomal protein S7	ATCG01240.1	3	1	4.0	10.0
Rieske (2Fe-2S) domain-containing protein	AT1G71500.1	3	1	2.3	5.7
TCP-1/cpn60 chaperonin family protein	AT5G56500.1	3	0	5.7	16.0
Thioredoxin superfamily protein	AT3G26060.1	3	1	3.3	10.7
Thioredoxin superfamily protein	AT3G11630.1	3	1	3.0	7.3

Table 3 continued.

Protein Name	Protein Accession	No. of replicates identified (n=7)	No. of control replicates identified (n=7)	Average Peptides	Average PSMs
Transketolase family protein	AT2G34590.1	3	0	3.7	10.3
2-cysteine peroxiredoxin B	AT5G06290.1	2	1	2.0	6.0
allene oxide synthase	AT5G42650.1	2	0	11.5	27.5
ascorbate peroxidase 4	AT4G09010.1	2	1	3.5	8.0
CLPC homologue 1	AT5G50920.1	2	0	5.5	8.5
cyclophilin 38	AT3G01480.1	2	0	6.5	11.0
dicarboxylate diiron protein, putative (Crd1)	AT3G56940.1	2	0	4.5	7.5
dicarboxylate transporter 1	AT5G12860.1	2	0	2.0	5.5
elongation factor Ts family protein	AT4G29060.1	2	0	3.5	6.0
heat shock protein 60-3A	AT3G13860.1	2	0	2.5	5.5
high cyclic electron flow 1	AT3G54050.1	2	0	3.5	6.0
one-helix protein 2	AT1G34000.1	2	0	2.0	4.0
photosystem II family protein	AT1G03600.1	2	0	2.0	5.0
Protein of unknown function (DUF1118)	AT5G08050.1	2	0	2.0	5.5
Ribosomal L28 family	AT2G33450.1	2	0	2.5	4.0
Ribosomal protein L10 family protein	AT5G13510.1	2	0	2.5	5.0
ribosomal protein L12-A	AT3G27830.1	2	0	3.5	8.0
ribosomal protein S11	ATCG00750.1	2	0	3.0	7.0
Ribosomal protein S13/S18 family	AT5G14320.1	2	0	3.0	6.0
ribosomal protein S2	ATCG00160.1	2	0	3.0	7.5
Ribosomal protein S21 family protein	AT3G27160.1	2	0	2.0	2.5
ribosomal protein S9	AT1G74970.1	2	0	3.5	5.5
unknown protein	AT4G01150.1	2	0	2.0	3.5
acclimation of photosynthesis to environment	AT5G38660.1	1	0	2.0	4.0
Aldolase-type TIM barrel family protein	AT3G14420.1	1	0	2.0	4.0
Aldolase-type TIM barrel family protein	AT4G18360.1	1	0	2.0	4.0

Table 3 continued.

Protein Name	Protein Accession	No. of replicates identified (n=7)	No. of control replicates identified (n=7)	Average Peptides	Average PSMs
allene oxide cyclase 1	AT3G25760.1	1	0	2.0	2.0
allene oxide cyclase 2	AT3G25770.1	1	0	2.0	4.0
ATP synthase alpha/beta family protein	AT5G08670.1	1	0	2.0	4.0
Chaperone protein htpG family protein	AT2G04030.2	1	0	3.0	4.0
Dihydrolipoamide acetyltransferase, long form protein	AT3G13930.1	1	0	2.0	3.0
Eukaryotic aspartyl protease family protein	AT3G54400.1	1	0	2.0	3.0
Flavin containing amine oxidoreductase family	AT4G01690.1	1	0	2.0	3.0
Glucose-6-phosphate/phosphate translocator-related	AT5G46110.2	1	0	3.0	11.0
high chlorophyll fluorescence phenotype 173	AT1G16720.1	1	0	2.0	2.0
lactate/malate dehydrogenase family protein	AT5G58330.1	1	0	2.0	2.0
Leucine-rich repeat protein kinase family protein	AT3G02880.1	1	0	2.0	4.0
Mog1/PsbP/DUF1795-like photosystem II reaction center PsbP family protein	AT5G27390.1	1	0	2.0	4.0
NAD(P)-linked oxidoreductase superfamily protein	AT1G14345.1	1	0	2.0	6.0
Nuclear transport factor 2 (NTF2) family protein	AT1G71480.1	1	0	3.0	5.0
Oxidoreductase, zinc-binding dehydrogenase family protein	AT1G23740.1	1	0	2.0	2.0
PGR5-LIKE A	AT4G22890.4	1	0	3.0	7.0
phosphoglycerate kinase 1	AT3G12780.1	1	0	8.0	33.0
Phosphoglycerate kinase family protein	AT1G56190.1	1	0	4.0	22.0
photosystem I light harvesting complex gene 2	AT3G61470.1	1	0	2.0	9.0
photosystem I P subunit	AT2G46820.1	1	0	4.0	12.0
Plastid-lipid associated protein PAP / fibrillin family protein	AT1G51110.1	1	0	2.0	3.0
Plastid-lipid associated protein PAP / fibrillin family protein	AT5G19940.1	1	0	2.0	2.0
Plastid-lipid associated protein PAP / fibrillin family protein	AT2G35490.1	1	0	2.0	2.0
P-loop containing nucleoside triphosphate hydrolases superfamily protein	AT1G80380.2	1	0	2.0	3.0

Table 3 continued.

Protein Name	Protein Accession	No. of replicates identified (n=7)	No. of control replicates identified (n=7)	Average Peptides	Average PSMs
Protein of unknown function (DUF1118)	AT1G74730.1	1	0	2.0	4.0
Protein of unknown function (DUF3353)	AT3G51140.1	1	0	2.0	3.0
Ribosomal protein L11 family protein	AT2G37190.1	1	0	2.0	4.0
ribosomal protein L14	ATCG00780.1	1	0	2.0	3.0
Ribosomal protein L21	AT1G35680.1	1	0	2.0	5.0
Ribosomal protein S10p/S20e family protein	AT3G13120.1	1	0	2.0	4.0
thioredoxin M-type 1	AT1G03680.1	1	0	2.0	3.0
Thioredoxin superfamily protein	AT3G52960.1	1	0	2.0	3.0
Translation elongation factor EFG/EF2 protein	AT1G62750.1	1	0	3.0	6.0
unknown protein	AT4G23890.1	1	0	2.0	3.0
unknown protein	AT1G67700.2	1	0	2.0	3.0
unknown protein	AT2G21960.1	1	0	2.0	4.0
vegetative storage protein 1	AT5G24780.1	1	0	2.0	6.0

Table 3 continued.

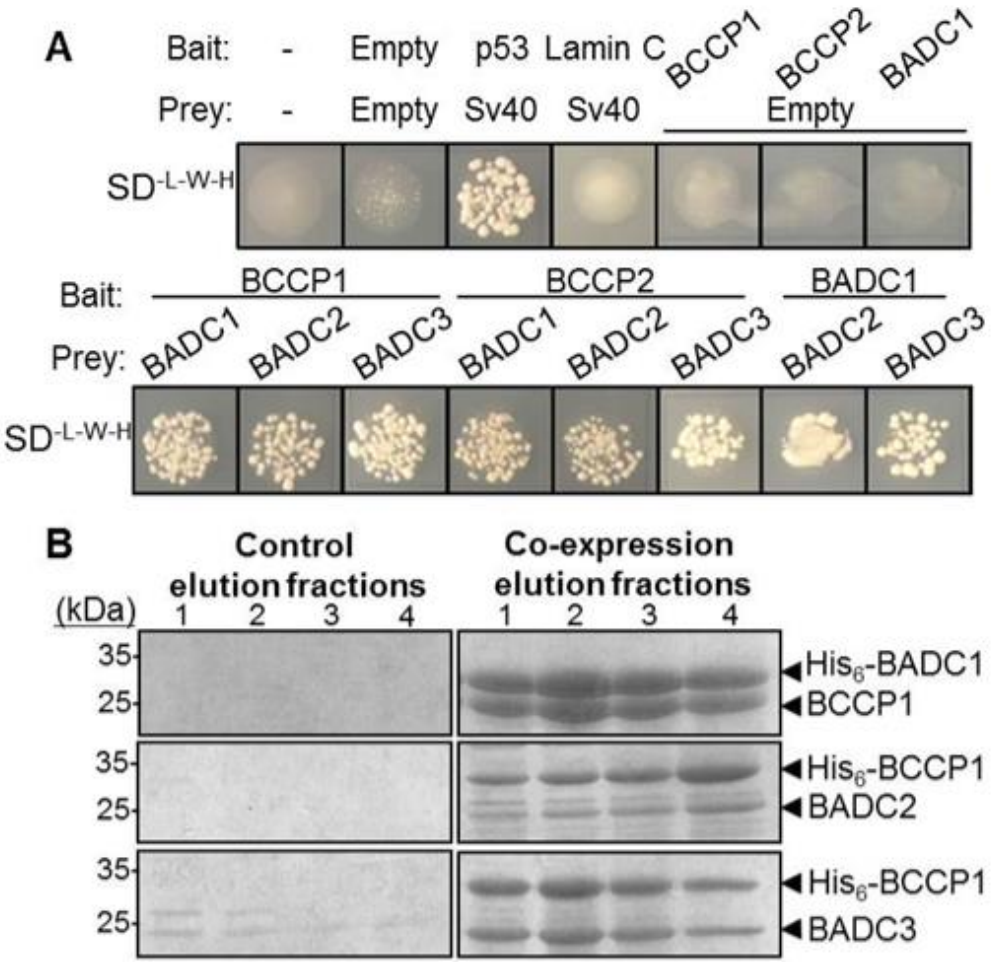

FIGURE 5. BADC proteins directly interact with BCCP subunits of ACCase. *A*, Strain AH109 yeast was transformed with bait and prey constructs containing the genes shown and plated on media lacking Trp, Leu, and His. Negative controls showed minimal or no growth. Sv40 and p53 were used as a positive control. Lamin C was used as a negative control. Results shown are representative of three biological replicates (*B*) Coomassie-stained gels showing the elution fractions of Ni^{2+}-NTA-purified protein from *E. coli*. At right, a native protein was co-expressed with a His_6-tagged protein. At left, the native protein was expressed alone. The native proteins were present strongly in the elution fractions only when co-expressed with the His_6-tagged protein. Protein identities were confirmed by LC-MS/MS.

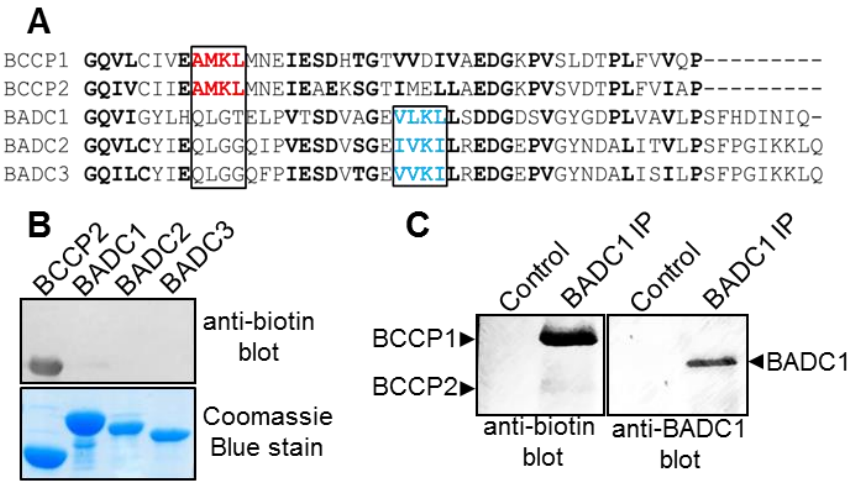

FIGURE 6. The BADC proteins resemble BCCP isoforms but are not biotinylated. *A*, Alignment of the C-termini of the *A. thaliana* BCCP and BADC proteins shows multiple conserved residues (bold). Highlighted in red is the canonical biotinylation motif containing the modified Lys in BCCP. Highlighted in blue is the chemically similar motif found in the BADC proteins. *B*, Western blotting analysis of recombinant *A. thaliana* proteins using a biotin-specific antibody. BCCP2 was observed to be biotinylated while the BADCs were not. *C*, Protein blot analysis of immunoprecipitated *in vivo* BADC1 from *A. thaliana* seedlings. Blotting precipitate with BADC1-specific antibody showed the presence BADC1 in the sample, while blotting with biotin-specific antibody showed no recognition of BADC1.

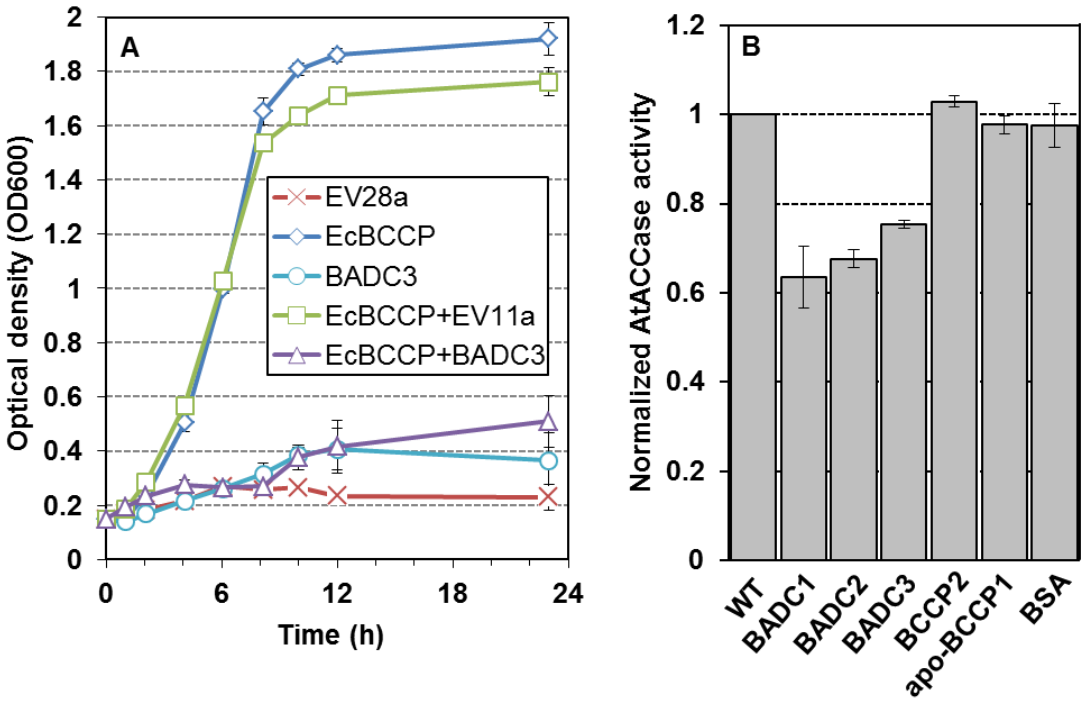

FIGURE 7. BADCs reduce ACCase activity in *E. coli* and *A. thaliana*. *A*, Growth curves showing the optical density of L8 *E. coli* cells over time. Cultures were grown in liquid culture at 37°C. Transformed cells contained the following vectors: empty pET28a (EV28a), pET28a containing the *E. coli* BCCP gene (EcBCCP), empty pET11a (EV11a), and/or pET11a containing the *A. thaliana* BADC3 gene (BADC3). BADC3 expression alone showed no statistical difference from EV control except at T=10 h, while co-expression of BADC3 with EcBCCP showed an approximate 72% reduction in growth compared to EcBCCP+EV11a at T = 24 h. Results shown are representative of three separate experiments. Error bars represent SD. *B*, Protein extracted from three 10 d old *A. thaliana* siliques was assayed for ACCase activity through incorporation of radiolabelled sodium bicarbonate into acid-stable products. Assays were performed in the absence (WT) or presence of 10 mM recombinant BADC1, BADC2, BADC3, BCCP2, apo-BCCP1, or BSA. Specific activities were calculated for each assay and then normalized to WT control. Four biological replicates were performed for each trial. Error bars denote SEM.

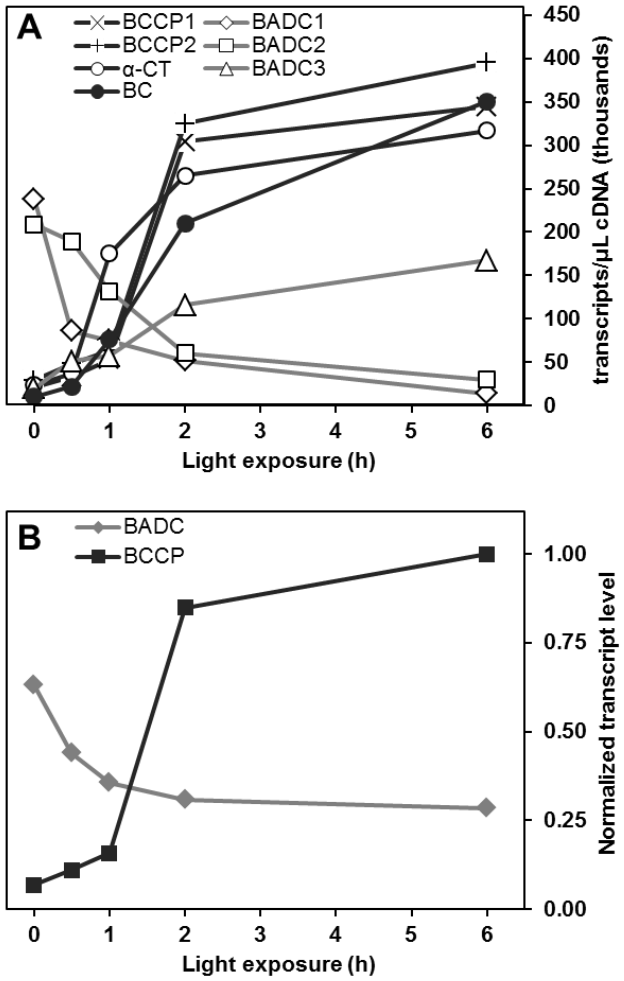

FIGURE 8. Light-dependent changes in gene expression of BADC and htACCase in *A. thaliana* siliques. *A,* Graph shows the absolute expression level of the given genes obtained by qPCR. Ten d old *A. thaliana* siliques were collected after various amounts of light exposure. RNA extracted from these tissues was used to create cDNA for this analysis. Average values of four biological replicates are shown. Standard error was approximately 5 to 10 percent for all data points. *B,* Graph depicts the shift in BADC and BCCP total transcript level in response to light. The sum of transcript levels from BCCPs and BADCs in (*A*) for each time point were normalized to the sum of BCCP transcripts at six hours light exposure. At T=0, the ratio of BADC:BCCP transcript is 9:1. At T=6, the ratio has shifted to 1:4.

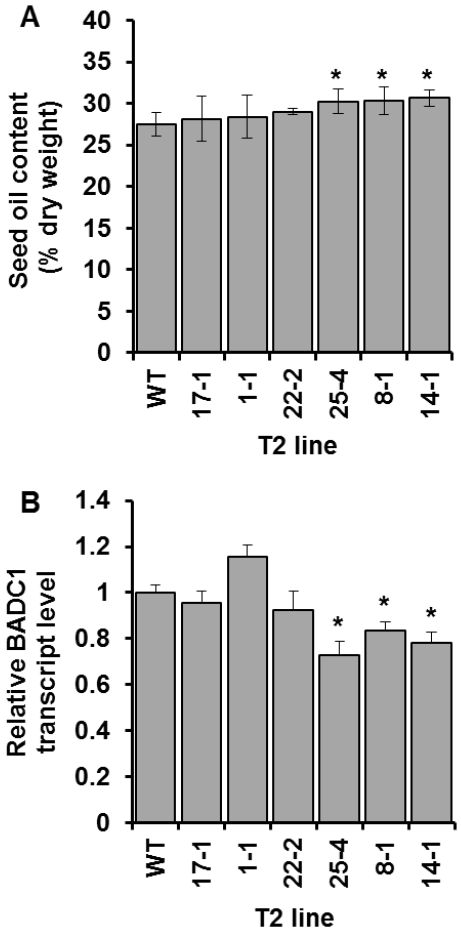

FIGURE 9. Seed specific RNAi silencing of BADC1 increases seed oil content in *A. thaliana*. *A*, Bar graph shows total seed oil content in WT and basta-resistant T_2 *A. thaliana* lines containing a construct that silences BADC1 expression in the seed. Each data point represents the average of four plants. Error bars denote SD. *B*, RT-PCR analysis of BADC1 RNAi silencing lines. BADC1 transcript level was quantified relative to Actin transcript level and normalized to WT. RNA used for analysis was extracted from four biological replicates of ten d old siliques. Error bars denote SEM. In both graphs, statistical significance was determined by Student's t-test (*, $P < 0.05$).

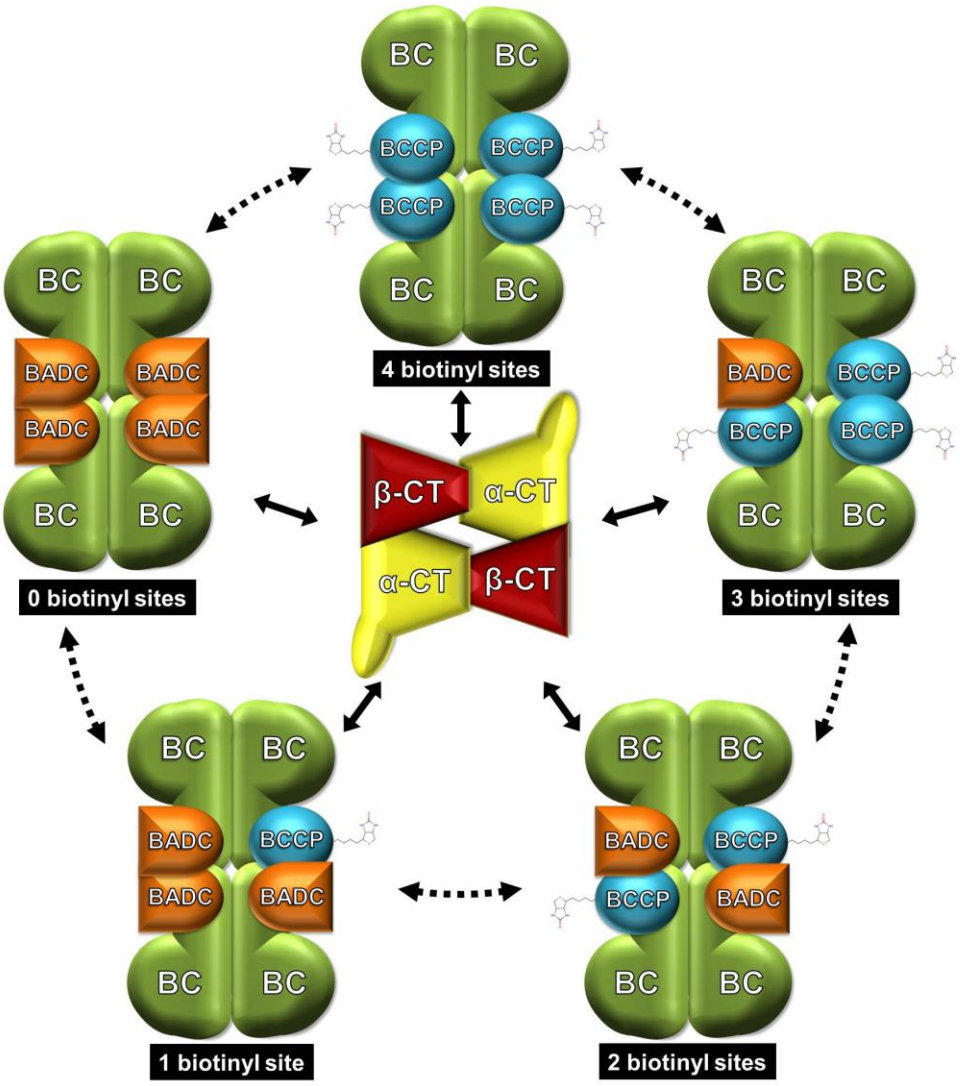

FIGURE 10. Model of BADC competitive inhibition of htACCase. Schematic illustrating the proposed mechanism of BADC inhibition. The BC/BCCP subcomplex design was made based on the crystal structure in *E. coli.* (97), consisting of two dimers of BC and four BCCP proteins. The BADC proteins compete with BCCP for binding to BC. Binding of BADC prevents binding of the essential BCCP subunit. The pool of BC/BCCP and BC/BCCP/BADC subcomplexes then compete for interaction with the CT subcomplex (design based on crystal structure in *E. coli* (20)) , leading to variable reductions in ACCase activity. While a transient association of the two ACCase half reactions is known, it is unclear whether BADC can displace BCCP from an assembled BC/BCCP subcomplex, hence the dashed arrows. Abbreviations: BC, biotin carboxylase; BCCP, biotin carboxyl carrier protein; BADC, biotin/lipoyl attachment domain protein; CT, carboxyltransferase.

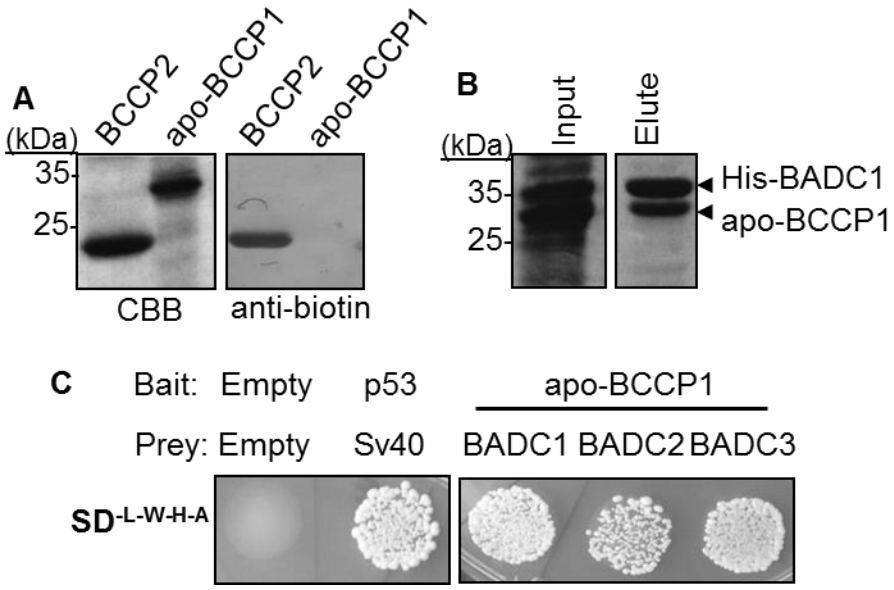

FIGURE 11. Biotinylation is not required for BADC-BCCP interaction. *A*, Purified recombinant His_6-tagged BCCP2 or apo-BCCP1 was resolved by SDS-PAGE and stained with Coommassie Brilliant Blue or blotted with anti-biotin antibody. *B,* Coomassie-stained gels showing the elution fractions of Ni^{2+}-NTA-purified protein from *E. coli*. Input shows both proteins are expressed. Apo-BCCP1 was strongly present in the elution fraction with His_6-BADC1. Protein identities were confirmed by LC-MS/MS. *C.* Strain AH109 yeast was transformed with bait and prey constructs containing the genes shown and plated on media lacking Trp, Leu, His, and Adenine. Empty vector negative control showed no growth. Sv40 and p53 were used as a positive control. Results shown are representative of three biological replicates.

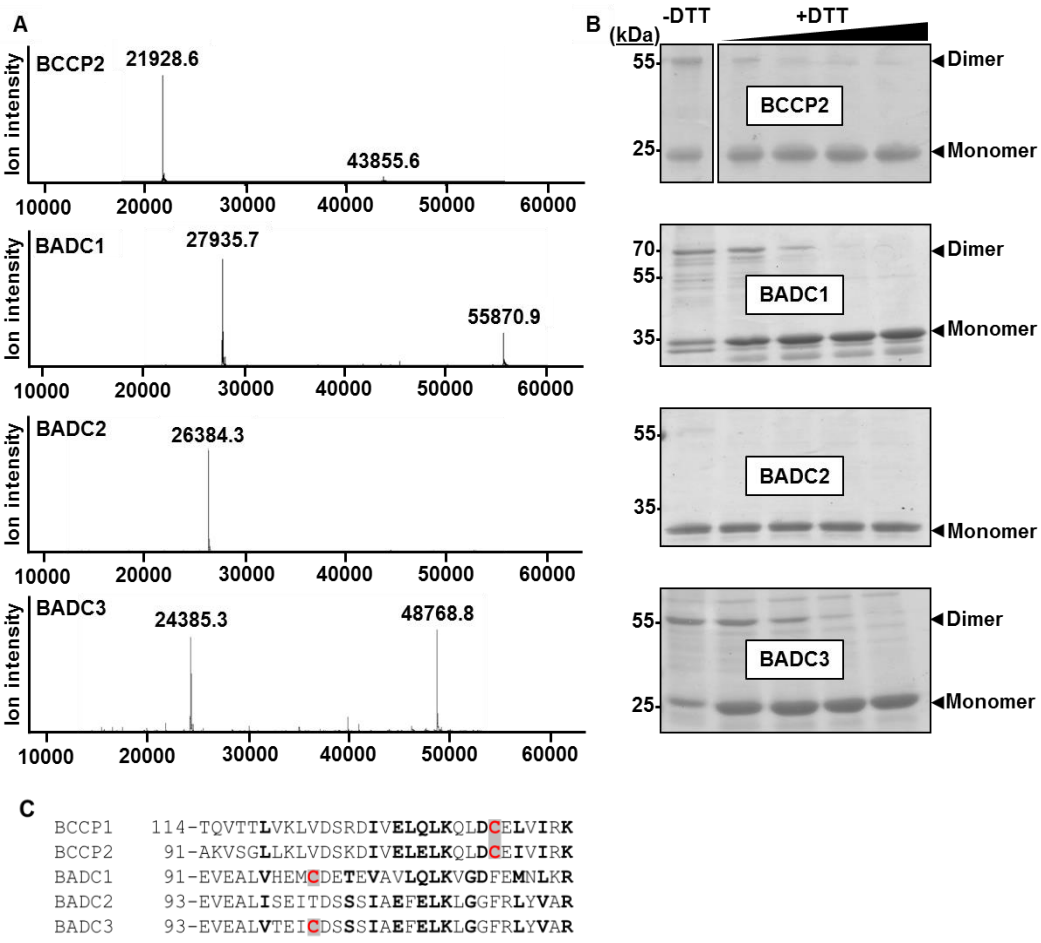

FIGURE 12. Recombinant BADC proteins form heterodimers through disulfide bonds. *A,* Spectra show the intact mass spectrometry analysis of purified recombinant BCCP2, BADC1, BADC2, and BADC3. All proteins showed a monomer and dimer peak except for BADC2. *B,* Purified recombinant proteins were incubated in 3x SDS sample buffer containing 0 mM, 1 mM, 2.5 mM, 5 mM, or 10 mM DTT and resolved by SDS-PAGE and Coomassie-stained. Monomer and dimer bands are marked. Protein identities were confirmed by mass spectrometry. Gels are representative of three replicates. *C,* Clustal alignment of partial protein sequences from the shown proteins. Cys residues are highlighted in red. Conserved residues are in bold.

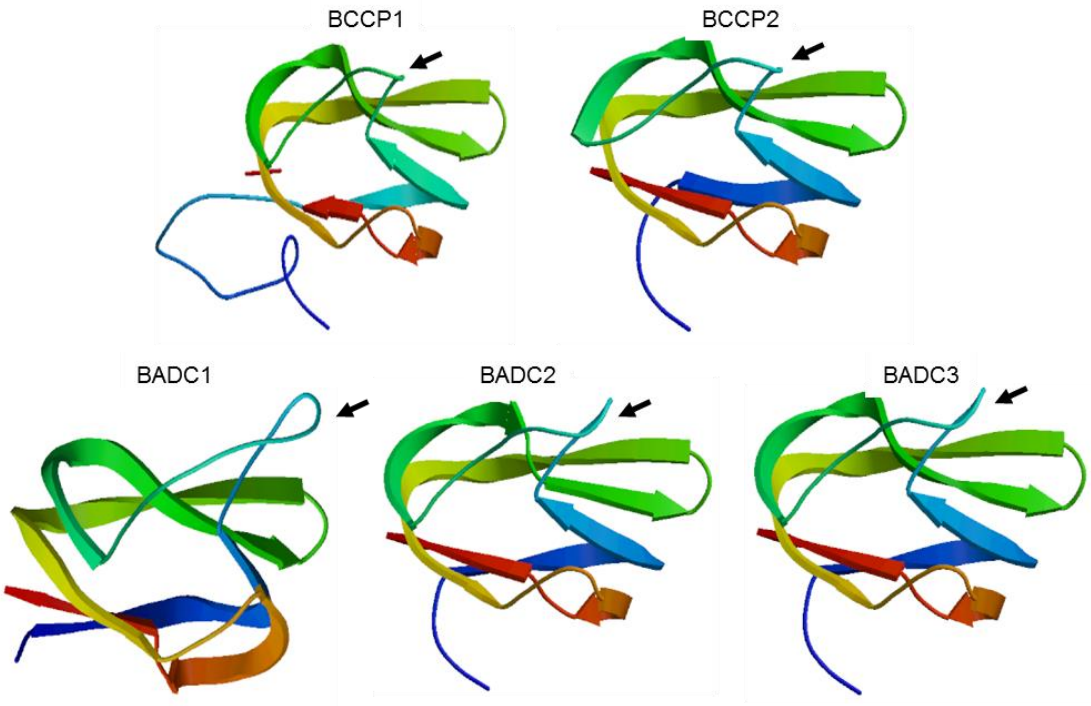

FIGURE 13. Predicted structures of BADC proteins resemble BCCP subunits of ACCase in *A. thaliana*. Structures of each protein were generated using SWISS-MODEL. The solved structure for *E. coli* BCCP (PDB 4HR7) was the closest matching solved structure to all five proteins and was used as a template. Protein sequences lacking the predicted transit peptide residues were used as the input. The N-and C-termini are colored blue and red, respectively. Arrows indicate thumb domain.

FIGURE 14 Alignment of BCCP and BADC isoforms in *Arabidopsis thaliana.* Multiple sequence alignment of the two BCCP and three BADC isoforms found in Arabidopsis. The full primary sequence was used in this alignment. *, residue identity conserved; :, residue chemistry/structure conserved in all proteins; ., residue chemistry/structure conserved in most proteins.

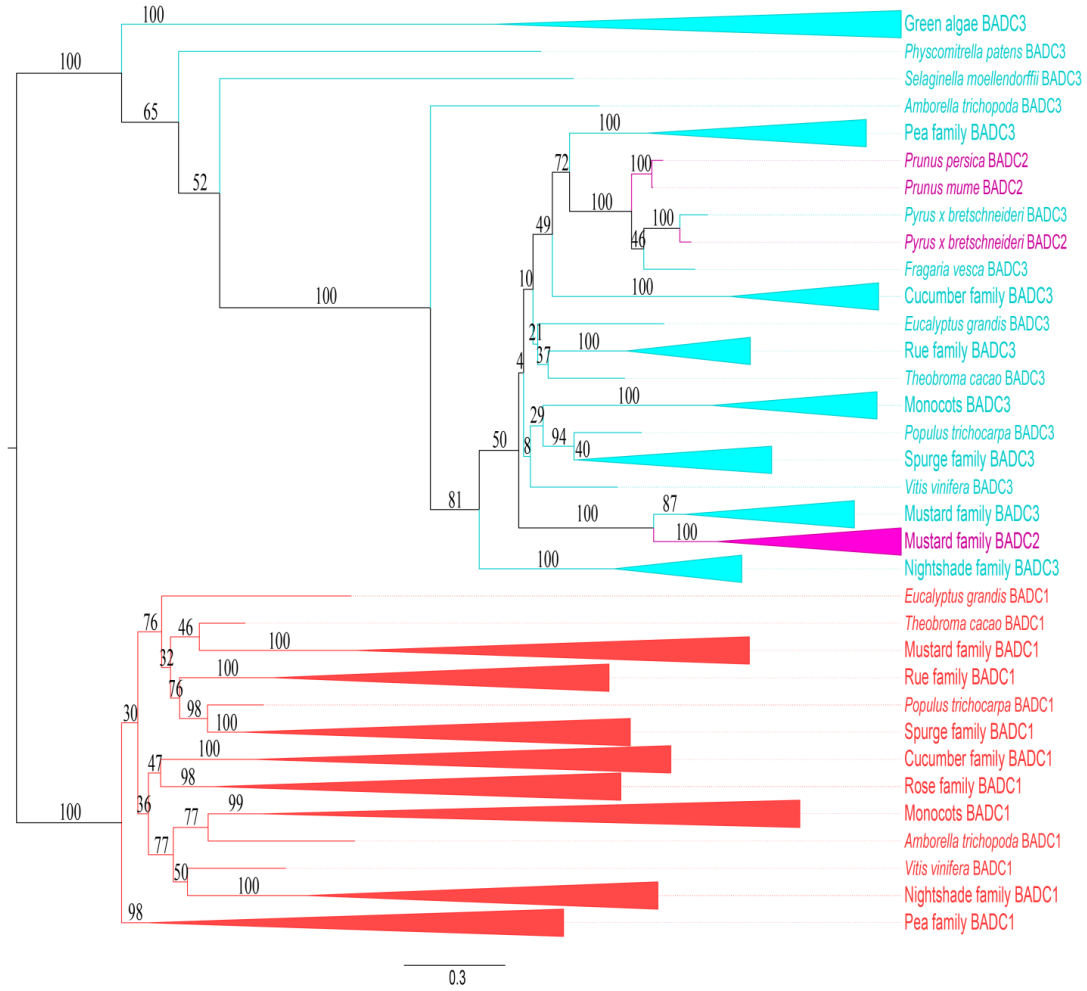

FIGURE 15. A maximum-likelihood phylogenetic tree of BADC full-length proteins: BADC1, BADC2, and BADC3 clades are shown in red, purple, and blue, respectively. The confidence support for each branch from 1000 bootstrapping iterations is noted. The unit length of branches represented 0.3 substitutions per amino acid site.

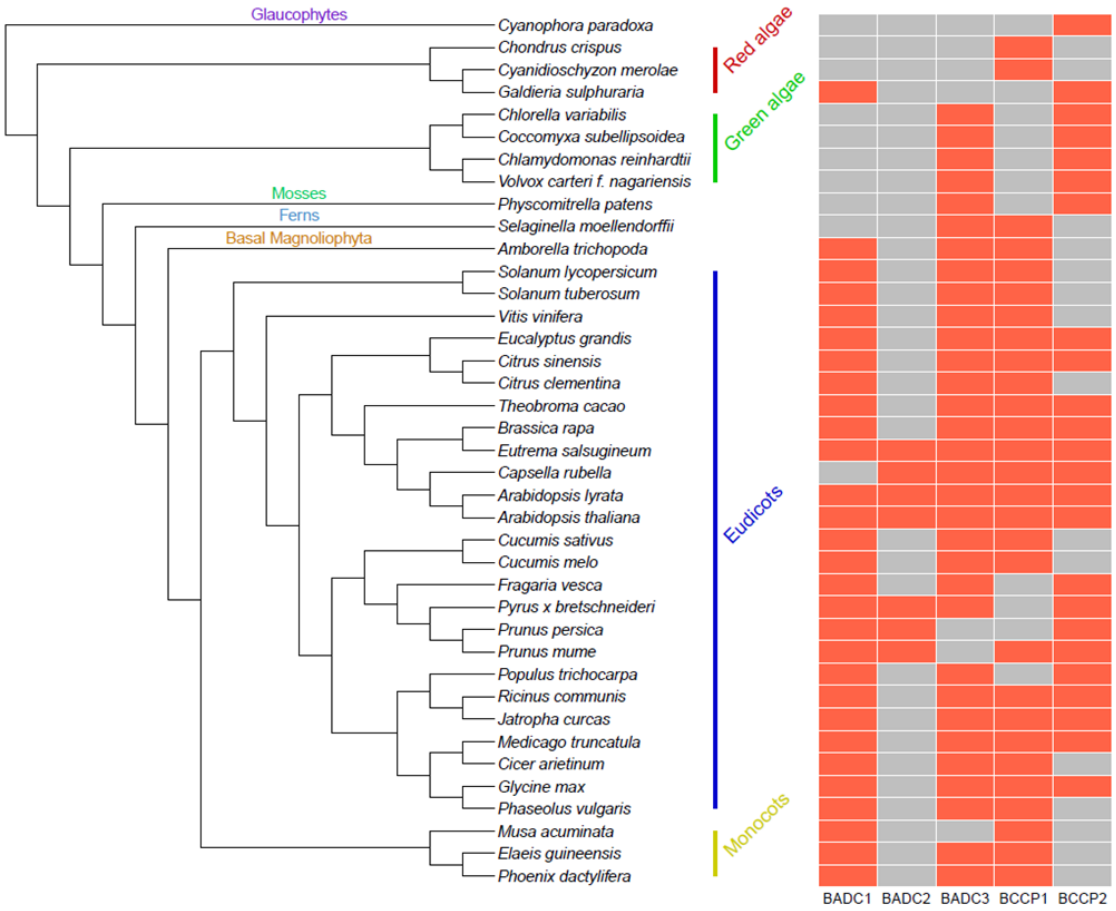

FIGURE 16. Co-occurrence of BADC and BCCP proteins during evolution of plant kingdom. A schematic illustrating the species included in the co-occurrence analysis. At left, an unrooted taxonomic tree depicting the relation of each species is shown. Species names are in black, clades are in various colors. At right, boxes indicate whether the given species contains an ortholog to AtBADC or AtBCCP (red, yes; grey, no).

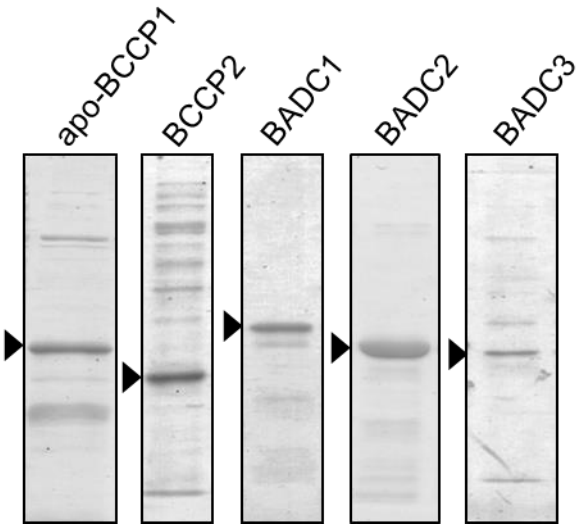

FIGURE 17. Purity of recombinant protein purifications for ACCase activity assays. Coomassie-stained SDS gels show the purity of Ni^{2+}-NTA purified recombinant proteins that were used in the ACCase activity assays.

A

Name	Accession	Sequence
BCCP1 sense	AT5G16390	5'-CATATGTCAGCTGAAGGAAAGGAGAAAAACTCATTG-3'
BCCP1 anti-sense		5'-GGATCCCTACGGTTGAACCACAAACAGAGGAG-3'
BCCP2 sense	AT5G15530	5'-CATATGGAATTTATGGCTAAAGTCTCTGGTCTT-3'
BCCP2 anti-sense		5'-GGATCCTCAAGGTGCGATGACAAAAAGAG-3'
BADC1 sense	AT3G56130	5'-GAATTCGCTAAGGCCGCTAAATCTTCGAC-3'
BADC1 anti-sense		5'-CTCGAGTCACTGGATGTTGATGTCGTG-3'
BADC2 sense	AT1G52670	5'-CATATGACGACTCTGCGATCTGTGAAAGCT-3'
BADC2 anti-sense		5'-GGATCCTTACTGAAGCTTCTTGATGCCAGGA-3'
BADC3 sense	AT3G15690	5'-CATATGGCTGTCCAAGTGTCTACTGTCCC-3'
BADC3 anti-sense		5'-GGATCCTTACTGAAGCTTCTTGATCCCAGGG-3'
apo-BCCP1 mutant sense	AT5G16390	5'-GCATTGTTGAAGCCATGAGGTTAATGAATGAAATA-3'
apo-BCCP1 mutant antisense		5'-TATTTCATTCATTAACCTCATGGCTTCAACAATGC-3'

B

Name	Predicted target peptide length
BCCP1	82
BCCP2	87
BADC1	56
BADC2	47
BADC3	54

FIGURE 18. Primers used in cloning experiments. Primer sequences used to create constructs for recombinant protein expression and yeast two hybrid experiments.

CHAPTER III

ESTABLISHING A ROLE FOR MULTISITE PHOSPHORYLATION OF THE ALPHA-CARBOXYLTRANSFERASE SUBUNIT TO PLASTID HETEROMERIC ACETYL-COA CARBOXYLASE

INTRODUCTION

Biochemical regulation can be exerted on an enzyme in multiple ways. One way is through protein-protein interactions. As was demonstrated in the previous chapter, protein-protein interactions can have significant effects on enzyme activity. A second mechanism of enzyme regulation is post-translational modifications (PTM). Over 300 different PTMs to proteins have been discovered (118,119). These PTMs expand the functionality of the genome by allowing single proteins to behave in more than one way. One of the most well documented PTMs is phosphorylation. Proteins can be phosphorylated on the side groups of multiple amino acid residues, namely Ser, Thr, and Tyr. Phosphorylation is involved in almost every cellular process, including protein localization, protein stability, multiprotein complex formation, and enzyme activity (120-122). Like most PTMs, phosphorylation occurs relatively quickly in relation to gene expression and is reversible, allowing for immediate changes to a specific cellular process when required.

Phosphorylation has been observed on htACCase in plants. The β-CT subunit was previously shown to undergo Ser phosphorylation (71). This PTM was shown to be prevalent after plastid light exposure and suggested to have a positive effect on CT activity, but the modified Ser residue(s) was never identified. Phosphorylation was also observed on the α-CT subunit through a 2D gel-based phosphoproteomic screen of developing rapeseed (72). Later, phosphorylation on Ser^{741} and Ser^{744} in the non-catalytic C-terminal domain was identified from three independent phosphoproteomic screens of Arabidopsis tissues, one of which was in developing *A. thaliana* seed (73-75).

The functional significance of these phosphorylation events on htACCase remains unknown. These sites are located near the C-terminus of α-CT in a region that is predicted to contain coiled-coil domains (Fig. 19). Coiled-coil domains are known to be involved in protein-protein interactions (for review, see (123)), so it is possible that phosphorylation at one or both of these sites could affect the interaction of α-CT with other proteins. For example, the CT subunits were previously shown to associate with the inner envelope of the plastid through a non-ionic interaction (69). Since no acyl modification to these subunits has been identified, it appears likely that CT interacts with an integral membrane protein in the inner envelope. Phosphorylation of α-CT may be involved in this interaction as envelope association is fractional (69). Additionally, α-CT phosphorylation could affect htACCase complex formation given the location of the phosphorylation events. The solved crystal structure of the CT subcomplex in *E. coli* was shown to be a $\alpha_2\beta_2$ heterotetramer (20). Phosphorylation of α-CT in plants could prevent or encourage the formation of the CT subcomplex.

A preliminary study of the functional role of α-CT phosphorylation by Swatek suggested that phosphorylation might have a negative effect on htACCase activity in *A. thaliana*. Stable transgenic lines expressing a phospho-mimic α-CT mutant, where Ser^{744} was mutated to Asp, showed a reduction in total seed oil content of approximately 30% in two lines (124). Additionally, amino acid sequence analysis of eudicot species containing the C-terminal domain showed that Ser^{744} is conserved among more species than Ser^{741} (124). Together, these results suggested that Ser^{744} might be an important phosphorylation site that negatively affects htACCase activity. It was hypothesized that

preventing phosphorylation at this site would increase htACCase activity and result in higher seed oil content. Increased ACCase activity has been shown to lead to higher seed oil content in at least one other case (13). To test this hypothesis, two stable transgenic lines expressing the phospho-deficient S744A α-CT mutant were analyzed (124). However, no increase in seed oil content was observed. One reason for this result could be that the change in seed oil content was marginal and could not be statistically differentiated from the control based on the two lines analyzed. It is possible that htACCase activity increased slightly, but enzyme activity was not measured in this study. Therefore, further analysis of more stable transgenic lines expressing α-CT mutants is necessary.

This chapter summarizes the analysis of 16 stable transgenic lines expressing different α-CT mutants. Specifically, phosphomimic or phospho-deficient mutations were made to Ser^{744}, as was done previously, as well as both Ser^{741} and Ser^{744} to test for any synergistic or antagonistic effects. As a result, some lines showed statistical differences from empty vector (EV) controls, but no consistent trends were observed among specific mutants. However, the results presented here suggest that over-expression of α-CT, regardless of mutation, can increase htACCase activity. This change could have masked the effect of the mutations to α-CT.

EXPERIMENTAL PROCEDURES

Plant Material and Growth Conditions

Transgenic plants (empty vector, GmUbi-α-CT, GmUbi-S741A, GmUbi-S741D, GmUbi-S744A, GmUbi-S744D, GmUbi-AA, GmUbi-DD) were grown in a growth chamber with

12 h day (23^{o} C, 50% humidity, light intensity 100 µmol m^{-2} s^{-1}) and 12 h night (20^{o}C, 50% humidity). Plants were grown to maturity in 8 cm x 8 cm pots and seed was harvested from dry plants. Four plants were grown in each pot. Pots were randomly placed throughout the growth chamber to control for variable growth conditions and natural plant-to-plant variation (116).

Gene Construct Design

α-CT (At2g38040) and site-directed mutant (S741A, S741D, S744A, S744D) genes were synthesized by GeneArt (Carlsbad, CA, USA) using GeneOptimzer® technology for stable and increased protein expression levels. α-CT and site-directed mutants were cloned into a pMD1 series plasmid containing a *Glycine max* ubiquitin promoter, pMGmUbi (125), using *Xba*I and *Xho*I restriction enzymes. The AA and DD double mutant constructs were created by performing site-directed mutagenesis on the S741A and S741D constructs previously (124). All assembled binary vectors were sequenced verified.

Arabidopsis transformation and selection

Binary vectors (pMGmUbi::α-CT, pMGmUbi::S741A, pMGmUbi::S741D, pMGmUbi::S744A, pMGmUbi::S744D) were transformed into *Agrobacterium tumefaciens* strain GV3101 (pMP90RK) using a previously described freeze-thaw transformation procedure (126). Insertion of the binary vectors into Agrobacterium was confirmed through kanamycin (Kan) selection and restriction enzyme digestion of

purified plasmids with *Xba*I and *Xho*I. Arabidopsis plants 5-6 weeks of age were transformed using a previously described floral dipping method (115). After Agrobacterium-mediated transformation, plants were grown for 3 weeks and seed was collected. Seeds harboring the transgene were identified through Kan selection (50 mg ml^{-1}) on sterile 1/2x Murashige and Skoog media containing 1% phyto agar. After 2 weeks of growth, Kan-resistant T1 plants were transferred to soil. This process was repeated until homozygous T3 plants were obtained. α-CT over-expression was monitored in two-week-old T3 leaf tissue with α-CT antibodies (*see western blotting section below*). This process was repeated until T3 homozygous plants with greater than two-fold α-CT over-expression were obtained.

Western blotting

Two-week-old Arabidopsis leaf tissue was harvested and pulverized in 100 µL of SDS-PAGE sample buffer (60 mM Tris-HCl, 60 mM SDS, 5% (v/v) glycerol, 2 mM DTT, pH 6.8), heated at 95^{o}C for 10 min, and centrifuged at 15,000 x g for 10 min. The supernatant was removed and used for protein quantitation using BCA protein assay. Total protein (10 µg) was resolved by SDS-PAGE and transferred to PVDF using standard conditions. Blots were probed using α-CT antibody similarly to Thelen et al., 2002 (47). Signal intensity of immunoblots was determined using ImageJ. Duplicate gels were stained in Coommassie Brilliant Blue and the intensity of RuBisCO large subunit was used as a loading control.

Lipid Analysis

Prior to analysis, seeds were dried over desiccant at 22 °C for one week. Approximately five milligrams of dry seeds was weighed using an analytical balance capable of measuring sub-milligram values. The derivitization process was performed in a glass round bottom Teflon lined cap tube. Fatty acid methyl ester (FAMEs) derivitization was performed in methanol containing 5% (v/v) sulfuric acid and 0.2% butylated hydroxyl toluene. Heptadecanoic acid (17:0) was added as an internal standard (75 µg). The final volume of toluene was brought up to 315 µL. Samples were heated at 95^{o}C for 1.5 h, removed from the heat block, and cooled to room temperature. FAMEs were extracted by adding 1.5 mL of 0.9% (w/v) NaCl and 1 mL hexanes. Samples were vortexed for 15 s and centrifuged at 3,000 x g for 1 min. The top hexane phase was transferred to a clean glass sample vial and stored at -80 °C until analysis.

FAMEs analysis was performed using gas chromatography (Agilent model 6890N gas chromatograph). FAMEs were loaded by split injection and separated using a 30 m, 0.25 mm i.d., cyanopropyl-methylpolysiloxane capillary column (Agilent Technologies, Santa Clara, CA) and detected using flame ionization detection. Standard method parameters included an oven temperature from 150^{o}C to 200^{o}C at 2^{o}C min^{-1} with an initial pressure of 120 kPa. Retention times and peak areas were used to identify and quantify individual FAs, respectively. Six to ten biological replicates were analyzed per transgenic line. Each biological replicate consisted of approximately 5 mg *A. thaliana* seeds from an individual plant.

Principal component analysis

Fatty acid mole percentages of all lines were collected and standardized. Then a principle component analysis was carried out to find the most significant principle dimensions. The most significant five dimensions were extracted since these five dimensions explain majority (> 85%) of the variation in observations.

ACCase activity assays

Activity of htACCase was detected using the method stated previously (*see Chapter II*). Three 21-d-old seedlings were pulverized in 150 µL ice-cold homogenization buffer and assayed immediately. Haloxyfop was included in the homogenization buffer to inhibit homomeric ACCase activity. Actual specific activity was calculated by subtracting minus acetyl-CoA controls from trials. Protein concentrations were quantified by Bradford assay using bovine gamma globulin as standard.

RESULTS

C-terminal domain of α-carboxyltransferase

Although the α-CT subunit of htACCase is present in prokaryotes, green algae, and land plants, the primary sequence is only semi-conserved among organisms. All α-CT orthologs share one characteristic carboxyltransferase domain (*Acc*A Pfam-A match), but eudicots contain an extended C-terminal domain that is not found in prokaryotes or ancient vascular plants (Fig. 19A). In *A. thaliana*, this C-terminal domain is approximately 370 amino acids long and contains three regions that are predicted to

form coiled coils (Fig. 19B). A previous study showed that Ser^{744} is more conserved than Ser^{741} among Brassicaceae species containing the C-terminal domain and suggested phosphorylation at this site may have a more pronounced regulatory role for htACCase (124) (Fig. 19C). To test this hypothesis, stable transgenic lines expressing various site-directed α-CT mutants (S744A, S744D, S741A + S744A (AA), and S741D + S744D (DD)) were created and analyzed. These mutations are depicted on the α-CT primary sequence in Fig. 19D.

Generation of homozygous transgenic lines and quantitation of α-carboxyltransferase protein content

To characterize the role of α-CT phosphorylation, native and site-directed mutagenized forms of codon optimized, synthetic α-CT genes were constitutively over-expressed or expressed, respectively, in *A. thaliana* tissues. Constructs containing Ser^{744} to Ala (S744A) or Ser^{744} to Asp (S744D) mutations in the α-CT gene were made previously by Swatek and transformed into *A. thaliana* (124). Bulk T_0 seed from this previous study was screened by Kan-resistance to identify more independent lines. Independent lines were propagated until homozygous T_3 lines were obtained. Additionally, site-directed mutagenesis was performed on the S744A and S744D constructs to mutate Ser^{741}. These constructs, termed 'double-mutants', were designed to contain a Ser to Ala mutation (AA) or Ser to Asp (DD) mutation to both Ser^{741} and Ser^{744}. Sequence-confirmed constructs were used to transform *A. thaliana* and T_0 seeds were screened for

gene insertion by Kan-resistance. Screening was repeated until homozygous T_3 lines were obtained.

One potential issue with these transgenic lines was the presence of endogenous α-CT. To outcompete the endogenous subunit effect, the α-CT transgenes were expressed under the control of a *Glycine max* ubiquitin promoter (GmUbi), reported to have 2- to 7-fold higher expression levels compared to a standard CaMV 35S promoter (125). Promoter expression was previously demonstrated to be ubiquitous in *A. thaliana* through GUS expression driven by the GmUbi promoter (124).

Expression level of α-CT in homozygous T_3 lines was monitored by western blotting (Fig. 20). Independent transgenic lines showing at least two-fold expression of α-CT compared to EV controls were used for further analysis.

Seed oil content of independent lines containing two-fold higher levels of α-carboxyltransferase protein

To determine the effect of native α-CT overexpression or mutant expression on seed oil content, total seed oil was quantified from plants of independent lines containing at least two-fold α-CT protein levels than EV controls. FAMEs extracted from dry T_4 seed were analyzed by gas chromatography-flame ionization detection (GC-FID). Results from this analysis showed that three lines were statistically lower than empty vector control, specifically α-CT OX 8-6, S744D 3-4, and S744D 9-3 (Fig. 21). Unexpectedly, the other α-CT OX and S744D lines showed no difference in seed oil content. Similarly, line

S744A 5-8 contained significantly higher seed oil content, while the other lines showed no difference.

Fatty acid profile of two-fold expressing independent lines

To further characterize the fatty acid (FA) composition in α-CT OX and mutant T_4 seeds, the mole percent distribution of individual FAs was calculated (Table 4). The oil content determinations described above are comprised of seven long-chain FAs (LCFA) and seven very-long chain FAs (VLCFA). The LCFAs are palmitic (16:0), palmitoleic acid ($16:1^{\Delta 9}$), stearic (18:0), oleic ($18:1^{\Delta 9}$), vaccenic ($18:1^{\Delta 11}$), linoleic ($18:2^{\Delta 9, 12}$), and linolenic ($18:3^{\Delta 9, 12, 15}$). The VLCFAs are arachidic (20:0), and eicosenoic ($20:1^{\Delta 11}$), paullinic ($20:1^{\Delta 13}$), eicosadienoic ($20:2^{\Delta 9, 12}$), eicosatrienoic ($20:3^{\Delta 9, 12, 15}$), behenic (22:0) and erucic ($22:1^{\Delta 13}$). Unexpectedly, almost all lines showed significantly increased levels of oleic and vaccenic LCFAs with compensatory reductions in levels of linolenic, eicosenoic, and eicosadienoic VLCFAs regardless of α-CT mutation. In previous reports, seed oil content was shown to directly correlate with oleic and linoleic acid levels, and inversely correlate with linolenic acid level (13,40,47). By these criteria, seed oil content should have been higher in most of the transgenic lines analyzed. Since only one line was observed to have increased seed oil content, these data are not consistent with the previous observations.

VLCFA-to-LCFA ratio suggests de novo fatty acid synthesis rate increased

Changes in the rate of *de novo* fatty acid synthesis (FAS) in seeds can be inferred by monitoring changes in the VLCFA-to-LCFA ratio. Previous studies have suggested a direct correlation between the VLCFA-to-LCFA ratio and *de novo* FAS rate (40,127,128). Interestingly, this ratio was significantly lower in all α-CT OX and S744A lines, as well as two DD lines. In addition, S744D line 1-2 was significantly lower, while lines 3-4 and 4-1 were significantly higher.

Principle component analysis of transgenic lines

To identify subtle differences between the transgenic lines, principle component analysis was performed using the fatty acid mole percentages from all lines. These analyses showed the most variation among the first three principle components. Visualization of principle components two and three showed very distinct groupings between EV line 3-14 and the two α-CT OX lines, suggesting the two groups are different (Fig. 22). Additionally, the majority of plants expressing the S744A mutant grouped with the α-CT OX cluster, while the majority of plants expressing the S744D mutant grouped with the EV cluster. Plants expressing the AA mutant showed no obvious grouping. Finally, plants expressing the DD mutant grouped in between the EV and α-CT OX clusters.

htACCase activity increases in transgenic lines regardless of mutation

The present data suggest that *de novo* FAS rates, as well as htACCase activity, are increased in transgenic plants that overexpress α-CT whether the protein is expressed natively or with a mutation. However, only one line, S744A 5-8, contained significantly

more oil than the EV control. These results could be explained by the fact that htACCase activity did not change in these transgenic lines, or that increased flux through *de novo* FAS resulted in a bottleneck prior to triacylglycerol synthesis. To clarify these hypotheses, htACCase activity was monitored in 21 d old leaves of the T_3 transgenic lines.

Surprisingly, all lines tested contained significantly higher specific htACCase activity compared to EV control (Fig. 23). No statistical difference was observed between α-CT OX, S744A, and S744D lines. This result demonstrated that htACCase activity, and possibly *de novo* FAS rates, did increase in these lines as a result of increased α-CT expression. Mutagenesis of Ser^{744} had no significant effect on enzyme activity, as these lines were similar to the wild type α-CT overexpression line.

DISCUSSION

The aim of this study was to determine the effect of α-CT phosphorylation on htACCase activity and seed oil content in *A. thaliana*. Since the phosphorylation sites are located near the C-terminus within the non-catalytic portion of α-CT, it was expected these mutations would not directly affect activity. However, preliminary evidence suggested that phosphorylation on site Ser^{744} can have a negative effect on htACCase activity (124). This hypothesis was inferred based on the observed reduction in seed oil content in transgenic lines expressing the S744D α-CT mutant. To further establish this finding we performed a more systematic analysis of the two principal phosphorylation sites for Brassicaceae α-CT, including double mutants and more independent transgenic events

to account for transgene positional effects. Furthermore, we also quantified the specific activity of ACCase in select varieties with strong expression and a phenotype.

Activity analysis was performed on plants that contained at least two-fold expression of α-CT protein (Fig. 20). Unexpectedly, all lines tested, whether expressing native, S744A mutant, or S744D mutant α-CT, showed increased htACCase activity by approximately 50% on average compared to the EV control (Fig. 23). Since all lines showed higher activity regardless of mutation, these results suggest that increased α-CT expression has a positive impact on htACCase activity which might offset any effect the mutation may have on htACCase function. Furthermore, it can be inferred that α-CT might be the limiting subunit in the htACCase complex, whereby increasing concentration of α-CT leads to a higher specific activity.

Other evidence from this study supports the hypothesis that α-CT over-expression increases the specific activity of htACCase. First, analysis of the fatty acid profile revealed significant changes to certain fatty acids (Table 4). Specifically, increased levels of oleic and vaccenic LCFAs as well as reduced levels of linolenic, eicosenoic, and eicosadienoic VLCFAs were observed in most lines tested. The major products of *de novo* FAS in the plastid are the LCFAs, specifically oleic acid (14). These LCFAs are then exported to the cytoplasm and endoplasmic reticulum for elongation and packaging into triacylglycerols. Therefore, the observed increase in LCFAs and decrease in VLCFAs suggests that *de novo* FAS rates, as well as htACCase activity, were higher (Fig 22). Second, principle component analysis revealed that plants containing two-fold higher levels of α-CT clustered differently than EV controls.

The data presented here suggest that seed oil content should increase in transgenic lines containing two-fold higher α-CT expression since these lines show higher specific htACCase acitivity. Previous reports have shown a direct correlation between htACCase activity and seed oil content (13,47). However, marginal, yet significant, changes to seed oil content were observed in only a few transgenic lines. In agreement with the previous study by Swatek, two lines expressing the S744D α-CT mutant showed an average 9% reduction in seed oil content compared to the EV control (Fig. 21). Additionally, analysis of one line expressing the S744A α-CT mutant showed an increase of about 7% seed oil content. However, one of the α-CT OX lines tested also contained 6% less seed oil content. This observation seems to counter the enzyme activity data. One explanation could be the positional effect of the transgene. There are approximately 600 genes known to be associated with acyl-lipid metabolism (14). Insertion of the transgene into any of these genes could affect total seed oil content. A second explanation could be that the conditions of growth were not optimal for maximal oil deposition in the seed. Although *in vitro* activity assays showed that htACCase activity was higher in lines containing more α-CT protein, these assays were performed using saturating substrate concentrations. Therefore the limiting factor in these experiments was the number of active htACCase complexes. *In vivo,* it is more likely that substrates will be limiting, especially since these plants were not grown under constant, high-intensity light. In this case, the increased amount of α-CT protein could not affect htACCase activity *in vivo*. A third explanation could be the margin of error in the analysis. While seed oil content in some independent lines differed from EV controls

by six to nine percent, the standard error for all lines was approximately six percent on average. Some of the statistical changes could simply be due to the large margin of error in these data.

Finally, no seed oil phenotype was observed for the double mutant transgenic lines. The hypothesis was that the AA and DD mutations would increase or decrease seed oil content, respectively. A conclusive determination of the effect of these mutations was prevented by a lack of statistically significant changes in seed oil content. First, although some of the lines contained approximately ten percent less seed oil content on average, the reductions were not significant due to large standard error. Second, the VLCFA/LCFA ratio was unchanged in six of the eight double mutant lines tested. Third, principle component analysis showed that these plants did not cluster with either the EV control or the α-CT OX lines. Therefore further research is required to determine the effect, if any, of the double mutations on α-CT function.

CONCLUDING REMARKS

This study was performed to determine the function of α-CT phosphorylation in *A. thaliana*. We chose the method described above due to several considerations: 1) Site-directed mutagenesis is the simplest way to mimic or prevent phosphorylation *in vivo*; 2) Seed is the most likely tissue to reveal changes in *de novo* FAS, relative to leaf tissue; 3) Mutant α-CT was expressed in a WT background because α-CT is an essential protein. Creating transgenic lines in an α-CT knockout background would be take a considerable amount of time. However, there was inherent risk in the chosen method for many

reasons. First, these experiments were performed under the assumption that a Ser to Asp mutation mimics a constitutive phosphorylation event. In fact, Asp is not a perfect substitute for phosphorylation due to the increased negative charge, polarity, and bulkiness of the phosphoryl group. At least one previous study has observed that phosphomimics cannot reproduce the effect of phosphorylation (129). Second, seed oil content is a complex phenotype. Although previous reports showed a correlation between htACCase activity and seed oil content, this phenotype can be affected by other factors. Therefore a seed oil phenotype is not strictly dependent on htACCase activity. Third, endogenous α-CT is still present in these transgenic lines and can compete with the mutant α-CT for access to the holo complex, thus producing a dilution effect for any potential mutant phenotype. With these factors, plus the newly observed effect of increased α-CT concentration on htACCase activity, it is not surprising that a consistent phenotype was not observed in the transgenic lines analyzed. Therefore it might be appropriate to focus future research on the testable biochemical effects of α-CT phosphorylation.

From the present data as well as the previous work by Swatek, it appears that the S744D mutation does have a negative effect on seed oil content. Therefore phosphorylation of Ser^{744} might affect α-CT in some way. Ser^{744} phosphorylation could be involved in one of these functions: 1) CT formation or α-CT dimerization; 2) CT activity; 3) CT association with the inner envelope. These possibilities could all be tested biochemically using the S744D mutant protein. First, to test the effect of the S744D mutation on CT formation, S744D mutant protein could be recombinantly

expressed in *E. coli* with β-CT. The *E. coli* CT subunits have been expressed together previously to identify the crystal structure of the subcomplex (20). A similar method could be employed here with the *A. thaliana* subunits by cloning the genes for β-CT and either native or S744D α-CT in tandem into the pETDuet vector. CT complexes could be purified by affinity and size exclusion chromatography and then quantified to determine changes in CT complex formation. Second, CT activity could be specifically tested in these *E. coli* cells using radiolabelling in cell lysates as described previously (63). Third, isolated chloroplasts from S744D expressing transgenic seedlings could be fractionated and analyzed to determine the localization of α-CT quantitatively as described previously (69). Obtaining these data would significantly advance our understanding of the mechanism of α-CT phosphorylation.

It would also be advantageous to identify the kinase responsible for phosphorylation, as well as the spatiotemporal presence of α-CT modification. Identification of the kinase involved could provide clues as to the function of this phosphorylation event given what else is known of the identified kinase. One established technique that could be applied is the KiC assay (130). A synthesized α-CT peptide containing the site Ser^{744} could be screened against a kinase library to identify potential client proteins. To determine the environmental factors affecting α-CT phosphorylation, quantitative identification of the phosphorylation event during different conditions (i.e. seed development, light-dark) could give clues as to when this phosphorylation event is necessary.

In conclusion, the data presented here suggest, but do not confirm, that phosphorylation of α-CT on Ser^{744} has a negative effect on seed oil content in *A. thaliana*. However, the expected negative effect on htACCase was likely mitigated by the observed positive effect of α-CT overexpression *in vivo*. This finding suggests that α-CT might be the limiting subunit of htACCase, whereby increased α-CT expression increases overall enzyme activity and prevents the observation of the negative effect of the mutation. To assess the true effect of α-CT phosphorylation on seed oil content, transgenic lines will need to be generated that lack the endogenous α-CT protein.

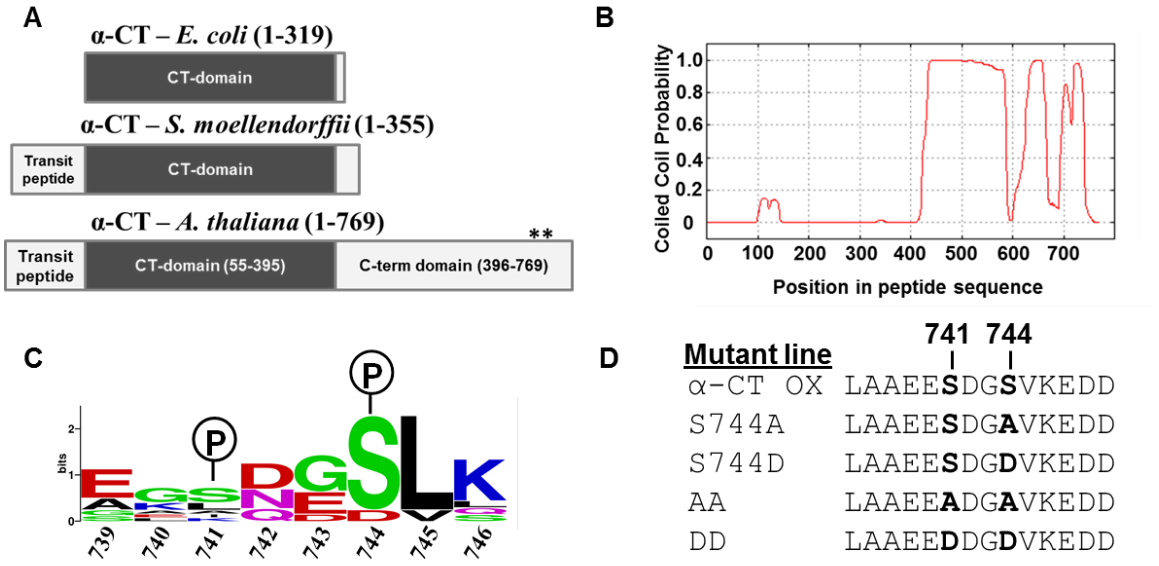

Figure 19. C-terminal domain of α-CT. *A,* Schematic of α-CT sequence in the prokaryote *Escherichia coli* and the vascular plants *Selaginella moellendorffii and Arabidopsis thaliana.* The primary protein sequence for each protein was aligned using ClustalW. The two proteins share a conserved catalytic domain (grey). The plant proteins contain an additional transit peptide, while only *A. thaliana* contains an extended C-terminal domain. Asterisks denote phosphorylation sites Ser^{741} and Ser^{744}. *B,* MARCOIL (131) prediction of coiled-coil domains in the *A. thaliana* α-CT protein. Three regions of the sequence have 100% probability of containing coiled coils. *C,* Conservation of the phosphosites among Brassicaceae species. Weblogo shows that site Ser^{744} is conserved in more species than Ser^{741}. *D,* Sequence alignment shows the various mutations made to the C-terminus of α-CT at site Ser^{741} and Ser^{744} in each mutant line. In α-CT OX lines, native α-CT was over-expressed.

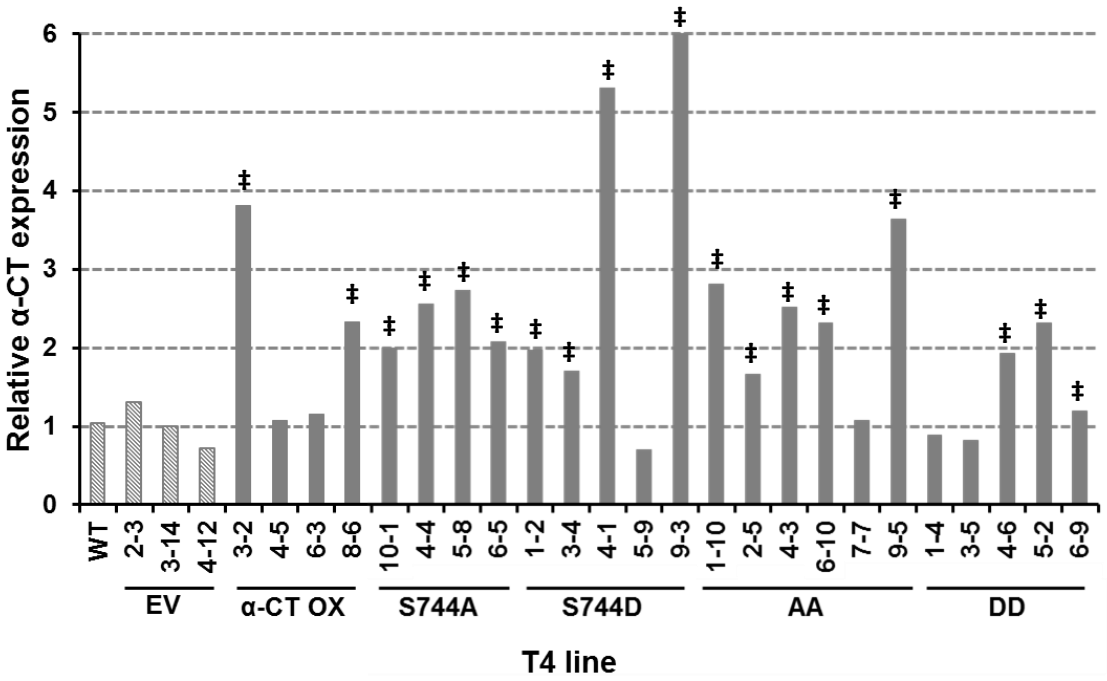

Figure 20. Protein blot densitometry analysis of α-CT and mutant overexpression lines. Total protein (10ug) isolated from two-week old seedlings was resolved by SDS-PAGE and electrophoretically transferred to PVDF membrane for antibody probing. Duplicate CBB-stained gels were used to ensure equal loading. Blots were probed with anti-α-CT antibody. Densitometry analysis was performed using ImageJ software and normalized to EV 3-14 control. ‡, lines showing above or near two-fold expression of α-CT compared to EV 3-14 were used for further analysis.

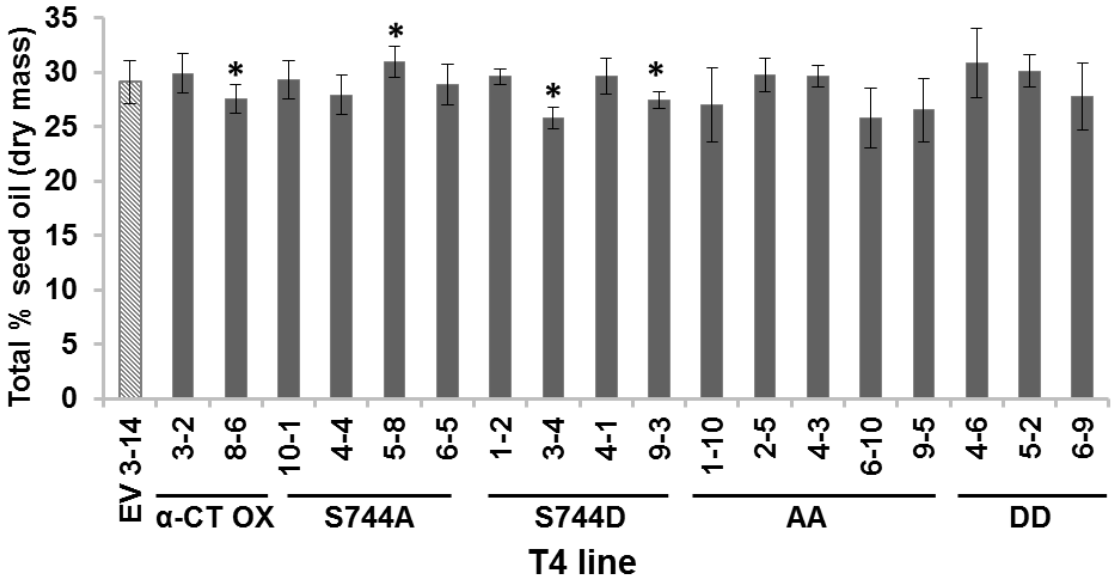

Figure 21. Total seed oil content of transgenic α-CT overexpression line T_4 seeds. Total FA levels were determined using gas chromatographic analysis of fatty acid methyl esters (FAMEs). T_4 seed was obtained from six to eight soil-germinated homozygous T_4 plants. Only lines observed to have two-fold α-CT expression were analyzed. Statistical significance compared to EV 3-14 was determined by Student's t-test (*, $P < 0.05$). Error bars denote standard deviation.

Plant line	Average fatty acid mol %													
	16:0	16:1(9)	18:0	18:1(9)	18:1(11)	18:2 (9,12)	18:3 (9,12,15)	20:0	20:1(11)	20:1(13)	20:2	20:3	22:0	22:1(13)
EV 3-14	8.53	0.36	3.41	14.22	1.36	28.42	18.91	2.12	16.77	1.72	1.81	0.45	0.30	1.63
α-CTox 3-2	8.52	0.36	4.17	16.54	1.61	28.80	16.65	2.30	15.78	1.80	1.52	0.32	0.31	1.31
α-CTox 8-6	8.27	0.37	3.88	16.31	1.68	29.70	15.98	2.29	15.94	1.98	1.57	0.28	0.34	1.42
S744A 4-4	8.94	0.40	3.97	14.90	1.96	28.37	17.51	2.24	15.35	2.12	1.67	0.57	0.34	1.65
S744A 5-8	8.49	0.35	3.40	14.70	1.44	28.71	18.39	2.08	16.65	1.81	1.78	0.41	0.29	1.51
S744A 6-5	8.58	0.37	3.77	15.51	1.70	29.94	16.64	2.20	15.84	1.87	1.64	0.32	0.29	1.33
S744A 10-1	8.71	0.38	4.02	15.86	1.68	29.03	16.84	2.25	15.67	1.90	1.62	0.36	0.32	1.38
S744D 1-2	8.25	0.35	3.40	15.79	1.46	28.89	17.45	2.10	16.63	1.80	1.71	0.37	0.31	1.49
S744D 3-4	8.25	0.41	3.57	14.72	1.89	27.18	18.83	2.58	14.99	2.39	1.82	0.79	0.40	2.16
S744D 4-1	8.34	0.39	3.52	13.85	1.59	27.28	19.36	2.46	16.36	2.14	1.87	0.60	0.37	1.87
S744D 9-3	8.42	0.38	3.74	15.35	1.85	28.50	17.32	2.34	15.87	2.00	1.73	0.48	0.34	1.67
AA -10	8.20	0.38	3.65	16.99	1.61	27.62	17.24	2.33	15.69	1.99	1.59	0.55	0.36	1.80
AA 2-5	8.37	0.34	3.33	14.70	1.41	28.52	18.43	2.11	16.75	1.82	1.82	0.46	0.31	1.61
AA 4-3	8.25	0.35	3.38	15.63	1.45	27.98	18.13	2.12	16.91	1.73	1.72	0.47	0.31	1.57
AA 6-10	8.69	0.43	3.90	14.18	1.84	27.02	18.76	2.57	15.25	2.37	1.81	0.75	0.39	2.04
AA 9-5	8.49	0.39	3.88	16.82	1.67	27.64	16.85	2.35	15.55	2.03	1.61	0.53	0.37	1.82
DD 4-6	8.06	0.34	3.35	15.99	1.61	28.96	16.28	1.96	16.29	3.56	1.63	0.33	0.26	1.39
DD 5-2	8.12	0.34	3.32	16.38	1.58	28.99	17.27	1.96	16.57	1.82	1.62	0.36	0.28	1.38
DD 6-9	8.14	0.38	3.89	15.57	1.71	27.78	17.78	2.45	16.01	2.04	1.64	0.49	0.35	1.75

Legend

= significantly higher than EV ($P < 0.05$)

= significantly lower than EV ($P < 0.05$)

Table 4. Fatty acid composition of transgenic α-CT overexpression line T_4 seeds. Values shown are expressed as average mole % for each fatty acid across six to ten biological replicates. Least squares mean estimate analysis was performed to determine statistical significance. Values in green are statistically higher ($P < 0.05$) and values in red are statistically lower ($P < 0.05$).

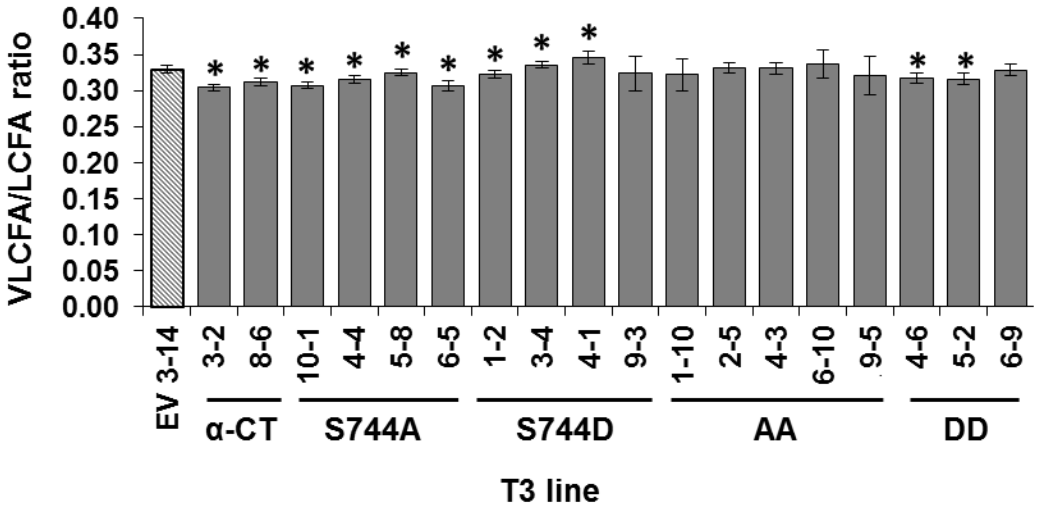

Figure 22. VLCFA/LCFA ratio in transgenic α-CT overexpression line T_4 seeds. Total FA levels were determined using gas chromatographic analysis of fatty acid methyl esters (FAMEs). T_4 seed was obtained from six to ten soil-germinated homozygous T_4 plants. Only lines observed to have two-fold α-CT expression were analyzed. Statistical significance was determined by Student's t-test (*, $P < 0.05$). Error bars denote standard deviation.

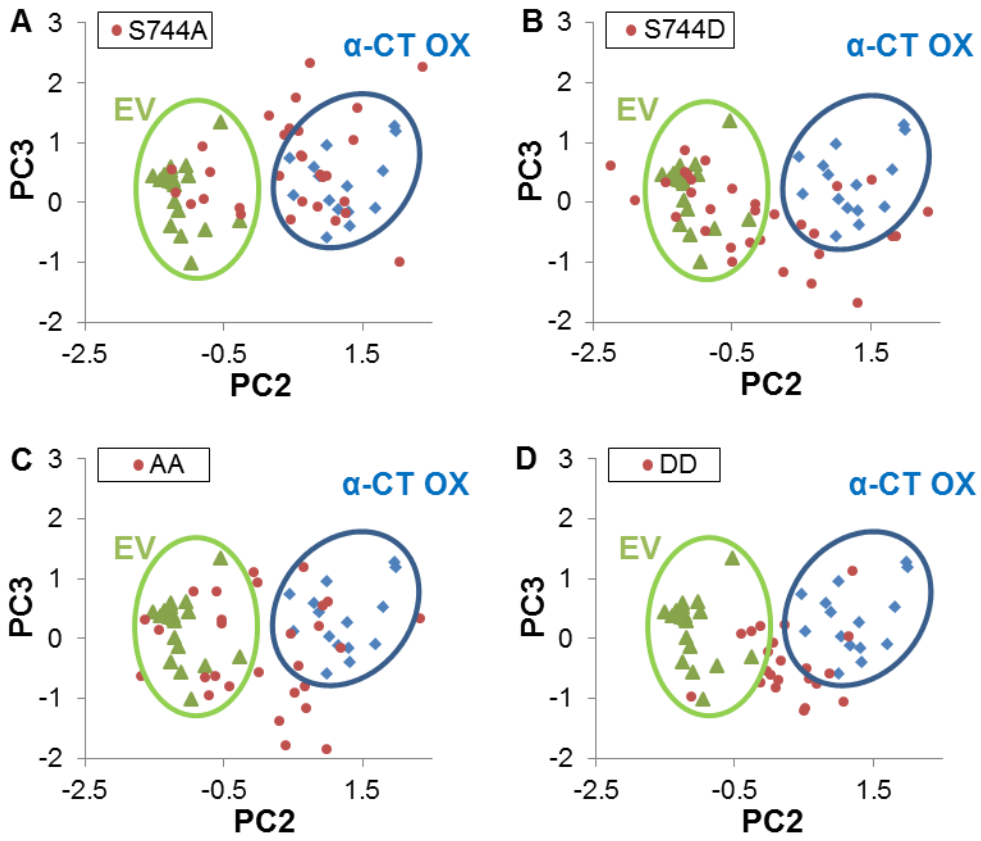

Figure 23. Principle component analysis of transgenic lines. Scatter plots depict the values given to each biological replicate along principle components two and three. Each point represents a single biological replicate (i.e. one plant). Empty vector plants (green triangles) and α-CT OX plants (blue diamonds) form separate clusters, shown with the ovals. Red dots denote the values for plants expressing S744A (*A*), S744D (*B*), AA (*C*), or DD (*D*).

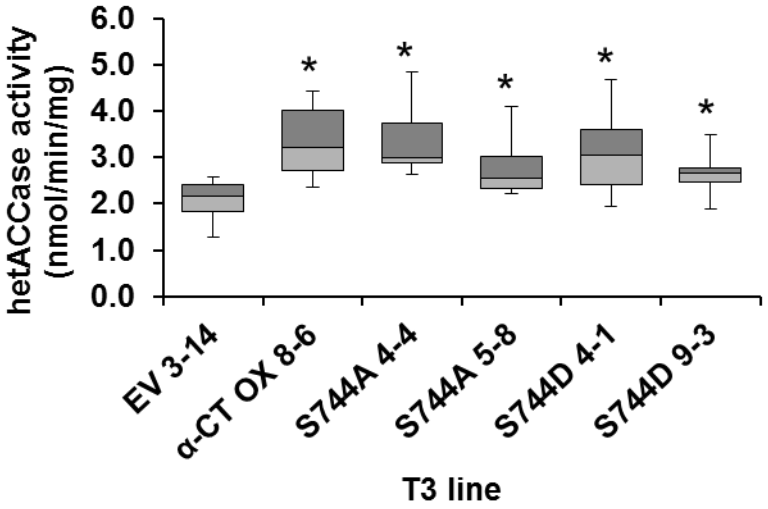

Figure 24. ACCase activity increases in α-CT overexpression lines regardless of mutation. Box and whisker plot shows the specific activity of htACCase in 21 d old leaves of each T4 homozygous line. Specific activity was calculated by dividing the total ^{14}C incorporated into acid-stable products per min per mg of leaf protein extract. Eight biological replicates containing three leaves each were assayed for each independent line. All overexpression lines showed statistically higher htACCase activity that the EV control according to Student's t-test (*, Pvalue < 0.05). S744A and S744D mutant lines were not statistically different from α-CT OX 8-6.

CHAPTER IV

SUMMARY

Fossil fuels have been the main feedstock of reduced carbon since the industrial revolution. The resulting mass relocation of carbon from underground storehouses to the atmosphere has resulted in unexpected consequences to the global climate. These changes, in addition to the estimated growth in global human population, mean that a renewable feedstock is necessary in order to sustain the energy consumption rates of developed and developing countries. Oilseed plants currently represent the best alternative, renewable feedstock of reduced carbon. Decades of research have been dedicated to understanding how plants produce, modify, and store fatty acids in their seed. As was summarized in Chapter I, much has been learned about *de novo* fatty acid synthesis regulation, particularly regarding one of the key enzymes, acetyl-coenzyme A carboxylase (htACCase). This information has attested to the essential role of htACCase in seed oil accumulation. Indeed, previous reports have shown the direct correlation between htACCase activity and seed oil

content (12,47). Therefore, htACCase is a major target of plant biotechnology research. Many of the regulatory mechanisms that have been discovered are still not fully understood. For example, it is well known that acyl-acyl carrier protein can exert feedback inhibition on htACCase, but the mechanism that mediates this inhibition remains unknown. Our understanding of these mechanisms is in part hindered by the lability of the htACCase complex, as it proved difficult to purify and study biochemically using conventional purification techniques. Therefore it was posited that unknown factors, namely protein-protein interactions or post-translational modifications, might be involved in regulating htACCase activity. Identification of these factors could allow for a novel method of increasing htACCase activity, as well as seed oil content, in crops.

The first aim of this study was to comprehensively identify any unknown protein-protein interactions involving htACCase in *Arabidopsis thaliana.* Using co-immunoprecipitation coupled with tandem mass spectrometry, this goal was achieved and led to an important discovery. An uncharacterized family of three proteins annotated as 'biotin/lipoyl attachment domain containing', termed BADCs, were found to directly interact with the biotin carboxyl carrier protein (BCCP) and biotin carboxylase (BC) subunits of htACCase. Not only do these proteins interact with the enzyme, but the BADCs directly inhibit htACCase

activity in both *A. thaliana* and *E. coli*. Furthermore, silencing of one of the BADC proteins in *A. thaliana* led to increased seed oil content, suggesting that htACCase activity was enhanced. Therefore, the BADCs appear to function as negative regulators of the htACCase enzyme.

Characterization of the BADC proteins from *A. thaliana* led to a potential model for their regulatory role. Interestingly, the BADCs share many characteristics with the BCCP subunits of htACCase, including size, primary sequence identity, predicted structure, and ability to form homodimers. However, one key difference between the BADCs and BCCPs is the former lacks the tetrapeptide biotinylation motif 'AMKL' and is not biotinylated. Since the BADCs were shown to negatively affect htACCase activity, the most logical mechanism of action is that BADCs act as apo-BCCP mimics and incorporate into the htACCase complex. In doing so, the resulting complex is less active due to a reduced number of biotinylated BCCP subunits. Consequently, the BADCs act as competitive inhibitors of the htACCase enzyme by competing with BCCP for incorporation into the complex.

Evolution analysis of the BADC gene family suggested that these genes arose early in the plant kingdom. In fact, the original BADC gene appears to reside in a species of red algae. This gene matches most closely to the BCCP2 gene in *A. thaliana*, but lacks the biotinylation motif. Therefore BADC appears to

have arisen as a result of a duplication and subsequent mutation of the BCCP gene. From an evolutionary standpoint, the earliest species found to contain an AtBADC ortholog is in the algae clade. This gene was then maintained and duplicated over time, and can be found in many different plant species, including the ancient vascular plant *S. moellendorffii*, mosses, non-graminaceous monocots, and eudicots. Graminaceous monocots, which lack the htACCase genes, contain no orthologs to AtBADC. Also, no AtBADC orthologs were identified in prokaryotes, suggesting that the BADC gene might have allowed for primitive algal species to maintain tighter control over carbon metabolism that was not required in prokaryotes.

This discovery could have significant implications on the vegetable oil industry. Orthologs to AtBADC were identified in almost every major oilseed crop that is currently being used to produce vegetable oil around the globe. In our preliminary experiment in *A. thaliana*, silencing of one BADC gene allowed for increases in total seed oil content of up to 13 % by dry mass. Translating this technology to a major oilseed crop such as soybean or canola could result in significant increases in vegetable oil production worldwide. The most recent data show a total production of approximately 9.9 million metric tons of soybean oil in the US last year that was sold at an average of $697 per metric ton (USDA, Oilseeds: World Markets and Trade, April, 2016). This commodity then amounts

to approximately seven billion dollars. Therefore, even an increase in yield of one percent could lead to hundreds of millions of dollars of increased revenue.

This discovery was also surprising given that htACCase is part of a well-known, central metabolic pathway. Both d*e novo* FAS and ACCase have been studied for at least 50 years (1,132), therefore one could assume that most of the major proteins and enzymes involved have already been discovered. But this study goes against that assumption and provides yet another example of the importance of basic biochemistry research to further our understanding of the cellular processes that are required to maintain life. In addition, the advancement of analytical techniques and the field of proteomics allowed for such a discovery to be made, and highlights the significance of these technologies to the scientific community.

The second aim of this study was to identify the role of a known phosphorylation event on the α-CT subunit of htACCase. To pursue this goal, it was decided to create phosphomimic and phospho-deficient mutants of α-CT and express these proteins in wild type *A. thaliana.* The resulting transgenic lines were then screened for seed oil content to determine the effect of the mutations. Testing of multiple independent lines showed no consistent trends for a particular mutation. This outcome is not surprising given that a single mutation was made to the non-catalytic domain of an approximately 80 kDa protien. However, further

analysis of these transgenic lines showed that htACCase specific activity was higher in lines that contained two-fold higher expression of native α-CT protein than the empty vector control. In the same manner, transgenic lines expressing mutant α-CT showed higher htACCase specific activity regardless of the mutation. These *in vitro* data suggest that increased expression of α-CT alone has a beneficial effect on htACCase activity. Furthermore, since the *in vitro* experiments were performed at saturating substrate concentrations, htACCase specific activity in α-CT overexpressing lines was likely increased due to the presence of higher number of active complexes. Therefore α-CT could be the limiting subunit of the complex.

This finding could also have significant implications on our understanding of htACCase regulation. It is still largely unknown how the plant cell coordinates the expression of the htACCase subunit genes and whether equimolar concentrations are maintained in the plastid. From this study, it appears that the subunits are not maintained at equimolar concentrations, since overexpression of α-CT increased htACCase activity *in vitro*. This implies that the concentration of the α-CT subunit determines the number of active htACCase complexes, and is the limiting subunit. If this trend can be confirmed in other htACCase-containing plant species, a potential biotechnological application could be realized.

Future work on these projects should be focused on the mechanistic details of regulation htACCase. For the BADC proteins, it is still unclear how they interact with the htACCase complex. Our understanding of this regulatory mechanism is limited by our knowledge of htACCase complex formation. Answering a number of questions regarding htACCase assembly would enable the characterization of this mechanism: 1) Does BADC replace BCCP or bind to another site; 2) Can BCCP and/or BADC incorporate into the complex as a monomer or dimer; 3) Can subunits be replaced once the complex is formed; 4) What is the half-life of the formed complex. These details will allow for educated biotechnology strategies to improve seed oil content in commercial crops.

In summary, the body of work presented here has introduced a new regulatory mechanism that has a direct affect to htACCase activity in plants. In addition, this mechanism requires an uncommon method of action whereby proteins engage in competition for binding to the BC subunit. Understanding this mechanism might not only lead to a better understanding of fatty acid synthesis, but also a better understanding of enzyme regulation.

REFERENCE LIST

1. Waite, M., and Wakil, S. J. (1962) Studies on the mechanism of fatty acid synthesis. XII. Acetyl coenzyme A carboxylase. *The Journal of biological chemistry* **237**, 2750-2757
2. Alberts, A. W., and Vagelos, P. R. (1968) Acetyl CoA carboxylase. I. Requirement for two protein fractions. *Proceedings of the National Academy of Sciences of the United States of America* **59**, 561-568
3. Guchhait, R. B., Polakis, S. E., Dimroth, P., Stoll, E., Moss, J., and Lane, M. D. (1974) Acetyl coenzyme A carboxylase system of Escherichia coli. Purification and properties of the biotin carboxylase, carboxyltransferase, and carboxyl carrier protein components. *The Journal of biological chemistry* **249**, 6633-6645
4. Konishi, T., Shinohara, K., Yamada, K., and Sasaki, Y. (1996) Acetyl-CoA carboxylase in higher plants: most plants other than gramineae have both the prokaryotic and the eukaryotic forms of this enzyme. *Plant & cell physiology* **37**, 117-122
5. Huerlimann, R., and Heimann, K. (2012) Comprehensive guide to acetyl-carboxylases in algae. *Critical reviews in biotechnology*
6. Kimura, Y., Miyake, R., Tokumasu, Y., and Sato, M. (2000) Molecular cloning and characterization of two genes for the biotin carboxylase and carboxyltransferase subunits of acetyl coenzyme A carboxylase in Myxococcus xanthus. *Journal of bacteriology* **182**, 5462-5469
7. Chuakrut, S., Arai, H., Ishii, M., and Igarashi, Y. (2003) Characterization of a bifunctional archaeal acyl coenzyme A carboxylase. *Journal of bacteriology* **185**, 938-947
8. Demirev, A. V., Lee, J. S., Sedai, B. R., Ivanov, I. G., and Nam, D. H. (2009) Identification and characterization of acetyl-CoA carboxylase gene cluster in Streptomyces toxytricini. *Journal of microbiology* **47**, 473-478
9. Fatland, B. L., Nikolau, B. J., and Wurtele, E. S. (2005) Reverse genetic characterization of cytosolic acetyl-CoA generation by ATP-citrate lyase in Arabidopsis. *The Plant cell* **17**, 182-203
10. Schulte, W., Topfer, R., Stracke, R., Schell, J., and Martini, N. (1997) Multi-functional acetyl-CoA carboxylase from Brassica napus is encoded by a multi-gene family: indication for plastidic localization of at least one isoform. *Proceedings of the National Academy of Sciences of the United States of America* **94**, 3465-3470
11. Cronan, J. E., Jr., and Waldrop, G. L. (2002) Multi-subunit acetyl-CoA carboxylases. *Progress in lipid research* **41**, 407-435
12. Davis, M. S., Solbiati, J., and Cronan, J. E., Jr. (2000) Overproduction of acetyl-CoA carboxylase activity increases the rate of fatty acid biosynthesis in Escherichia coli. *The Journal of biological chemistry* **275**, 28593-28598
13. Roesler, K., Shintani, D., Savage, L., Boddupalli, S., and Ohlrogge, J. (1997) Targeting of the Arabidopsis homomeric acetyl-coenzyme A carboxylase to plastids of rapeseeds. *Plant physiology* **113**, 75-81

14. Li-Beisson, Y., Shorrosh, B., Beisson, F., Andersson, M. X., Arondel, V., Bates, P. D., Baud, S., Bird, D., Debono, A., Durrett, T. P., Franke, R. B., Graham, I. A., Katayama, K., Kelly, A. A., Larson, T., Markham, J. E., Miquel, M., Molina, I., Nishida, I., Rowland, O., Samuels, L., Schmid, K. M., Wada, H., Welti, R., Xu, C., Zallot, R., and Ohlrogge, J. (2013) Acyl-lipid metabolism. *The Arabidopsis book / American Society of Plant Biologists* **11**, e0161
15. Nikolau, B. J., Ohlrogge, J. B., and Wurtele, E. S. (2003) Plant biotin-containing carboxylases. *Archives of biochemistry and biophysics* **414**, 211-222
16. Sasaki, Y., and Nagano, Y. (2004) Plant acetyl-CoA carboxylase: structure, biosynthesis, regulation, and gene manipulation for plant breeding. *Bioscience, biotechnology, and biochemistry* **68**, 1175-1184
17. Reverdatto, S., Beilinson, V., and Nielsen, N. C. (1999) A multisubunit acetyl coenzyme A carboxylase from soybean. *Plant physiology* **119**, 961-978
18. Fall, R. R. (1976) Stabilization of an acetyl-coenzyme A carboxylase complex from Pseudomonas citronellolis. *Biochimica et biophysica acta* **450**, 475-480
19. Mooney, B. P., Miernyk, J. A., and Randall, D. D. (2002) The complex fate of alpha-ketoacids. *Annual review of plant biology* **53**, 357-375
20. Bilder, P., Lightle, S., Bainbridge, G., Ohren, J., Finzel, B., Sun, F., Holley, S., Al-Kassim, L., Spessard, C., Melnick, M., Newcomer, M., and Waldrop, G. L. (2006) The structure of the carboxyltransferase component of acetyl-coA carboxylase reveals a zinc-binding motif unique to the bacterial enzyme. *Biochemistry* **45**, 1712-1722
21. Alberts, A. W., Nervi, A. M., and Vagelos, P. R. (1969) Acetyl CoA carboxylase, II. Deomonstration of biotin-protein and biotin carboxylase subunits. *Proceedings of the National Academy of Sciences of the United States of America* **63**, 1319-1326
22. Li, S. J., and Cronan, J. E., Jr. (1992) The gene encoding the biotin carboxylase subunit of Escherichia coli acetyl-CoA carboxylase. *The Journal of biological chemistry* **267**, 855-863
23. Li, S. J., and Cronan, J. E., Jr. (1992) The genes encoding the two carboxyltransferase subunits of Escherichia coli acetyl-CoA carboxylase. *The Journal of biological chemistry* **267**, 16841-16847
24. Sasaki, Y., Hakamada, K., Suama, Y., Nagano, Y., Furusawa, I., and Matsuno, R. (1993) Chloroplast-encoded protein as a subunit of acetyl-CoA carboxylase in pea plant. *The Journal of biological chemistry* **268**, 25118-25123
25. Choi, J. K., Yu, F., Wurtele, E. S., and Nikolau, B. J. (1995) Molecular cloning and characterization of the cDNA coding for the biotin-containing subunit of the chloroplastic acetyl-coenzyme A carboxylase. *Plant physiology* **109**, 619-625
26. Shorrosh, B. S., Roesler, K. R., Shintani, D., van de Loo, F. J., and Ohlrogge, J. B. (1995) Structural analysis, plastid localization, and expression of the biotin carboxylase subunit of acetyl-coenzyme A carboxylase from tobacco. *Plant physiology* **108**, 805-812

27. Shorrosh, B. S., Savage, L. J., Soll, J., and Ohlrogge, J. B. (1996) The pea chloroplast membrane-associated protein, IEP96, is a subunit of acetyl-CoA carboxylase. *The Plant journal : for cell and molecular biology* **10**, 261-268
28. Thelen, J. J., Mekhedov, S., and Ohlrogge, J. B. (2000) Biotin carboxyl carrier protein isoforms in Brassicaceae oilseeds. *Biochemical Society transactions* **28**, 595-598
29. Mekhedov, S., de Ilarduya, O. M., and Ohlrogge, J. (2000) Toward a functional catalog of the plant genome. A survey of genes for lipid biosynthesis. *Plant physiology* **122**, 389-402
30. Ohlrogge, J., and Browse, J. (1995) Lipid biosynthesis. *The Plant cell* **7**, 957-970
31. Meades, G., Jr., Benson, B. K., Grove, A., and Waldrop, G. L. (2010) A tale of two functions: enzymatic activity and translational repression by carboxyltransferase. *Nucleic acids research* **38**, 1217-1227
32. Goremykin, V. V., Holland, B., Hirsch-Ernst, K. I., and Hellwig, F. H. (2005) Analysis of Acorus calamus chloroplast genome and its phylogenetic implications. *Molecular biology and evolution* **22**, 1813-1822
33. Guisinger, M. M., Kuehl, J. V., Boore, J. L., and Jansen, R. K. (2011) Extreme reconfiguration of plastid genomes in the angiosperm family Geraniaceae: rearrangements, repeats, and codon usage. *Molecular biology and evolution* **28**, 583-600
34. Haberle, R. C., Fourcade, H. M., Boore, J. L., and Jansen, R. K. (2008) Extensive rearrangements in the chloroplast genome of Trachelium caeruleum are associated with repeats and tRNA genes. *Journal of molecular evolution* **66**, 350-361
35. Hu, S., Sablok, G., Wang, B., Qu, D., Barbaro, E., Viola, R., Li, M., and Varotto, C. (2015) Plastome organization and evolution of chloroplast genes in Cardamine species adapted to contrasting habitats. *BMC genomics* **16**, 306
36. Magee, A. M., Aspinall, S., Rice, D. W., Cusack, B. P., Semon, M., Perry, A. S., Stefanovic, S., Milbourne, D., Barth, S., Palmer, J. D., Gray, J. C., Kavanagh, T. A., and Wolfe, K. H. (2010) Localized hypermutation and associated gene losses in legume chloroplast genomes. *Genome research* **20**, 1700-1710
37. Martin, W., Stoebe, B., Goremykin, V., Hapsmann, S., Hasegawa, M., and Kowallik, K. V. (1998) Gene transfer to the nucleus and the evolution of chloroplasts. *Nature* **393**, 162-165
38. Rousseau-Gueutin, M., Huang, X., Higginson, E., Ayliffe, M., Day, A., and Timmis, J. N. (2013) Potential functional replacement of the plastidic acetyl-CoA carboxylase subunit (accD) gene by recent transfers to the nucleus in some angiosperm lineages. *Plant physiology* **161**, 1918-1929
39. Ruuska, S. A., Girke, T., Benning, C., and Ohlrogge, J. B. (2002) Contrapuntal networks of gene expression during Arabidopsis seed filling. *The Plant cell* **14**, 1191-1206
40. Focks, N., and Benning, C. (1998) wrinkled1: A novel, low-seed-oil mutant of Arabidopsis with a deficiency in the seed-specific regulation of carbohydrate metabolism. *Plant physiology* **118**, 91-101

41. Cernac, A., and Benning, C. (2004) WRINKLED1 encodes an AP2/EREB domain protein involved in the control of storage compound biosynthesis in Arabidopsis. *The Plant journal : for cell and molecular biology* **40**, 575-585
42. Fukuda, N., Ikawa, Y., Aoyagi, T., and Kozaki, A. (2013) Expression of the genes coding for plastidic acetyl-CoA carboxylase subunits is regulated by a location-sensitive transcription factor binding site. *Plant molecular biology* **82**, 473-483
43. Baud, S., Wuilleme, S., To, A., Rochat, C., and Lepiniec, L. (2009) Role of WRINKLED1 in the transcriptional regulation of glycolytic and fatty acid biosynthetic genes in Arabidopsis. *The Plant journal : for cell and molecular biology* **60**, 933-947
44. Baud, S., Mendoza, M. S., To, A., Harscoet, E., Lepiniec, L., and Dubreucq, B. (2007) WRINKLED1 specifies the regulatory action of LEAFY COTYLEDON2 towards fatty acid metabolism during seed maturation in Arabidopsis. *The Plant journal : for cell and molecular biology* **50**, 825-838
45. Shintani, D., Roesler, K., Shorrosh, B., Savage, L., and Ohlrogge, J. (1997) Antisense expression and overexpression of biotin carboxylase in tobacco leaves. *Plant physiology* **114**, 881-886
46. Madoka, Y., Tomizawa, K., Mizoi, J., Nishida, I., Nagano, Y., and Sasaki, Y. (2002) Chloroplast transformation with modified accD operon increases acetyl-CoA carboxylase and causes extension of leaf longevity and increase in seed yield in tobacco. *Plant & cell physiology* **43**, 1518-1525
47. Thelen, J. J., and Ohlrogge, J. B. (2002) Both antisense and sense expression of biotin carboxyl carrier protein isoform 2 inactivates the plastid acetyl-coenzyme A carboxylase in Arabidopsis thaliana. *The Plant journal : for cell and molecular biology* **32**, 419-431
48. Chen, M., Mooney, B. P., Hajduch, M., Joshi, T., Zhou, M., Xu, D., and Thelen, J. J. (2009) System analysis of an Arabidopsis mutant altered in de novo fatty acid synthesis reveals diverse changes in seed composition and metabolism. *Plant physiology* **150**, 27-41
49. Li, X., Ilarslan, H., Brachova, L., Qian, H. R., Li, L., Che, P., Wurtele, E. S., and Nikolau, B. J. (2011) Reverse-genetic analysis of the two biotin-containing subunit genes of the heteromeric acetyl-coenzyme A carboxylase in Arabidopsis indicates a unidirectional functional redundancy. *Plant physiology* **155**, 293-314
50. Sasaki, Y., Kozaki, A., Ohmori, A., Iguchi, H., and Nagano, Y. (2001) Chloroplast RNA editing required for functional acetyl-CoA carboxylase in plants. *The Journal of biological chemistry* **276**, 3937-3940
51. Robbins, J. C., Heller, W. P., and Hanson, M. R. (2009) A comparative genomics approach identifies a PPR-DYW protein that is essential for C-to-U editing of the Arabidopsis chloroplast accD transcript. *Rna* **15**, 1142-1153
52. Tseng, C. C., Sung, T. Y., Li, Y. C., Hsu, S. J., Lin, C. L., and Hsieh, M. H. (2010) Editing of accD and ndhF chloroplast transcripts is partially affected in the Arabidopsis vanilla cream1 mutant. *Plant molecular biology* **73**, 309-323
53. Yu, Q. B., Jiang, Y., Chong, K., and Yang, Z. N. (2009) AtECB2, a pentatricopeptide repeat protein, is required for chloroplast transcript accD RNA

editing and early chloroplast biogenesis in Arabidopsis thaliana. *The Plant journal : for cell and molecular biology* **59**, 1011-1023
54. Zhang, H. D., Cui, Y. L., Huang, C., Yin, Q. Q., Qin, X. M., Xu, T., He, X. F., Zhang, Y., Li, Z. R., and Yang, Z. N. (2015) PPR protein PDM1/SEL1 is involved in RNA editing and splicing of plastid genes in Arabidopsis thaliana. *Photosynthesis research* **126**, 311-321
55. Browse, J., Roughan, P. G., and Slack, C. R. (1981) Light control of fatty acid synthesis and diurnal fluctuations of fatty acid composition in leaves. *The Biochemical journal* **196**, 347-354
56. Bao, X., Focke, M., Pollard, M., and Ohlrogge, J. (2000) Understanding in vivo carbon precursor supply for fatty acid synthesis in leaf tissue. *The Plant journal : for cell and molecular biology* **22**, 39-50
57. Sauer, A., and Heise, K. P. (1983) On the light dependence of Fatty Acid synthesis in spinach chloroplasts. *Plant physiology* **73**, 11-15
58. Sasaki, Y., Kozaki, A., and Hatano, M. (1997) Link between light and fatty acid synthesis: thioredoxin-linked reductive activation of plastidic acetyl-CoA carboxylase. *Proceedings of the National Academy of Sciences of the United States of America* **94**, 11096-11101
59. Hunter, S. C., and Ohlrogge, J. B. (1998) Regulation of spinach chloroplast acetyl-CoA carboxylase. *Archives of biochemistry and biophysics* **359**, 170-178
60. Heath, R. J., and Rock, C. O. (1996) Regulation of fatty acid elongation and initiation by acyl-acyl carrier protein in Escherichia coli. *The Journal of biological chemistry* **271**, 1833-1836
61. Davis, M. S., and Cronan, J. E., Jr. (2001) Inhibition of Escherichia coli acetyl coenzyme A carboxylase by acyl-acyl carrier protein. *Journal of bacteriology* **183**, 1499-1503
62. Andre, C., Haslam, R. P., and Shanklin, J. (2012) Feedback regulation of plastidic acetyl-CoA carboxylase by 18:1-acyl carrier protein in Brassica napus. *Proceedings of the National Academy of Sciences of the United States of America*
63. Kozaki, A., Mayumi, K., and Sasaki, Y. (2001) Thiol-disulfide exchange between nuclear-encoded and chloroplast-encoded subunits of pea acetyl-CoA carboxylase. *The Journal of biological chemistry* **276**, 39919-39925
64. Feria Bourrellier, A. B., Valot, B., Guillot, A., Ambard-Bretteville, F., Vidal, J., and Hodges, M. (2010) Chloroplast acetyl-CoA carboxylase activity is 2-oxoglutarate-regulated by interaction of PII with the biotin carboxyl carrier subunit. *Proceedings of the National Academy of Sciences of the United States of America* **107**, 502-507
65. Rodrigues, T. E., Gerhardt, E. C., Oliveira, M. A., Chubatsu, L. S., Pedrosa, F. O., Souza, E. M., Souza, G. A., Muller-Santos, M., and Huergo, L. F. (2014) Search for novel targets of the PII signal transduction protein in Bacteria identifies the BCCP component of acetyl-CoA carboxylase as a PII binding partner. *Molecular microbiology* **91**, 751-761

66. Ninfa, A. J., and Jiang, P. (2005) PII signal transduction proteins: sensors of alpha-ketoglutarate that regulate nitrogen metabolism. *Current opinion in microbiology* **8**, 168-173
67. Gerhardt, E. C., Rodrigues, T. E., Muller-Santos, M., Pedrosa, F. O., Souza, E. M., Forchhammer, K., and Huergo, L. F. (2014) The Bacterial signal transduction protein GlnB regulates the committed step in fatty acid biosynthesis by acting as a dissociable regulatory subunit of acetyl-CoA carboxylase. *Molecular microbiology*
68. Olinares, P. D., Ponnala, L., and van Wijk, K. J. (2010) Megadalton complexes in the chloroplast stroma of Arabidopsis thaliana characterized by size exclusion chromatography, mass spectrometry, and hierarchical clustering. *Molecular & cellular proteomics : MCP* **9**, 1594-1615
69. Thelen, J. J., and Ohlrogge, J. B. (2002) The multisubunit acetyl-CoA carboxylase is strongly associated with the chloroplast envelope through non-ionic interactions to the carboxyltransferase subunits. *Archives of biochemistry and biophysics* **400**, 245-257
70. Joyard, J., Ferro, M., Masselon, C., Seigneurin-Berny, D., Salvi, D., Garin, J., and Rolland, N. (2010) Chloroplast proteomics highlights the subcellular compartmentation of lipid metabolism. *Progress in lipid research* **49**, 128-158
71. Savage, L. J., and Ohlrogge, J. B. (1999) Phosphorylation of pea chloroplast acetyl-CoA carboxylase. *The Plant journal : for cell and molecular biology* **18**, 521-527
72. Agrawal, G. K., and Thelen, J. J. (2006) Large scale identification and quantitative profiling of phosphoproteins expressed during seed filling in oilseed rape. *Molecular & cellular proteomics : MCP* **5**, 2044-2059
73. Reiland, S., Messerli, G., Baerenfaller, K., Gerrits, B., Endler, A., Grossmann, J., Gruissem, W., and Baginsky, S. (2009) Large-scale Arabidopsis phosphoproteome profiling reveals novel chloroplast kinase substrates and phosphorylation networks. *Plant physiology* **150**, 889-903
74. Meyer, L. J., Gao, J., Xu, D., and Thelen, J. J. (2012) Phosphoproteomic analysis of seed maturation in Arabidopsis, rapeseed, and soybean. *Plant physiology* **159**, 517-528
75. Nakagami, H., Sugiyama, N., Mochida, K., Daudi, A., Yoshida, Y., Toyoda, T., Tomita, M., Ishihama, Y., and Shirasu, K. (2010) Large-scale comparative phosphoproteomics identifies conserved phosphorylation sites in plants. *Plant physiology* **153**, 1161-1174
76. Michelet, L., Zaffagnini, M., Vanacker, H., Le Marechal, P., Marchand, C., Schroda, M., Lemaire, S. D., and Decottignies, P. (2008) In vivo targets of S-thiolation in Chlamydomonas reinhardtii. *The Journal of biological chemistry* **283**, 21571-21578
77. Dixon, D. P., Skipsey, M., Grundy, N. M., and Edwards, R. (2005) Stress-induced protein S-glutathionylation in Arabidopsis. *Plant physiology* **138**, 2233-2244

78. Noctor, G., Mhamdi, A., Chaouch, S., Han, Y., Neukermans, J., Marquez-Garcia, B., Queval, G., and Foyer, C. H. (2012) Glutathione in plants: an integrated overview. *Plant, cell & environment* **35**, 454-484
79. Broussard, T. C., Kobe, M. J., Pakhomova, S., Neau, D. B., Price, A. E., Champion, T. S., and Waldrop, G. L. (2013) The three-dimensional structure of the biotin carboxylase-biotin carboxyl carrier protein complex of E. coli acetyl-CoA carboxylase. *Structure* **21**, 650-657
80. Lu, P., Vogel, C., Wang, R., Yao, X., and Marcotte, E. M. (2007) Absolute protein expression profiling estimates the relative contributions of transcriptional and translational regulation. *Nature biotechnology* **25**, 117-124
81. Ishihama, Y., Schmidt, T., Rappsilber, J., Mann, M., Hartl, F. U., Kerner, M. J., and Frishman, D. (2008) Protein abundance profiling of the Escherichia coli cytosol. *BMC genomics* **9**, 102
82. Choi-Rhee, E., and Cronan, J. E. (2003) The biotin carboxylase-biotin carboxyl carrier protein complex of Escherichia coli acetyl-CoA carboxylase. *The Journal of biological chemistry* **278**, 30806-30812
83. Li, G. W., Burkhardt, D., Gross, C., and Weissman, J. S. (2014) Quantifying absolute protein synthesis rates reveals principles underlying allocation of cellular resources. *Cell* **157**, 624-635
84. Benson, B. K., Meades, G., Jr., Grove, A., and Waldrop, G. L. (2008) DNA inhibits catalysis by the carboxyltransferase subunit of acetyl-CoA carboxylase: implications for active site communication. *Protein science : a publication of the Protein Society* **17**, 34-42
85. Crepin, T., Schmitt, E., Blanquet, S., and Mechulam, Y. (2004) Three-dimensional structure of methionyl-tRNA synthetase from Pyrococcus abyssi. *Biochemistry* **43**, 2635-2644
86. Serre, L., Verdon, G., Choinowski, T., Hervouet, N., Risler, J. L., and Zelwer, C. (2001) How methionyl-tRNA synthetase creates its amino acid recognition pocket upon L-methionine binding. *Journal of molecular biology* **306**, 863-876
87. Glasfeld, E., and Schimmel, P. (1997) Zinc-dependent tRNA binding by a peptide element within a tRNA synthetase. *Biochemistry* **36**, 6739-6744
88. Cronan, J. E., Jr. (2001) The biotinyl domain of Escherichia coli acetyl-CoA carboxylase. Evidence that the "thumb" structure id essential and that the domain functions as a dimer. *The Journal of biological chemistry* **276**, 37355-37364
89. Thelen, J. J., Mekhedov, S., and Ohlrogge, J. B. (2001) Brassicaceae express multiple isoforms of biotin carboxyl carrier protein in a tissue-specific manner. *Plant physiology* **125**, 2016-2028
90. Troncoso-Ponce, M. A., Nikovics, K., Marchive, C., Lepiniec, L., and Baud, S. (2015) New insights on the organization and regulation of the fatty acid biosynthetic network in the model higher plant Arabidopsis thaliana. *Biochimie*
91. Roughan, P. G., and Ohlrogge, J. B. (1996) Evidence That Isolated Chloroplasts Contain an Integrated Lipid-Synthesizing Assembly That Channels Acetate into Long-Chain Fatty Acids. *Plant physiology* **110**, 1239-1247

92. Ferro, M., Salvi, D., Brugiere, S., Miras, S., Kowalski, S., Louwagie, M., Garin, J., Joyard, J., and Rolland, N. (2003) Proteomics of the chloroplast envelope membranes from Arabidopsis thaliana. *Molecular & cellular proteomics : MCP* **2**, 325-345
93. Roughan, P. G. (1997) Stromal concentrations of coenzyme A and its esters are insufficient to account for rates of chloroplast fatty acid synthesis: evidence for substrate channelling within the chloroplast fatty acid synthase. *The Biochemical journal* **327 (Pt 1)**, 267-273
94. Dyer, J. M., Stymne, S., Green, A. G., and Carlsson, A. S. (2008) High-value oils from plants. *The Plant journal : for cell and molecular biology* **54**, 640-655
95. Dyer, J. M., and Mullen, R. T. (2008) Engineering plant oils as high-value industrial feedstocks for biorefining: the need for underpinning cell biology research. *Physiologia plantarum* **132**, 11-22
96. Konishi, T., and Sasaki, Y. (1994) Compartmentalization of two forms of acetyl-CoA carboxylase in plants and the origin of their tolerance toward herbicides. *Proceedings of the National Academy of Sciences of the United States of America* **91**, 3598-3601
97. Baud, S., and Lepiniec, L. (2009) Regulation of de novo fatty acid synthesis in maturing oilseeds of Arabidopsis. *Plant physiology and biochemistry : PPB / Societe francaise de physiologie vegetale* **47**, 448-455
98. Blough, N. V., and Sauer, K. (1984) The effects of mono- and divalent salts on the O2-evolution activity and low temperature multiline EPR spectrum of Photosystem II preparations from spinach. *Biochimica et biophysica acta* **767**, 377-381
99. Alban, C., Job, D., and Douce, R. (2000) Biotin Metabolism in Plants. *Annual review of plant physiology and plant molecular biology* **51**, 17-47
100. Tissot, G., Job, D., Douce, R., and Alban, C. (1996) Protein biotinylation in higher plants: characterization of biotin holocarboxylase synthetase activity from pea (Pisum sativum) leaves. *The Biochemical journal* **314 (Pt 2)**, 391-395
101. Kanehisa, M., Sato, Y., Kawashima, M., Furumichi, M., and Tanabe, M. (2016) KEGG as a reference resource for gene and protein annotation. *Nucleic acids research* **44**, D457-462
102. Chapman-Smith, A., Morris, T. W., Wallace, J. C., and Cronan, J. E., Jr. (1999) Molecular recognition in a post-translational modification of exceptional specificity. Mutants of the biotinylated domain of acetyl-CoA carboxylase defective in recognition by biotin protein ligase. *The Journal of biological chemistry* **274**, 1449-1457
103. Shevchenko, A., Tomas, H., Havlis, J., Olsen, J. V., and Mann, M. (2006) In-gel digestion for mass spectrometric characterization of proteins and proteomes. *Nature protocols* **1**, 2856-2860
104. Swatek, K. N., Graham, K., Agrawal, G. K., and Thelen, J. J. (2011) The 14-3-3 isoforms chi and epsilon differentially bind client proteins from developing Arabidopsis seed. *Journal of proteome research* **10**, 4076-4087

105. Swatek, K. N., Wilson, R. S., Ahsan, N., Tritz, R. L., and Thelen, J. J. (2014) Multisite phosphorylation of 14-3-3 proteins by calcium-dependent protein kinases. *The Biochemical journal* **459**, 15-25
106. Stevenson, S. E., Chu, Y., Ozias-Akins, P., and Thelen, J. J. (2009) Validation of gel-free, label-free quantitative proteomics approaches: applications for seed allergen profiling. *Journal of proteomics* **72**, 555-566
107. Nielsen, H., Engelbrecht, J., Brunak, S., and von Heijne, G. (1997) Identification of prokaryotic and eukaryotic signal peptides and prediction of their cleavage sites. *Protein engineering* **10**, 1-6
108. Emanuelsson, O., Nielsen, H., Brunak, S., and von Heijne, G. (2000) Predicting subcellular localization of proteins based on their N-terminal amino acid sequence. *Journal of molecular biology* **300**, 1005-1016
109. Gietz, R. D., and Schiestl, R. H. (2007) Quick and easy yeast transformation using the LiAc/SS carrier DNA/PEG method. *Nature protocols* **2**, 35-37
110. Smith, T. F., and Waterman, M. S. (1981) Identification of common molecular subsequences. *Journal of molecular biology* **147**, 195-197
111. Eddy, S. R. (1998) Profile hidden Markov models. *Bioinformatics* **14**, 755-763
112. Finn, R. D., Coggill, P., Eberhardt, R. Y., Eddy, S. R., Mistry, J., Mitchell, A. L., Potter, S. C., Punta, M., Qureshi, M., Sangrador-Vegas, A., Salazar, G. A., Tate, J., and Bateman, A. (2016) The Pfam protein families database: towards a more sustainable future. *Nucleic acids research* **44**, D279-285
113. Edgar, R. C. (2004) MUSCLE: multiple sequence alignment with high accuracy and high throughput. *Nucleic acids research* **32**, 1792-1797
114. Stamatakis, A. (2014) RAxML version 8: a tool for phylogenetic analysis and post-analysis of large phylogenies. *Bioinformatics* **30**, 1312-1313
115. Clough, S. J., and Bent, A. F. (1998) Floral dip: a simplified method for Agrobacterium-mediated transformation of Arabidopsis thaliana. *The Plant journal : for cell and molecular biology* **16**, 735-743
116. Li, Y., Beisson, F., Pollard, M., and Ohlrogge, J. (2006) Oil content of Arabidopsis seeds: the influence of seed anatomy, light and plant-to-plant variation. *Phytochemistry* **67**, 904-915
117. Chen, M., and Thelen, J. J. (2013) ACYL-LIPID DESATURASE2 is required for chilling and freezing tolerance in Arabidopsis. *The Plant cell* **25**, 1430-1444
118. Garavelli, J. S. (2003) The RESID Database of Protein Modifications: 2003 developments. *Nucleic acids research* **31**, 499-501
119. Lanucara, F., and Eyers, C. E. (2013) Top-down mass spectrometry for the analysis of combinatorial post-translational modifications. *Mass spectrometry reviews* **32**, 27-42
120. Krebs, E. G., and Beavo, J. A. (1979) Phosphorylation-dephosphorylation of enzymes. *Annual review of biochemistry* **48**, 923-959
121. Humphrey, S. J., James, D. E., and Mann, M. (2015) Protein Phosphorylation: A Major Switch Mechanism for Metabolic Regulation. *Trends in endocrinology and metabolism: TEM* **26**, 676-687

122. Cohen, P. (2002) The origins of protein phosphorylation. *Nature cell biology* **4**, E127-130
123. Mason, J. M., and Arndt, K. M. (2004) Coiled coil domains: stability, specificity, and biological implications. *Chembiochem : a European journal of chemical biology* **5**, 170-176
124. Swatek, K. N. (2013) Characterization of the 14-3-3 client protein interactome from developing Arabidopsis seed and regulation by protein phosphorylation. University of Missouri-Columbia
125. Hernandez-Garcia, C. M., Bouchard, R. A., Rushton, P. J., Jones, M. L., Chen, X., Timko, M. P., and Finer, J. J. (2010) High level transgenic expression of soybean (Glycine max) GmERF and Gmubi gene promoters isolated by a novel promoter analysis pipeline. *BMC plant biology* **10**, 237
126. Hofgen, R., and Willmitzer, L. (1988) Storage of competent cells for Agrobacterium transformation. *Nucleic acids research* **16**, 9877
127. Baud, S., Feria Bourrellier, A. B., Azzopardi, M., Berger, A., Dechorgnat, J., Daniel-Vedele, F., Lepiniec, L., Miquel, M., Rochat, C., Hodges, M., and Ferrario-Mery, S. (2010) PII is induced by WRINKLED1 and fine-tunes fatty acid composition in seeds of Arabidopsis thaliana. *The Plant journal : for cell and molecular biology* **64**, 291-303
128. Baud, S., Wuilleme, S., Dubreucq, B., de Almeida, A., Vuagnat, C., Lepiniec, L., Miquel, M., and Rochat, C. (2007) Function of plastidial pyruvate kinases in seeds of Arabidopsis thaliana. *The Plant journal : for cell and molecular biology* **52**, 405-419
129. Paleologou, K. E., Schmid, A. W., Rospigliosi, C. C., Kim, H. Y., Lamberto, G. R., Fredenburg, R. A., Lansbury, P. T., Jr., Fernandez, C. O., Eliezer, D., Zweckstetter, M., and Lashuel, H. A. (2008) Phosphorylation at Ser-129 but not the phosphomimics S129E/D inhibits the fibrillation of alpha-synuclein. *The Journal of biological chemistry* **283**, 16895-16905
130. Huang, Y., and Thelen, J. J. (2012) KiC assay: a quantitative mass spectrometry-based approach for kinase client screening and activity analysis [corrected]. *Methods Mol Biol* **893**, 359-370
131. Delorenzi, M., and Speed, T. (2002) An HMM model for coiled-coil domains and a comparison with PSSM-based predictions. *Bioinformatics* **18**, 617-625
132. Newcomb, E. H., and Stumpf, P. K. (1953) Fat metabolism in higher plants. I. Biogenesis of higher fatty acids by slices of peanut cotyledons in vitro. *The Journal of biological chemistry* **200**, 233-239

VITA

Matthew J. Salie was born on April 23, 1989, in Bellflower, California to Marvin and Mary Salie. He attended Valley Christian schools from elementary to high school in Cerritos, California. He then moved to Grand Rapids, Michigan, to study Biochemistry at Calvin College. He received his Bachelors of Science in Biochemistry in 2011 and obtained almost two years research experience under the guidance of Larry L. Louters. He then went to the University of Missouri-Columbia and earned a PhD in Biochemistry under the guidance of Jay J. Thelen. Matthew is currently deciding between offers for postdoc positions from the Scripps Research Institute and Salk Institute in San Diego, California.